2015

Role of Nuclear Factor E2 Related Factor 2 (Nrf2) in Environmental Chemical Induced Steatosis and Adipogenesis

Prajakta Shimpi
University of Rhode Island, prajishimpi@gmail.com

ROLE OF NUCLEAR FACTOR E2 RELATED FACTOR 2 (NRF2) IN ENVIRONMENTAL CHEMICAL INDUCED STEATOSIS AND ADIPOGENESIS

BY

PRAJAKTA SHIMPI

A DISSERTATION SUBMITTED IN PARTIAL FULFILLMENT OF THE REQUIREMENTS FOR THE DEGREE OF

DOCTOR OF PHILOSOPHY

IN

PHARMACOLOGY AND TOXICOLOGY

UNIVERSITY OF RHODE ISLAND

2015

DOCTOR OF PHILOSOPHY IN PHARMACOLOGY AND TOXICOLOGY

OF

PRAJAKTA SHIMPI

APPROVED:

Thesis Committee:

Major Professor Angela Slitt

Roberta King

Niall Howlett

Naseer Zawia

DEAN OF THE GRADUATE SCHOOL

UNIVERSITY OF RHODE ISLAND

2015

ABSTRACT

Prevalence of non-alcoholic fatty liver disease (NAFLD) and obesity both in the young and adult population is increasing at an alarming rate globally. Along with traditional risk factors, such as diet and sedentary life style, exposure of environmental chemicals is suspected to be a risk factor for metabolic disruption. Moreover, the 'fetal basis of adult disease' hypothesis implicates that early life exposure to environmental chemicals is more impactful in causing lipid homeostasis disturbances than exposure in maturity. Nuclear factor E2 related factor 2 (Nrf2) is a cytoprotective transcription factor known to combat oxidative stress. The contribution of Nrf2 to other cellular functions, such as lipid homeostasis relevant to liver and adipose tissue is relatively new emerging area. The work herein assessed the role of Nrf2 in augmenting environmental chemical induced NAFLD and adipogenesis. CD-1 mice were exposed to bisphenol A (BPA) perinatally and peripubertally until age of 5 week at 25 μg/kg BW/day and effect of this exposure on hepatic lipid disturbances was evaluated at pubertal (week 5) and adult age (week 39). Developmental exposure of BPA increased hepatic lipid accumulation in both young, as well as adult mice. BPA also increased Nrf2 expression in these animals at both ages. Nrf2 binding to predicted anti-oxidant response elements on the Srebp-1c promoter, a master regulator of denovo lipogenesis, elucidated a potential regulatory role of Nrf2 in lipogenesis. BPA exposure also increased Nrf2 binding to this new putative ARE by about 2 fold. Epigenetic reprogramming of chromatin upon developmental exposure of

environmental xenobiotics is a potential mechanism for increasing susceptibly to diseases, such as like NALFD. BPA exposure from gestation day 8 through purberty caused hypomethylation in select regions of promoters that encode for proteins involved in lipogenesis (e.g. Srebp-1c), as well as the antioxidant response (e.g. Nrf2). The work further depicts an undescribed role for Nrf2 in the regulation of lipogenesis via regulation of Srebp-1c.

In connection to the findings above, as well as other findings in our laboratory that pointed to Nrf2 having a role in promoting hepatic lipid accumulation, it was decided to evaluate whether chemicals that induce lipid accumulation can do so in association with Nrf2 activation. Next, the role of Nrf2 in lipid accumulation was further characterized using adipose tissue in presence of perfluorooctane sulfonic acid (PFOS). In rodent and human preadipocytes, PFOS exposure elevated adipogenic process by increasing expression of key regulators of adipose differentiation. PFOS-induced adipogenesis was associated with increase in Nrf2 expression and its transcriptional activity.

In conclusion, the environmental contaminants, BPA and PFOS alter lipid homeostasis in liver and adipose tissue respectively. Concurrent increase in Nrf2 expression, and its transcription regulation on lipogenic mediators was demonstrated.

ACKNOWLEDGEMENTS

I would like to acknowledge everyone who supported me, guided me, helped me and inspired me to achieve my goals during this pleasant journey of graduate school.

First of all, I would like to thank my advisor Dr. Angela Slitt for her enormous support and inspiration along with an opportunity to work in her lab. She has helped me mature as a scientist and as a human being. Her expert guidance and enthusiasm about work has always motivated me to finish work in timely manner, and with utmost quality and ethics. She has willingly written many letters of recommendations for me throughout the years and supported me.

I also want to thank my defense committee- Dr. Niall Howlett, Dr. Roberta King, Dr. Nasser Zawia, and Dr. Thomas Manfredi for their continued support, and prompt guidance during comprehensive exams as well as thesis defense.

I would like to thank the Chemistry Department Chair, Dr. William Euler, who has given me financial support by providing me teaching assistantship opportunities Chemistry Department.

I also want to thank my friends from department- Dr. Yuan Chen, Dr. Leila Valanejad, Marek Marczak and Aseel Eid for their valuable help in learning new research techniques in lab. I really appreciate contribution of our collaborators from outside the URI to multiple projects - Dr. Dana Dolinoy, Jackie Goodrich (U. Michigan), Dr. Michel Skinner (Washington State U.) Christine Chio, Swetha Rudraiah (U. Conn). I also want to thank RI INBRE and GSC facilities for making available necessary technology for advanced research.

I would also like to acknowledge my lab mate Laura - as well as past members Jialin, Maureen, Wei, Ajay, Vijay and Supriya, for their help at intellectual level through emails or in lab meeting discussions, comments on the posters, manuscripts, comprehensive exam, an many more things along the way. I also want to thank lab undergraduate students, including Eileen, Megan and Kristen who worked with me for helping me gain valuable mentoring and leadership skills.

Lastly, I would like to acknowledge my family- mom, dad, my sister and brother for their tremendous moral support, who have always believed in me, motivated me and taught me the way to pursue a dream. Lastly but importantly, I would like to thank the most precious person of my life and my lovely husband Vijay. There are not enough words for me to express gratitude about his contribution in this entire journey. I would say, without his support it would have been impossible to complete this process. He has been there with me through all the ups and downs and kept me focused. He has been most wonderful partner in this journey.

PREFACE

The following dissertation titled “Role of nuclear factor E2 related factor 2 (Nrf2) in environmental chemical induced hepatic steatosis and adipogenesis” is presented in manuscript format. There are three manuscripts in this dissertation. First manuscript is a review, prepared for “Int J of Toxicology”, and also serves as general background for manuscript two, three. Manuscript two is formatted in *“Hepatology”* journal style, second manuscript is in *“Toxicology and Applied Pharmacology (TAAP)”* style. At the end of the thesis, there are two ‘appendices’, which present data that has not been included in any of the manuscripts, but was generated by student while working towards PhD research.

TABLE OF CONTENTS

ABSTRACT..... ii

ACKNOWLEDGEMENTS..... iv

PREFACE..... vi

TABLE OF CONTENTS..... vii

LIST OF TABLES..... xi

LIST OF FIGURES..... xii

MANUSCRIPT 1..... 1

1.1 Abstract..... 2

1.2 Obesity..... 3

1.3 Non-alcoholic Fatty Liver Disease (NAFLD)..... 4

1.4 Environmental chemicals and adipose tissue lipid alterations..... 6

1.5 Environmental chemicals and hepatic lipid alteration..... 10

1.6 Mechanisms of the environmental chemical induced lipid disturbances. 11

1.7 Conclusion..... 12

1.8 References..... 14

1.9 Tables..... 21

MANUSCRIPT 2...... 27

2.1 Abstract..... 28

2.2 Introduction..... 30

2.3 Materials and methods..... 33

2.3.1 Animals and dosing..... 33

2.3.2 Triglyceride quantification..... 34

2.3.3 Oil Red O staining..... 34

2.3.4 RNA isolation and quantitative real time PCR..... 34
2.3.5 Determination of relative protein expression by western blot.. 35
2.3.6 Chromatin immunoprecipitation (ChIP) assay..... 36
2.3.7 Methylation analysis..... 37
2.3.8 Cell culture and transient transfection reporter gene assay... 39
2.3.9 Statistical analysis..... 40
2.4 Results..... 41
2.4.1 Effects of perinatal peripubertal bisphenol A exposure on body weight, liver weight and hepatic lipid accumulation..... 41
2.4.2 Effect of PNPP BPA exposure on expression hepatic lipogenic gene expression in female mice at puberty (week 5) and adult (week 39) age..... 41
2.4.3 PNPP BPA exposure enhanced Nrf2 and Nrf2-dependent protein expression..... 42
2.4.4 PNPP BPA exposure was associated with hypomethylation in regions of the mouse Srepb-1c, Fas and Nrf2 promoters..... 43
2.4.5 PNPP BPA exposure enhances recruitment of Nrf2 to the promoter of lipogenic genes..... 44
2.4.6 Effect of NRF2 over-expression on transactivation of human Srebp-1c promoter..... 44
2.5 Discussion..... 45
2.6 Figure legends..... 50
2.7 Funding information..... 54
2.8 Acknowledgement..... 54

2.9 Tables..... 55

2.10 References..... 57

2.11 Figures..... 61

2.12 Supplementary data information..... 69

MANUSCRIPT 3..... 77

3.1 Abstract..... 78

3.2 Introduction..... 80

3.3 Materials and methods..... 84

3.3.1 Chemicals..... 84

3.3.2 Animals and PFOS administration..... 84

3.3.3 Acute cytotoxicity assay..... 85

3.3.4 Cell culture and 3T3-L1 pre-adipocyte differentiations..... 85

3.3.5 Human visceral preadipocytes culture and induction to adipocytes..... 86

3.3.6 RNA isolation and quantitative real-time PCR..... 86

3.3.7 Oil Red O staining..... 87

3.3.8 Measurement of triglycerides in 3T3-L1 preadipocytes..... 87

3.3.9 Glucose uptake assay..... 87

3.3.10 hPAP induction assay..... 88

3.3.11 Chromatin immunoprecipitation (ChIP) assay..... 89

3.3.12 Statistical analysis..... 89

3.4 Results..... 90

3.4.1 PFOS induces adipogenesis in 3T3-L1 preadipocytes..... 90

3.4.2 PFOS increases adipogenic gene expression in 3T3-L1 preadipocytes..... 90

3.4.3 PFOS promotes insulin-stimulated glucose uptake in 3T3-L1 adipocytes..... 91

3.4.4 Adipogenic gene expression and Nrf2 signaling is increased in white adipose tissue from mice administered PFOS..... 92

3.4.5 PFOS increased lipid accumulation in differentiated human visceral preadipocytes..... 93

3.4.6 PFOS increases Antioxidant Response Element activity and enhances Nrf2 enrichment at the ARE element in mouse Nqo1 promoter..... 94

3.5 Discussion..... 95

3.6 Acknowledgements..... 100

3.7 Reference..... 101

3.8 Figure Legends..... 104

3.9 Figures..... 108

3.10 Supplementary Material..... 115

SUMMARY AND CONCLUSION..... 116

APPENDIX 1..... 117

APPENDIX 2..... 124

LIST OF TABLES

MANUSCRIPT 1:

Table 1: Human cohort studies correlating environmental chemical levels with obesity parameters..... 21

Table 2: In-vitro studies linking environmental chemicals to adipose tissue lipid accumulation..... 22

Table 3: Human correlation studies linking early life exposure of environmental chemicals to obesity outcomes..... 24

Table 4: Rodent developmental exposure to environmental chemicals and obesity studies..... 25

Table 5: Studies linking environmental chemical exposure to NAFLD..... 26

MANUSCRIPT 2:

Table 1: Site specific methylation (%) of 4 CpG sites for Nrf2 promoter upon PNPB BPA exposure in Week 5 and Week 39 age of mice..... 55

Table 2: PCR conditions for Pyro-Sequencing..... 56

MANUSCRIPT 3: None

LIST OF FIGURES

MANUSCRIPT 1: None

MANUSCRIPT 2:

Figure 1: Perinatal peripubertal (PNPP) exposure to bisphenol A affects body weight and hepatic lipid accumulation in female CD1 mice..... 61

Figure 2: Perinatal peripubertal (PNPP) exposure to bisphenol A increases mRNA expression of lipogenic targets in livers of female CD1 mice..... 62

Figure 3: Perinatal peripubertal (PNPP) exposure to bisphenol A increases protein expression of lipogenic transcription factors in livers of female CD1 mice..... 63

Figure 4: Perinatal peripubertal (PNPP) exposure to bisphenol A increases protein expression of lipid synthesis enzymes in livers of female CD1 mice (A. Week 5; B. Week 39)..... 64

Figure 5: Perinatal peripubertal (PNPP) exposure to bisphenol A and nuclear factor E2 related factor 2 (Nrf2) signaling in livers of female CD1 mice..... 65

Figure 6: Effect of Perinatal peripubertal exposure of BPA on promoter methylation of Srebp-1c, Fas and Nrf2 analyzed by methylated DNA immunoprecipitation (MeDIP)..... 66

Figure 7: Chromatin immunoprecipitation of nuclear factor E2 related factor 2 (Nrf2) on Srebp-1c gene promoter..... 67

Figure 8: Nrf2 mediated transactivation of human Srebp-1 *in vitro.....* 68

MANUSCRIPT 3:

Figure 1: Illustration of study design and MTT assay of PFOS on 3T3-L1 preadipocytes..... 108

Figure 2: Non-cytotoxic levels of PFOS enhances lipid content in differentiated 3T3-L1 preadipocytes..... 109

Figure 3: PFOS increases adipogenic gene expression and induced Nrf2 signaling in 3T3-L1 preadipocytes..... 110

Figure 4 PFOS promotes insulin-stimulated glucose uptake in 3T3-L1 adipocytes..... 111

Figure 5: Adipogenic gene expression and Nrf2 signaling of Nrf2 and Nqo1 expression increase in white adipose tissue (WAT) from mice administered PFOS..... 112

Figure 6: PFOS increased lipid accumulation in differentiated human visceral preadipocytes..... 113

Figure 7: PFOS increases hPAP expression and enhances Nrf2 enrichment at ARE sites in mouse Nqo1 promoter..... 114

MANUSCRIPT 1

ENVIRONMENTAL ORIGIN OF METABOLIC DYSFUNCTION AND DISTURBANCES OF LIPID HOMEOSTASIS

Prajakta C Shimpi, Angela Slitt

Biomedical and Pharmaceutical Sciences, University of Rhode Island,

Kingston RI, USA

Manuscript prepared for submission to *"Int J of toxicology"*

1.1 ABSTRACT:

Prevalence of obesity and its associated metabolic disorders including non-alcoholic fatty liver disease (NAFLD), are rising at an alarming rate, and hence need a careful search for all possible pathogenic factors contributing this epidemic. Although imbalance of energy intake and energy expenditure is considered most traditional risk factors for obesity and NAFLD, recently "environmental obesogens" hypothesis is the gaining interest in research community, which links exposure of environmental chemicals and obesity. Terms like toxicants associated fatty liver diseases (TAFLD) are being increasingly used. The current paper has reviewed some the most recent findings of these obesogens and TAFLD contributing chemicals which are studied in rodent, in-vitro model as well as human correlation studies. Chemical exposures during vulnerable windows in development play a critical role in etiology of diseases. This paper reviewed few developmental exposure studies, which correlated positive correlation between concentration of exposure of these xenobiotic and obesity phenotype both in human and rodent model to understand fetal basis of adult diseases. However, most of studies are only demonstrating link of environment and metabolic effect without elucidating possible mechanism of pathogenesis. Further work is required to better characterize the molecular targets responsible for environmental origin of metabolic dysfunction and disturbances of lipid homeostasis.

1.2 Obesity. Globally the rising prevalence of obesity and its associated diseases is major public health concern in adult, children as well as adolescent population. According to results from the 2011–2012 National Health and Nutrition Examination Survey (NHANES), more than one-third (34.9%) of adults were obese in United States (1). Childhood obesity prevalence is also increasing at an alarming rate. It is estimated that 20.5% of adolescents (12-19 years of age) and 17.7% children (6-11 years age) are obese (2). Obesity is characterized by structural and functional changes to and distribution of white adipose tissue (WAT) in body. Adipose tissue plays a prominent role of balancing energy status of the body by storing excess of fat in form of triglyceride. Initially, excess fat is stored in mature adipocyte, and because of its plasticity it can expand by undergoing hypertrophy. Along with hypertrophy, hyperplasia of adipocytes, which means increasing number of fat cells through differentiation of stem cells to adipocyte lineage, can also contribute for disturbances of normal lipogenic and lipolysis process of adipose tissue (3). Apart from considering WAT as fuel storage depot, is also recognized as an active endocrine organ because of secretion of hormones and cytokines that play crucial role in maintaining of metabolic homeostasis like appetite, inflammation and insulin sensitivity (4). Adipocyte biology is significant to pathogenesis of obesity and hence maintenance of normal adipogenesis and mature adipocyte is very significant. Mature adipocytes form from its precursor mesenchymal stem cells through adipogenesis process, which involves very complex transcriptional cascade regulating programs. Multiple transcription regulators, including CCAAT/ enhancer-binding proteins (Cebpα,

Cebpβ), and peroxisome proliferator-activated receptor (Ppar-γ), are involved in inducing adipogenic programming (5).

1.3 Non-alcoholic Fatty Liver Disease (NAFLD). Obesity associated disturbance of adipogenesis process has deleterious consequences on insulin resistance, which can contribute to pathogenesis of metabolic syndrome comprising type-2 diabetes, dyslipidemia, atherosclerosis, hypertension and NAFLD. Prevalence of suspected NAFLD increased from 3.9% in 1988-1994 to 10.7% in 2007-2010. Globally, 10-39% and in United States 20% of general adult population is suspected to have NAFLD (6). About 3-17% of children in the United States are detected with fatty liver diseases. As expected, nearly 75% adults and 38% children from overweight/ obese BMI have NAFLD (7, 8). NAFLD is a broad spectrum liver disease ranging from preliminary hepatic steatosis to more aggressive form of nonalcoholic steatohepatitis (NASH), which in turn may lead to cirrhosis and hepatocellular carcinoma (HCC). Although pathogenesis of NAFLD is not well understood, globally accepted “two-hit hypothesis” explain the progression of disease. “First hit” is associated accumulation of lipids, especially triglycerides, in the hepatocytes cytoplasm, contributing to 5% or more of the liver weight. Although steatosis is asymptomatic and reversible, this chronic fat accumulation in liver triggers “second hit” covering various inflammatory cytokines and oxidative stress. Steatotic liver is more susceptible for low-grade inflammation and disease progression like steatohepatitis. Dyslipidemia and lipid deposition in liver are not only involved in first hit of NAFLD. Non-

esterified free fatty acids not only contribute to the steatosis, but also in hastening the progression to NASH, challenging two-hit hypothesis (9). Recent research also points towards “multi-hit theory” as opposed to two hits for pathogenesis of NAFLD- reviewed by (10). Considering the complexity of steatogenesis, necroinflammation of the hepatocytes, oxidative stress and fibrogenesis, multi-hit theory is being considered more thorough approach towards pathogenesis of NAFLD.

Because of this increasing prevalence, numerous studies are focusing on early diagnosis and treatment for NAFLD. There is no specific biochemical marker or serological test for the diagnosis of NAFLD. Liver biopsy is the gold standard for diagnosis and staging of NAFLD, particularly for the diagnosis of NASH. Due to the invasive nature of liver biopsy and risk associated with procedure, it cannot be extensively used for large-scale population. Different imaging techniques like ultrasonography (US), computed tomography (CT), magnetic resonance imaging and magnetic resonance spectroscopy have been approved as noninvasive alternative methods to detect hepatic steatosis (11, 12). Association of NAFLD with cardiovascular disease, type 2 diabetes, cirrhosis, and hepatocellular carcinoma along with difficulty in diagnosis and lack of exact therapeutic intervention for these conditions make NAFLD a serious public health concern.

There are multiple sources that contribute to the hepatic fatty acid pool. 1) Dietary TG that reach the liver as chylomicron particles from the intestine; 2) Denovo synthesis in the liver under a transcriptionally regulated process; 3) Fatty acid influx into the liver from lipolysis of adipose tissue in obese and

insulin-resistant state ; 4) diminished export of lipids from the liver in very-low-density lipoproteins; and 5) reduced oxidation of fatty acids. The accumulated fatty acids are stored in liver in the form of TG, eventually contributing to steatosis.

NAFLD pathogenesis may involve disturbances of proliferator-activated receptor alpha (Pparα) and/ or sterol regulatory element binding protein-1c (Srebp-1c), transcription factors that control enzymes responsible for oxidation and synthesis of fatty acids respectively. The regulation of lipid metabolism in liver is usually integrated with adipose tissue. Both of these organs play a very critical role in trafficking and handling of lipid based on energy status of the body (13). Hepatic triglyceride (TG) can transport to adipose tissues in\ very low-density lipoprotein where TG can store. Under hormonal regulation, fatty acids are released from adipose tissue and are transported to liver for oxidation. The control of whole body lipid homeostasis is mainly depending on efficient regulation of this cycle (14). Therefore, disturbances at one organ lipid homeostasis can have an impact on the other organ. This is why NAFLD prevalence is high in obese population, and it remains major cause of mortality and morbidity in obese people.

1.4 Environmental chemicals and adipose tissue lipid alterations. Imbalances of energy intake and energy expenditure either because of sedentary lifestyle or some genetic predisposition are well-recognized risk factors for obesity and NAFLD. However, increases in rates of health concerns like metabolic syndrome and co-ordinate increase in synthetic

chemical production, toxic burden in our air, food and water since last few of decades, it seems prudent approach to study the effects of the environmental chemicals that are found in the majority of people, in increasing obesity epidemic. It has generated significant interest of studying “nontraditional” risk factors (e.g., environmental chemicals, stress, micronutrients, gut microbiome) to the etiology of these health conditions. Moreover, because of lipophilic property of most environmental chemicals like endocrine disruptors (EDC),, adipocytes are an obvious target organ for their biological effects (15). Many bioactive EDCs predicted to bioaccumulate in lipid droplets of mature adipocyte that can be released into the systemic circulation slowly, which may results into chronic exposure of chemical (16).

Alterations in adipose tissue function can modulate EDC flux from this storage depot, thereby influencing the function of other metabolic tissues. In 2006 Blumberg and Grun postulated “environmental obesogen hypothesis” suggesting possible link between environmental contaminants and the epidemic of metabolic disease (17). Different classes of chemicals have been proposed as environmental obesogens. Some examples include endocrine disturbing chemicals (DES: diethylstilbestrol, genestein, BPA: bisphenol A and it’s derivatives), organotins (TBT: tributyltin, TPT: triphenyltin, and DBT: dibutyltin), organophosphate pesticicdes (parathion, diazinon, chlorpyrifos), phthalates (MEHP: mono-ethylhexyl phthalate, DEHP: di-2-ethylhexyl phthalate), polyfluoroalkyl chemicals (PFOA: perfluorooctanoic acid, PFNA: perfluorononanoic acid, PFOS: perfluorooctane sulfonic acid, and PFHxS:

perfluorohexane sulfonic acid), polybrominated diphenyl ethers(PBDE), persistent organic pollutant (non-dioxin PCBs, HCB: Hexachlorobenzene , DDE: dichlorodiphenyldichloroethylene). Human get exposed to these chemicals on routine basis either through occupational or non-occupational means. Food, water, air contamination is the most common route of exposure. Some chemicals get into food by leaching out of products that food and beverages are stored. A prime example is BPA, which is used in polycarbonate reusable food and beverage storage containers and the resin lining of cans, which can lead to substantial levels of human exposure. PFAs are stain repellent, and also used in firefighting foams, whereas PBDEs are primarily used in flame retardant applications for manufacturing household rugs, carpets, non-stick utensils and so on (18-21). Although actual acute exposure of chemicals may be at nanomolar or lower concentrations, persistent exposure through these routes cannot be ignored.

In order to assess environmental xenobiotic induced obesogenic effects, numerous in-vivo as well as in-vitro approaches have been employed. Many population epidemiological studies have identified intriguing link between environmental chemical levels in biological fluids and metabolic syndrome parameters. Importantly, although these human correlation studies provide valuable information in predicting the risk associated with xenobiotic exposure, precise mechanisms for underlying effects remain largely unknown. Table 1 summarizes representative human correlation studies which associate serum, urinary, or tissue specific levels of xenobiotic with obesity parameters including

BMI, waist circumference, body weight, plasma insulin, leptin levels, systemic inflammation and so on (22-31). Majority of these data are gathered from participants of the National Health and Nutrition Examination Surveys (NHANES).

3T3L-1 murine preadipocyte, adipocyte or bone barrow derived mesenchymal stem cells (hADSC, mADSC), are most commonly used in-vitro model for studying effect environmental chemicals on adipogenesis. Through in-vitro studies, these chemicals are tested for its potential effect on adipogenic differentiation and increasing number of fat cells in body. Alteration of frequency with which MSCs are induced into adipogenic lineage to form preadipocyte and the rate of differentiation of preadipocytes to adipocyte upon exposure of these chemicals have been considered as one the possible mechanism for their obesogenic nature. Table 2 enlists in-vitro studies of chemicals tested for their adipogenesis potential (32-41).

For specific chemical induced obesogenic effects, in-vivo studies are also conducted. Food intake, energy expenditure by using metabolic cages, body weight, visceral and subcutaneous adipose tissue weight are some of the end point considered while designing these in-vivo experiments. Considering adipose tissue as an endocrine organ, serum leptin, adiponectin, cytokine levels are also considered as markers of adipose tissue hypertrophy or hyperplasia. Moreover, physiological consequences of the lipid accumulation including insulin resistance, glucose tolerance, urinary glucose elimination,

serum insulin levels, blood glucose levels, and serum lipid levels are measured as advanced markers of obesity.

1.5 Environmental chemicals and hepatic lipid alterations. Liver is the primary line of defense against potentially harmful xenobiotic therefore that is target organ, most commonly affected by environmental chemicals. Attributing to the relevance of environmental contaminants in inducing NAFLD in recent years, term toxicants associated fatty liver diseases (TAFLD) and it's sever form toxicants associated steatohepatitis (TASH) were coined (42). As reviewed by Kneeman some of the xenobiotics like amiodarone, methotrexate, tamoxifen and corticosteroids are implicated as possible contributing factors to cause NAFLD (43). The effect of numerous environmental/ industrial chemicals enlisted by The Toxicological Reference Database (ToxRefDB, EPA) and Chemical Effects in Biological Systems (CEBS, National Toxicology Program) were studied for liver effects. Hundreds of chemicals including toxic heavy metals (lead, mercury, cadmium, chromium), industrial chemicals include organoclorine pesticides DDT and dieldrin, perfluolochemicals, brominated fire retardants, PCBs, polyaromatic hyrocarbons, polychlorinated and polybrominated diaxins and furans, polychlorinated naphthalenes, fungicides, insecticides, biphenyls/dioxins, TCDD have potential to modify fat metabolism in liver, and hence elevating the susceptibility to NAFLD (44, 45).

Although lots of chemicals have been suspected for their ability to induce fatty liver independently of obesity, very few have been examined in-vivo. Table 5

enlists chemicals which have been tested in in-vitro as well as in-vivo, and human correlation studies for their NAFLD inducing abilities.

As mentioned earlier, diagnosis of NAFLD is difficult and non-invasive methods are not as reliable as biopsy, prevalence of NAFLD may be higher than anticipated. As listed in table 5, environmental chemicals contribute to the epidemic of the NAFLD, and unless disease progresses to advanced stages, diagnosis is difficult, this points towards importance of the mechanistic investigation of these environmental chemical induced effects. Few markers used in in-vivo studies for NAFLD include hepatic and serum TG, free fatty acid levels and oil red o staining of the frozen liver sections. Environmental NAFLD warrants detailed mechanism based, and biomarker research in order to better predict the prevalence in the population.

1.6 Mechanisms of the environmental chemical induced lipid disturbances. Molecular mechanisms of these environmental exposure induced dyslipidemia are largely unknown. Some of these chemicals are structural ligands of lipogenic transcription factors whereas some other chemicals like EDC interact of with hormone receptors and they mimic endogenous hormones and thus disturb the programming of endocrine signaling pathways and thus adipose tissue biology (46). TBT is a Ppar-γ ligand and thus stimulate adipogenesis. Because of having long carbon chain in their structure, PFAs mimic fatty acid structures and bind to Ppar-α (47). Phenylsulfamide and fungicide tolylfluanid mimic the action of endogenous glucocorticoids and function as a glucocorticoids agonist and augment

adipogenesis in 3T3-L1 preadipocytes (48).

Owing to the rising prevalence of the childhood obesity and NAFLD, nutrition and exposure to environmental chemicals during critical early life development are newly emerging etiological factors of metabolic syndrome (49). From biomonitoring studies, several environmental chemicals that can cause obesity in offspring because of gestational exposure were found in humans (49, 50). Increasing evidences are being generated from animal studies of in-utero exposure to relevant exposure levels of xenobiotics contributing to increase in parameters of obesity/ NAFLD (summarized in tables 3, 4 and 5) (45, 51-68).

From the mechanistic point of view, it is likely that gene-environment interactions and epigenetic modification of gene functions by alteration of DNA methylation, histone acetylation, and chromatin remodeling that results in genetic reprogramming (69). These epigenetic alterations during a vulnerable window of development usually result in non-reversible changes in tissue structure and function. These changes make body sensitize or programmed eventually lead to increases incidences of variety of diseases later in life. This hypothesis also referred as “fetal basis of adult diseases” (69).

For obesogenic compounds, few recent investigations link early epigenetic reprogramming of the adipogenic process to the incidence of obesity in adult life (37, 70).

1.7 Conclusion: Rising prevalence of dyslipidemic disorders suggests etiological factors beyond traditional lifestyle and genetic predisposition.

Obesity and NAFLD increase risk of cardiometabolic diseases, as evident from overlapping population prevalence. Moreover treatment of NAFLD is also a concern, as currently there are barely any therapies available in market targeting specifically on NAFLD/ NASH in people. Ongoing pharmaceutical research on these therapies is also constantly challenged by difficulty of diagnosis and unreliable non-invasive tools (71).

Based on research from government agencies, and also academic findings, few of the manufacturing chemicals have been banned for use in some countries, however, majority of chemicals listed in this review remain in industrial use. Also, the replacement chemicals being investigated for manufacturing use seem to have similar structural and chemical profiles, indicating real possibility of these new chemicals also not being risk-free. Another issue with few such environmental chemicals is their prolonged half-life in nature as well as inside the living system. PFAs exemplify bioaccumulating chemicals that are not degraded to inactive form for years in the food chain (72). Overall, rising awareness about environmental chemical exposure contribution to the epidemic of obesity/ NAFLD seems imperative.

More studies are necessary for thorough mechanistic investigation of these environmental origins of the childhood and adulthood diseases, so that preventive or therapeutic approaches can be guided.

1.8 REFERENCES:

1. Ogden CL, Carroll MD, Kit BK, Flegal KM. Prevalence of obesity among adults: United States, 2011-2012. NCHS Data Brief 2013:1-8.

2. Ogden CL, Carroll MD, Flegal KM. Prevalence of obesity in the United States. Jama 2014;312:189-190.

3. Hirsch J, Batchelor B. Adipose tissue cellularity in human obesity. Clin Endocrinol Metab 1976;5:299-311.

4. Kershaw EE, Flier JS. Adipose tissue as an endocrine organ. J Clin Endocrinol Metab 2004;89:2548-2556.

5. Tang QQ, Otto TC, Lane MD. CCAAT/enhancer-binding protein beta is required for mitotic clonal expansion during adipogenesis. Proc Natl Acad Sci U S A 2003;100:850-855.

6. Patrick L. Nonalcoholic fatty liver disease: relationship to insulin sensitivity and oxidative stress. Treatment approaches using vitamin E, magnesium, and betaine. Altern Med Rev 2002;7:276-291.

7. Schwimmer JB, Pardee PE, Lavine JE, Blumkin AK, Cook S. Cardiovascular risk factors and the metabolic syndrome in pediatric nonalcoholic fatty liver disease. Circulation 2008;118:277-283.

8. Verrijken A, Francque S, Mertens I, Talloen M, Peiffer F, Van Gaal L. Visceral adipose tissue and inflammation correlate with elevated liver tests in a cohort of overweight and obese patients. Int J Obes (Lond) 2010;34:899-907.

9. Gentile CL, Pagliassotti MJ. The role of fatty acids in the development and progression of nonalcoholic fatty liver disease. J Nutr Biochem 2008;19:567-576.

10. Charlton M. Noninvasive indices of fibrosis in NAFLD: starting to think about a three-hit (at least) phenomenon. Am J Gastroenterol 2007;102:409-411.

11. Chalasani N, Younossi Z, Lavine JE, Diehl AM, Brunt EM, Cusi K, Charlton M, et al. The diagnosis and management of non-alcoholic fatty liver disease: practice Guideline by the American Association for the Study of Liver Diseases, American College of Gastroenterology, and the American Gastroenterological Association. Hepatology 2012;55:2005-2023.

12. Koplay M, Sivri M, Erdogan H, Nayman A. Importance of imaging and recent developments in diagnosis of nonalcoholic fatty liver disease. World J Hepatol 2015;7:769-776.

13. Solinas G, Boren J, Dulloo AG. De novo lipogenesis in metabolic homeostasis: More friend than foe? Mol Metab 2015;4:367-377.

14. Fuchs CD, Claudel T, Trauner M. Role of metabolic lipases and lipolytic metabolites in the pathogenesis of NAFLD. Trends Endocrinol Metab 2014;25:576-585.

15. Mullerova D, Kopecky J. White adipose tissue: storage and effector site for environmental pollutants. Physiol Res 2007;56:375-381.

16. Tonnelier A, Coecke S, Zaldivar JM. Screening of chemicals for human bioaccumulative potential with a physiologically based toxicokinetic model. Arch Toxicol 2012;86:393-403.

17. Grun F, Blumberg B. Environmental obesogens: organotins and endocrine disruption via nuclear receptor signaling. Endocrinology 2006;147:S50-55.

18. Fromme H, Albrecht M, Appel M, Hilger B, Volkel W, Liebl B, Roscher E. PCBs, PCDD/Fs, and PBDEs in blood samples of a rural population in South Germany. Int J Hyg Environ Health 2015;218:41-46.

19. Fromme H, Becher G, Hilger B, Volkel W. Brominated flame retardants - Exposure and risk assessment for the general population. Int J Hyg Environ Health 2015.

20. Fromme H, Schutze A, Lahrz T, Kraft M, Fembacher L, Siewering S, Burkardt R, et al. Non-phthalate plasticizers in German daycare centers and human biomonitoring of DINCH metabolites in children attending the centers (LUPE 3). Int J Hyg Environ Health 2015.

21. Vestergren R, Cousins IT. Tracking the pathways of human exposure to perfluorocarboxylates. Environ Sci Technol 2009;43:5565-5575.

22. Bhandari R, Xiao J, Shankar A. Urinary bisphenol A and obesity in U.S. children. Am J Epidemiol 2013;177:1263-1270.

23. Trasande L, Attina TM, Blustein J. Association between urinary bisphenol A concentration and obesity prevalence in children and adolescents. Jama 2012;308:1113-1121.

24. Li DK, Miao M, Zhou Z, Wu C, Shi H, Liu X, Wang S, et al. Urine bisphenol-A level in relation to obesity and overweight in school-age children. PLoS One 2013;8:e65399.

25. Wang HX, Zhou Y, Tang CX, Wu JG, Chen Y, Jiang QW. Association between bisphenol A exposure and body mass index in Chinese school children: a cross-sectional study. Environ Health 2012;11:79.

26. Savastano S, Tarantino G, D'Esposito V, Passaretti F, Cabaro S, Liotti A, Liguoro D, et al. Bisphenol-A plasma levels are related to inflammatory markers, visceral obesity and insulin-resistance: a cross-sectional study on adult male population. J Transl Med 2015;13:169.

27. Pereira-Fernandes A, Dirinck E, Dirtu AC, Malarvannan G, Covaci A, Van Gaal L, Vanparys C, et al. Expression of obesity markers and Persistent Organic Pollutants levels in adipose tissue of obese patients: reinforcing the obesogen hypothesis? PLoS One 2014;9:e84816.

28. Hatch EE, Nelson JW, Qureshi MM, Weinberg J, Moore LL, Singer M, Webster TF. Association of urinary phthalate metabolite concentrations with body mass index and waist circumference: a cross-sectional study of NHANES data, 1999-2002. Environ Health 2008;7:27.

29. Oktar S, Sungur S, Okur R, Yilmaz N, Ustun I, Gokce C. The relationship between phthalates and obesity: serum and urinary concentrations of phthalates. Minerva Endocrinol 2015.

30. Trasande L, Attina TM, Sathyanarayana S, Spanier AJ, Blustein J. Race/ethnicity-specific associations of urinary phthalates with childhood body mass in a nationally representative sample. Environ Health Perspect 2013;121:501-506.

31. Yaghjyan L, Sites S, Ruan Y, Chang SH. Associations of urinary phthalates with body mass index, waist circumference and serum lipids among females: National Health and Nutrition Examination Survey 1999-2004. Int J Obes (Lond) 2015;39:994-1000.

32. Grun F, Watanabe H, Zamanian Z, Maeda L, Arima K, Cubacha R, Gardiner DM, et al. Endocrine-disrupting organotin compounds are potent inducers of adipogenesis in vertebrates. Mol Endocrinol 2006;20:2141-2155.

33. Inadera H, Shimomura A. Environmental chemical tributyltin augments adipocyte differentiation. Toxicol Lett 2005;159:226-234.

34. Kanayama T, Kobayashi N, Mamiya S, Nakanishi T, Nishikawa J. Organotin compounds promote adipocyte differentiation as agonists of the peroxisome proliferator-activated receptor gamma/retinoid X receptor pathway. Mol Pharmacol 2005;67:766-774.

35. Watt J, Schlezinger JJ. Structurally-diverse, PPARgamma-activating environmental toxicants induce adipogenesis and suppress osteogenesis in bone marrow mesenchymal stromal cells. Toxicology 2015;331:66-77.

36. Kirchner S, Kieu T, Chow C, Casey S, Blumberg B. Prenatal exposure to the environmental obesogen tributyltin predisposes multipotent stem cells to become adipocytes. Mol Endocrinol 2010;24:526-539.

37. Bastos Sales L, Kamstra JH, Cenijn PH, van Rijt LS, Hamers T, Legler J. Effects of endocrine disrupting chemicals on in vitro global DNA methylation and adipocyte differentiation. Toxicol In Vitro 2013;27:1634-1643.

38. Li X, Pham HT, Janesick AS, Blumberg B. Triflumizole is an obesogen in mice that acts through peroxisome proliferator activated receptor gamma (PPARgamma). Environ Health Perspect 2012;120:1720-1726.

39. Kamstra JH, Hruba E, Blumberg B, Janesick A, Mandrup S, Hamers T, Legler J. Transcriptional and epigenetic mechanisms underlying enhanced in vitro adipocyte differentiation by the brominated flame retardant BDE-47. Environ Sci Technol 2014;48:4110-4119.

40. Ferrante MC, Amero P, Santoro A, Monnolo A, Simeoli R, Di Guida F, Mattace Raso G, et al. Polychlorinated biphenyls (PCB 101, PCB 153 and PCB 180) alter leptin signaling and lipid metabolism in differentiated 3T3-L1 adipocytes. Toxicol Appl Pharmacol 2014;279:401-408.

41. Nakao T, Akiyama E, Kakutani H, Mizuno A, Aozasa O, Akai Y, Ohta S. Levels of tetrabromobisphenol A, tribromobisphenol A, dibromobisphenol A, monobromobisphenol A, and bisphenol a in Japanese breast milk. Chem Res Toxicol 2015;28:722-728.

42. Wahlang B, Beier JI, Clair HB, Bellis-Jones HJ, Falkner KC, McClain CJ, Cave MC. Toxicant-associated steatohepatitis. Toxicol Pathol 2012;41:343-360.

43. Kneeman JM, Misdraji J, Corey KE. Secondary causes of nonalcoholic fatty liver disease. Therap Adv Gastroenterol 2012;5:199-207.

44. Al-Eryani L, Wahlang B, Falkner KC, Guardiola JJ, Clair HB, Prough RA, Cave M. Identification of Environmental Chemicals Associated with the Development of Toxicant-associated Fatty Liver Disease in Rodents. Toxicol Pathol 2014;43:482-497.

45. Wahlang B, Beier JI, Clair HB, Bellis-Jones HJ, Falkner KC, McClain CJ, Cave MC. Toxicant-associated steatohepatitis. Toxicol Pathol 2013;41:343-360.

46. Regnier SM, Kirkley AG, Ye H, El-Hashani E, Zhang X, Neel BA, Kamau W, et al. Dietary exposure to the endocrine disruptor tolylfluanid promotes global metabolic dysfunction in male mice. Endocrinology 2015;156:896-910.

47. Elcombe CR, Elcombe BM, Foster JR, Chang SC, Ehresman DJ, Butenhoff JL. Hepatocellular hypertrophy and cell proliferation in Sprague-Dawley rats from dietary exposure to potassium perfluorooctanesulfonate

results from increased expression of xenosensor nuclear receptors PPARalpha and CAR/PXR. Toxicology 2012;293:16-29.

48. Neel BA, Brady MJ, Sargis RM. The endocrine disrupting chemical tolylfluanid alters adipocyte metabolism via glucocorticoid receptor activation. Mol Endocrinol 2013;27:394-406.

49. Ashley-Martin J, Dodds L, Arbuckle TE, Ettinger AS, Shapiro GD, Fisher M, Morisset AS, et al. A birth cohort study to investigate the association between prenatal phthalate and bisphenol A exposures and fetal markers of metabolic dysfunction. Environ Health 2014;13:84.

50. Heggeseth B, Harley K, Warner M, Jewell N, Eskenazi B. Detecting Associations between Early-Life DDT Exposures and Childhood Growth Patterns: A Novel Statistical Approach. PLoS One 2015;10:e0131443.

51. Valvi D, Mendez MA, Garcia-Esteban R, Ballester F, Ibarluzea J, Goni F, Grimalt JO, et al. Prenatal exposure to persistent organic pollutants and rapid weight gain and overweight in infancy. Obesity (Silver Spring) 2014;22:488-496.

52. Valvi D, Mendez MA, Martinez D, Grimalt JO, Torrent M, Sunyer J, Vrijheid M. Prenatal concentrations of polychlorinated biphenyls, DDE, and DDT and overweight in children: a prospective birth cohort study. Environ Health Perspect 2012;120:451-457.

53. Warner M, Wesselink A, Harley KG, Bradman A, Kogut K, Eskenazi B. Prenatal exposure to dichlorodiphenyltrichloroethane and obesity at 9 years of age in the CHAMACOS study cohort. Am J Epidemiol 2014;179:1312-1322.

54. Karmaus W, Osuch JR, Eneli I, Mudd LM, Zhang J, Mikucki D, Haan P, et al. Maternal levels of dichlorodiphenyl-dichloroethylene (DDE) may increase weight and body mass index in adult female offspring. Occup Environ Med 2009;66:143-149.

55. Valvi D, Casas M, Mendez MA, Ballesteros-Gomez A, Luque N, Rubio S, Sunyer J, et al. Prenatal bisphenol a urine concentrations and early rapid growth and overweight risk in the offspring. Epidemiology 2013;24:791-799.

56. Harley KG, Aguilar Schall R, Chevrier J, Tyler K, Aguirre H, Bradman A, Holland NT, et al. Prenatal and postnatal bisphenol A exposure and body mass index in childhood in the CHAMACOS cohort. Environ Health Perspect 2013;121:514-520.

57. Braun JM, Lanphear BP, Calafat AM, Deria S, Khoury J, Howe CJ, Venners SA. Early-life bisphenol a exposure and child body mass index: a prospective cohort study. Environ Health Perspect 2014;122:1239-1245.

58. Miyawaki J, Sakayama K, Kato H, Yamamoto H, Masuno H. Perinatal and postnatal exposure to bisphenol a increases adipose tissue mass and serum cholesterol level in mice. J Atheroscler Thromb 2007;14:245-252.

59. Somm E, Schwitzgebel VM, Toulotte A, Cederroth CR, Combescure C, Nef S, Aubert ML, et al. Perinatal exposure to bisphenol a alters early adipogenesis in the rat. Environ Health Perspect 2009;117:1549-1555.

60. Faulk C, Barks A, Sanchez BN, Zhang Z, Anderson OS, Peterson KE, Dolinoy DC. Perinatal lead (Pb) exposure results in sex-specific effects on food intake, fat, weight, and insulin response across the murine life-course. PLoS One 2014;9:e104273.

61. Branchi I, Alleva E, Costa LG. Effects of perinatal exposure to a polybrominated diphenyl ether (PBDE 99) on mouse neurobehavioural development. Neurotoxicology 2002;23:375-384.

62. Suvorov A, Battista MC, Takser L. Perinatal exposure to low-dose 2,2',4,4'-tetrabromodiphenyl ether affects growth in rat offspring: what is the role of IGF-1? Toxicology 2009;260:126-131.

63. Cave M, Appana S, Patel M, Falkner KC, McClain CJ, Brock G. Polychlorinated biphenyls, lead, and mercury are associated with liver disease in American adults: NHANES 2003-2004. Environ Health Perspect 2010;118:1735-1742.

64. Lv Z, Li G, Li Y, Ying C, Chen J, Chen T, Wei J, et al. Glucose and lipid homeostasis in adult rat is impaired by early-life exposure to perfluorooctane sulfonate. Environ Toxicol 2013;28:532-542.

65. Wan HT, Zhao YG, Wei X, Hui KY, Giesy JP, Wong CK. PFOS-induced hepatic steatosis, the mechanistic actions on beta-oxidation and lipid transport. Biochim Biophys Acta 2012;1820:1092-1101.

66. Bijland S, Rensen PC, Pieterman EJ, Maas AC, van der Hoorn JW, van Erk MJ, Havekes LM, et al. Perfluoroalkyl sulfonates cause alkyl chain length-dependent hepatic steatosis and hypolipidemia mainly by impairing lipoprotein production in APOE*3-Leiden CETP mice. Toxicol Sci 2011;123:290-303.

67. Zuo Z, Chen S, Wu T, Zhang J, Su Y, Chen Y, Wang C. Tributyltin causes obesity and hepatic steatosis in male mice. Environ Toxicol 2011;26:79-85.

68. Chamorro-Garcia R, Sahu M, Abbey RJ, Laude J, Pham N, Blumberg B. Transgenerational inheritance of increased fat depot size, stem cell reprogramming, and hepatic steatosis elicited by prenatal exposure to the obesogen tributyltin in mice. Environ Health Perspect 2013;121:359-366.

69. Heindel JJ, vom Saal FS. Role of nutrition and environmental endocrine disrupting chemicals during the perinatal period on the aetiology of obesity. Mol Cell Endocrinol 2009;304:90-96.

70. Stel J, Legler J. The Role of Epigenetics in the Latent Effects of Early Life Exposure to Obesogenic Endocrine Disrupting Chemicals. Endocrinology 2015;156:3466-3472.

71. Satapathy SK, Kuwajima V, Nadelson J, Atiq O, Sanyal AJ. Drug-induced fatty liver disease: An overview of pathogenesis and management. Ann Hepatol 2015;14:789-806.

72. Numata J, Kowalczyk J, Adolphs J, Ehlers S, Schafft H, Fuerst P, Muller-Graf C, et al. Toxicokinetics of seven perfluoroalkyl sulfonic and carboxylic acids in pigs fed a contaminated diet. J Agric Food Chem 2014;62:6861-6870.

1.9 TABLES:

Table 1: Human cohort studies correlating environmental chemical levels with obesity parameters

Chemical	Study design	Outcome	Ref
BPA	NHANES cross-sectional children age 6-19 yrs	Positive correlation between urinary BPA (median 2.9ng/mL) and obesity prevalence.	22, 23
BPA	School age children (1326 students in grades 4-12), urinary BPA measurement	BPA urinary level associated increased risk of heavy weight among girls of age 9-12 with gender differences in result	24, 25
BPA	Male adults, Caucasian, cross-sectional study	Plasma BPA levels associated with waist circumference, and risk factors for metabolic syndrome (inflammation, triglyceride, glucose intolerance)	26
Persistent organic pollutants (POPs)	Prospective study with adult obese subjects conducted at weights managements clinic on Antwerp University Hospital	Gender specific association of POPs concentration in adipose tissue and adiponectin levels on blood, significant correlation with gene expression of obesity marker genes	27
Phthalate metabolites	NHANES, 6-19 yrs	Positive correlation to obesity, in non-hispanic black population	28
Phthalate metabolites	Overweight and obese individuals	Positive correlation total serum and urinary phthalates levels and BMI	29
Phthalate metabolites	Cross sectional study of women and men more than 18 years of age	Urinary phthalates associated with BMI, waist circumferences and serum lipids	30, 31

Table 2: In-vitro studies linking environmental chemicals to adipose tissue lipid accumulation

Chemical	Study design	Outcome	Published mechanism	Ref
Tributyltin (TBT)	Murine 3T3L-1 preadipocytes	TBT promoted differentiation of preadiocyte, in absence of adipogenic sensitizing cocktail	None	32-34
TBT	Mouse bone barrow mesenchymal stem cells	Increased activity of Ppar-γ, increased adipogenesis, lipid accumulation and Fabp4	None	35
TBT	Human and mouse adipose-derived stromal stem cells	Increased adipogenesis, cellular lipid content and expression of adipogenic gene	Activation of Ppar-γ	36
TBT	Adipose derived stromal cell retrieved from animal exposed in-utero	Sensitized multipotent stem cells to undergo adipogenesis	Epigenetic alterations in the methylation status of the CpG islands of Fabp4 and Ppar-γ	36
Triphenyltin (TPT)	Murine 3T3L1 preadipocytes	Increase adipogenesis, lipid deposition, lipogenic gene expression	As ligand and activation of Ppar-γ and RXR transcription factors	34
TPT	Mouse bone barrow mesenchymal stem cells	Increased adipogenesis	None	35

Table 2 continued: In-vitro studies linking environmental chemicals to adipose tissue lipid accumulation

Chemical	Study design	Outcome	Published mechanism	Ref
Triflumizole (TFZ)	3T3L1, human mesenchymal stromal stem cells (MSCs)	Induced adipogenic differentiation	None	37
BDE-47 (Polybrominated biphenyls)	Mouse 3T3-L1 preadipocytes	Increase adipocyte differentiation	Hypomethylation of Ppar-γ2 promoter	38, 39
Polychlorinated biphenyls (PCBs)	Mouse 3T3-L1 preadipocytes	Increase lipid content, leptin gene expression and reduction in leptin receptor and signaling	None	40
Phthalate metabolites	Mouse bone barrow mesenchyal stem cells	Increased expression of Ppar- γ, increased adipogensis, lipid accumulation and Fabp4	None	35
Tetrabromobisphenol-a, (TBBPA)	Mouse bone marrow mesenchyal stem cells	Increases activity of ppar-g, increased adipogensis, lipid accumulation and Fabp4	None	35
TBBPA	Japanese women, breast milk analysis	TBBPA and its debrominated congeners accumulate in breast milk, and affect 3T3-L1 differentiation in-vitro	None	41

Table 3: Human correlation studies linking early life exposure of environmental chemicals to obesity outcomes

Chemical	Study design	Outcome	Ref
Persistent organic pollutants (POPs)	Maternal serum measurement at 1st trimester	DDE, HCB serum level were positively associated with postnatal growth until 6 month and overweight at age of 14 month old offsprings	51
POPs	Mass index, obesity, waist circumference, and percentage of body fat in 9-year-old children	Positive correlation DDT and increased waist circumference in boys not in girls at the age of 9	53
POPs	Pregnant women form Michigan fish eater cohort	Weight and BMI of daughters of age 20-50 years significantly associated with maternal DDE	54
BPA	BPA measurement from urinary samples from mother at 1st trimester and 3rd trimester	At the 4 years of age, BPA showed association with increased Waist circumferences, not associated with obesity related outcomes. 25% overweight at age of 14 month and 21 % at age of 4 years	55
BPA	CHAMACOS cohort study, urinary BPA level from pregnant mother and from children at 5 and 9 years of age	Mother urinary BPA concentration associated with increased BMI, body fat and overweight and obesity among their daughters at age of 9 years in girls but not in boys. BPA concentration at 9 years positively correlate with all these parameters both in boys and girls	56
BPA	Urinary BPA concentration in second and third trimester in pregnant women and from their children at age of 1 and 2 years.	Mother and early childhood BPA not associated with BMI both in girls and boys at age of 2-5 years. Early childhood BPA concentration associated with growth acceleration	57

Table 4: Rodent developmental exposure to environmental chemicals and obesity studies

Chemical	Study design	Outcome	Ref
BPA	Perinatal and prenatal exposure of BPA-1ug/ml and 10ug/ml through drinking water. BW, adipose tissue weight measured in the offspring at PND 31	BW and adipose tissue weight increased both in male and female offspring	58
BPA	Sprague-Dawley rats. Perinatal BPA exposure (1mg/L BPA) through drinking water from G6 to through lactation.	At weaning age (PND21), increased pWAT weight and increased expression of lipogenic genes both in adipose tissue and liver.	59
Lead	Perinatal exposure (before mating through lactation though drinking water) to mice. At the age of 3,6 and 9 months of the offspring food intake	Body weight increased only male. Total body fat and other physiological effect vary according to sex and age. Obesity related phenotype observed in adulthood.	60
PCB mixture Aroclor 1254	Developmental exposure to mice	Increased body weight of mouse pups on post natal days 16-20	61
PBDEs-47	Pre and postnatal exposure to rats	Increased Body weight from birth to puberty in pups	62

Table 5: Studies linking environmental chemical exposure to NAFLD

Chemical	Study design	Outcomes	Ref
PCBs In-vivo	Male mice fed with control or HFD with PCB 153 exposure	PCB153 had minimal effect in control fed diet. In HFD mice showed increased visceral adiposity, hepatic steatosis plasma cytokines	45
PCBs Human correlation	Adult participants NHANES study 2003-2004	Elevated serum ALT level, as proxy marker of NAFLD	63
Perfluorooctane sulfonate (PFOS)	Pregnant rats exposed to PFOS from exposure (GD0 to PND21)	Hepatic steatosis and increases fat pad weight observed in offspring in adulthood	64
PFOS	C57Bl/6 mice	Accumulation of fatty acids and Triglyceride in hepatocyte with significantly reduction in mitochondrial β-oxidation	65, 66
Tributyltin (TBT)	Transgenerational study in mice. Hepatic steatosis phenotype was studied in F1, F2 and F3 generation	Prenatal TBT exposure led to hepatic lipid accumulation and up-regulated hepatic expression of genes involved in lipid storage/transport, lipogenesis, and lipolysis in all three subsequent generations.	67
TBT	Low doses (0.5, 5, and 50μg/kg) exposure to male mice	Induced hepatic steatosis and insulin, leptin resistance	68

MANUSCRIPT 2

EPIGENETIC MODULATION OF NRF2 AND LIPOGENIC GENES BY PNPP EXPOSURE OF BISPHENOL A IS ASSOCIATED WITH HEPATIC STEATOSIS IN FEMALE MICE

Prajakta C Shimpi[1], Maneesha Paranjpe[2], Vijay More[1], Ajay Donepudi[1], Jaclyn M. Goodrich[4], Michael Skinner[3], Dana C Dolinoy[4], Beverly Rubin[2], Angela Slitt[1]

[1]Biomedical and Pharmaceutical Sciences, University of Rhode Island, Kingston RI, USA; [2]Sackler School of Graduate Biomedical Sciences, Tufts University, Boston MA, USA; [3]School of Biological Sciences, Washington State University, Pullman, WA, USA; [4]Department of Environmental Health Sciences, University of Michigan School of Public Health, Ann Arbor, MI USA

Manuscript prepared for submission to "*Hepatology*"

2.1 ABSTRACT

Bisphenol A (BPA) is chemical used in manufacturing of consumer products containing polycarbonate and epoxy resins. In humans, urinary BPA levels have been positively associated with general and abdominal obesity, with increased adverse liver effects described in children. Rodent studies have demonstrated increased hepatic lipid accumulation after developmental BPA exposure. Nuclear Factor E2-Related Factor 2 (Nrf2) has been recently shown to be a possible contributor to hepatic lipid accumulation. It was hypothesized that epigenetic changes occur before BPA-induced steatosis, possibility via induction of Nrf2 expression. Pregnant CD-1 mice were administered 25μg BPA/kg/day via osmotic pump, and then after weaning on postnatal day 21, the resulting daughters were exposed to BPA via drinking water until PND 35. Tissues were collected at postnatal day 32 (Week 5) and 39 weeks of age and mRNA and protein expression profiling was performed. BPA increased hepatic lipid content along with increased pro-lipogenic enzyme mRNA and protein expression and induction of Nrf2 protein expression at week 39. Transcription factor binding was assayed in liver by chromatin immunoprecipitation (ChIP) and result showed at week 5 and week 39 , BPA exposure increased Nrf2 binding to a putative ARE consensus sequence in the Srebp-1c promoter. Known Nrf2 activators increased Srebp-1c promoter reporter activity in HepG2 cells. Effect on gene specific and CpG site specific DNA methylation modification of was assesses by immunoprecipation and pyrosequencing respectively. Hypomethylation of the Nrf2 and Srebp-1c promoters was observed in livers from offspring that were

developmentally exposed to BPA. Overall, the work herein presents new findings that developmental BPA exposure induces fat accumulation via hypomethylation of key lipogenic genes and promotes Nrf2 binding to the Srebp-1c promoter.

Keywords: BPA, NAFLD, Nrf2, methylation, Srebp-1c, epigenetic

Abbreviations: Acetyl CoA carboxylase, Acc; antioxidant response element, ARE; β2-microglobulin, B2M; Bisphenol A, BPA; chromatin immunoprecipitation, ChIP; fatty acid synthase, Fas; gestational day, GD; glycerol 3 phosphate acetyl transferase, Gpat; glutamate cysteine ligase, Gclc; methylated DNA immunoprecipitation, MeDIP; nonalcoholic fatty liver disease, NAFLD; Nuclear factor E2 related factor 2, Nrf2; oil red o, ORO; peroxisome proliferated activated receptor, Ppar; phosphate buffered saline, PBS; postnatal day, PND; perinatal peripubertal, PNPP; sterol regulatory element binding protein 1c, Srebp-1c; tris-buffered saline, TBS

2.2 INTRODUCTION

Nonalcoholic fatty liver disease (NAFLD) is a broad-spectrum liver disorder. American Association for Liver Diseases guidelines define NAFLD as the presence of hepatic steatosis with no evidence of hepatocellular injury in the form of ballooning of the hepatocytes (1). In past two decades, NAFLD prevalence has risen in adults and children, with suspected NAFLD having increased from 3.9% in 1988-1994 to 10.7% in 2007-2010 (2). In addition to more accepted risk factors such as obesity, energy imbalance, and sedentary lifestyle (3), drugs and chemicals of environmental exposure have also been implicated in increasing predisposition to NAFLD. Multiple classes of chemicals of environmental exposure including pesticides, insecticides, dioxins, and polychlorinated biphenyls (PCBs) are potential modifiers of fat metabolism in liver, and are suspected to increase the risk for developing NAFLD (4, 5).

Specifically, exposure to Bisphenol A (BPA), a plastics component used in manufacturing of polycarbonate and epoxy resins containing plastic bottles, food containers, metal cans, and thermal receipts has been recently associated with NAFLD (6, 7). BPA exposure is ubiquitous, and it was detected in more than 90% of the urine samples from the US population (8). BPA has also been detected in human breast milk, amniotic fluid and cord blood samples, which demonstrates the potential for fetal and neonatal exposure (9-11). A positive correlation between urinary BPA levels and obesity risk has been reported in adults and children, especially in adolescent females (12). Recently, increased markers for NAFLD were positively

associated with urine BPA levels in a small cohort of children (13). Therefore, there is growing health concern for early-life BPA exposure that has not been fully addressed (14). In rodents, perinatal BPA exposure increased hepatic lipid content and lipogenic gene expression, along with imbalance in adipokine levels and insulin signaling disturbances in female offspring during adolescence and adulthood (15-17). The mechanisms by which BPA induces fat accumulation are largely undescribed, but likely involve induction of lipogenesis through both direct (6) and epigenetic mechanisms (18).

Epigenetic mechanisms, such as DNA methylation and histone modifications contribute to NAFLD (19-21). DNA methylation patterns and lipogenic gene expression has been correlated in liver biopsy tissues from NAFLD patients (22). Induction of fatty liver via a high-fat, high-sucrose diet was associated with hypomethylation at some CpG sites and increased transcripts for lipogenic proteins, such as sterol regulatory element binding protein 1c (Srebp-1c) and glycerol-3-phosphate dehydrogenase (Gpat) (23). Similarly, hypomethylation at specific CpG sites of the Fatty acid synthase (Fas) promoter was induced by short-term or long-term high fat diet feeding and correlated with up-regulation of Fas expression (24, 25). The mechanism by which induction of Srebp1-c in rodents with early-life exposure to BPA has not been elucidated, and it is hypothesized that it could also occur through promoter hypomethylation (7).

Nuclear factor E2 related factor 2 (Nrf2) functions primarily as an antioxidant defense system of the cell. Recently, Nrf2 has been linked to adipose

differentiation and lipid homeostasis- reviewed by (26). Our previous work suggests positive regulation of Nrf2 on hepatic lipid accumulation. In leptin-deficient ob/ob mice, constitutive activation of Nrf2, by means of Keap1 knockdown, enhanced hepatic steatosis (27). Also, hepatic lipid deposition and glucose tolerance worsened in Keap1 knockdown mice subjected to long-term high fat diet challenge (28). In rodent preadipocyte experiments, Nrf2 transcriptionally regulated Ppar-γ and Cebp-β to enhance adipocyte differentiation and consequently lipid synthesis (29, 30).

Here, we studied how early life exposure to BPA through perinatal and peripubertal exposure exerts epigenetic modifications in mice, and whether the modifications persist into adulthood. First, it was hypothesized that PNPP BPA exposure induces hypomethylation of CpG sites in promoters of lipogenic genes (e.g. Srebp-1c and Fas) early in development, which would persist into adulthood. Second, it was also determined whether Nrf2 expression increases with BPA exposure, and whether it can be correlated with promoter methylation status. Overall, our findings herein confirmed that PNPP BPA exposure increases the expression of lipogenic enzymes in conjunction with hypomethylation at CpG sites in the promoter regions. Moreover, we described increased Nrf2 recruitment to the Srebp-1c promoter in livers of BPA exposed mice.

2.3 MATERIALS AND METHODS

2.3.1 Animals and dosing. CD-1 female mice (10-12 weeks of age) and proven breeder male mice (Charles River Laboratories, Wilmington, MA) were maintained in temperature- and light-controlled (14/10-hr light/dark cycle) conditions at the at Tufts University Human Nutrition and Research Center animal facility (approved by the Association for Assessment and Accreditation of Laboratory Animal Care International). All experimental procedures were approved by the Tufts University New England Medical Center Institutional Animal Care and Use Committee. Cages, water, and bedding all tested negligible for estrogenicity. Water was supplied *ad libitum* from glass bottles. Food (Teklad 2018; Harlan, Indianapolis, IN) was supplied *ad libitum*. The estrogenicity of food lots used was measured and found to be negligible (<20 pmol estrogen equivalents per gram of feed). Mice were paired to mate and breed. The day on which a vaginal plug was detected, considered gestational day 1 (GD 1). On GD 8, dams were implanted subcutaneously with Alzet osmotic pumps (model 1004; Alza Corp., Palo Alto, CA) following the manufacturer recommendations. Pumps were designed to deliver vehicle alone (50% DMSO in water) and BPA (25 µg/kg bw/day). Care was taken to limit BPA contamination through housing or feeding. These exposures to dams were continued until weaning age of pups, which is postnatal day 21 (PND 21) and pups exposed to BPA through lactation. After weaning age, exposure of BPA to pups continued through drinking water until PND 32 (week 5). Livers and serum were collected from female pups at week 5 and at week

39 and stored at -80°C until analysis (n=10 or 5/ group for week 5 and week 39 respectively).

2.3.2 Triglyceride quantification. Total lipids were extracted from liver tissue by method previously described (28). Briefly, liver tissue (50mg) was homogenized in 1 ml of phosphate buffer saline (PBS) and extracted with chloroform-methanol mixture (2:1). Lipid extracts were vacuum-dried by using a Speedvac (Thermo Scientific) at 45°C. The lipid residue was re-suspended in 1% Triton X-100 in 100% ethanol. Triglyceride quantification was performed using a commercially available kit from Pointe Scientific Inc. (Canton, MI).

2.3.3 Oil Red O staining. About 5 µM thick sections were cut from frozen liver tissue using Vibratome UltraPro 5000 Cryostat (GMI, Ramsey, MN, USA). After acclimating to room temperature, the sections were fixed with 10% buffered formalin for 10 min and then stained with Oil red O (ORO) working solution. ORO stock solution was 0.5% Oil Red O in isopropanol. A fresh working solution was prepared by combining 3 parts of stock solution with 2 parts of deionized water. Tissue sections were incubated in the working solution for 15 min at room temperature, the ORO solution was removed, and sections were quickly rinsed 2 times with fresh 60% isopropanol. Sections were next counterstained with hematoxylin, washed to water, and mounted in glycerin jelly.

2.3.4 RNA isolation and quantitative real time PCR. Total RNA was isolated using TRIzol reagent (Invitrogen, CA) according to the manufacturer's instruction. RNA concentrations were determined by using spectrophotometer (Nanodrop ND1000, ThermoFischer Scientific, Waltham, MA, USA). 2µg of

RNA was converted to single stranded cDNA using a High-Capacity cDNA Reverse Transcription Kit (Invitrogen, Grand Island, NY). Expression of genes at mRNA level were measured with quantitative real-time PCR using Light-Cycler® 480 and SYBR Green (Roche Applied Science, Mannheim, Germany) detection system. Levels of β2-microglobulin (B2M) used as reference housekeeping gene to normalize all data. Lipogenic target genes such as sterol regulatory element binding protein 1c (Srebp-1c), proliferator-activated receptor –gamma (Ppar–γ), acetyl CoA carboxylase-1 (Acc-1), fatty acid synthase (Fas) and glycerol 3 phosphate acyltrasferase (Gpat) and stearoyl CoA desaturase-1 (Scd) were analyzed for mRNA expression and primers for all these genes are listed in Supplementary table S1.

2.3.5 Determination of relative protein expression by western blot. 50mg of liver tissue was homogenized in 1ml of RIPA buffer using a Dounce homogenizer. The lysate was centrifuged a 12,000 rpm for 15 min at 4°C and the resulting supernatant was collected as a total protein extract. Nuclear proteins were extracted from liver tissue using a NE-PER® kit (Thermo Scientific, Rockford, IL) and according to manufacturer's protocol. The extract was quantified for protein content by a DC Lowry assay (Bio-Rad, Hercules, CA). 30 µg of protein/well was resolved by SDS-polyacrylamide gel electrophoresis and then proteins were transferred on PVDF membrane (Millipore Corporation, Billerica, MA) at 100 V for 45 min. Membranes were blocked with 5% non-fat dry milk in tris-buffered saline with 0.1% tween-20 (TBS-T). The membranes were then incubated overnight with primary antibody diluted in 2% milk in TBS-T. Following washing with TBS-T, the membranes

were incubated with species-specific peroxidase-labeled secondary antibody (1:5000) in TBS-T for 1 hour at room temperature. Next, membranes were washed in TBS-T, incubated in ECL+ (GE Healthcare, Waukesha, WI, USA). The resulting protein bands were visualized by autoradiography films, which were quantified using Quantity One software (Biorad, Hercules, CA). Specific information about the source, dilution, type, and molecular weight of primary and secondary antibodies is detailed in Supplementary Table S2.

2.3.6 Chromatin Immunoprecipitation (ChIP) assay. Chip assays using liver tissues were performed according to the Active Motif ChIP-IT express kit protocol with modifications (Active Motif, Carlsbad, CA). Briefly, 100 mg of liver tissue was homogenized with 4 ml of phosphate-buffered saline containing protease inhibitor. Homogenate was cross-linked by adding 1% formaldehyde for 10 min and crosslinking was stopped by 125 mM glycine solution. After washing twice with ice-cold PBS containing protease inhibitor followed by centrifugation, the pellet was suspended in SDS-lysis buffer for 40 min on ice. Dounce homogenizer was used to release nuclei from cells. Lysates were sonicated using a Branson Sonifier 250 (Branson Ultrasonics Corporation, Danbury, CT) 3 times with 12 seconds per stroke and a 1 min rest in between. Cell debris was removed by centrifugation for 10 min at 12,000 g at 4°C. Shearing efficiency was optimized to obtain chromatin fragments between 200-800 bp and determined by 2% agarose gel electrophoresis. A portion of sheared chromatin was used to determine the DNA concentration and equal amount of sheared chromatin (equivalent to 15

µg of DNA) was incubated with ChIP validated rabbit anti-Nrf2 antibody (C-20, sc-722x, Santa Cruz Biotechnologies, Dallas, TX) or anti-rabbit IgG antibody (Cell Signaling, Danvers, MA) overnight at 4°C with rotation. A portion of sheared chromatin was preserved as input (10 µl). Antibody-chromatin complex was recovered by adding pre-blocked Dynabeads Protein A (Life Tech, Grand Island, NY). Using magnetic racks, beads were pelleted and sequentially washed. Antibody and beads bound to chromatin were eluted by adding reverse crosslinking buffer and elution buffer sequentially. DNA was purified by adding proteinase K and via phenol: chloroform: isoamyl alcohol extraction. DNA fragments were analyzed by end-point PCR or real time PCR using different primers that cover putative antioxidant response element (ARE) sequences on mouse Srebp-1c, Fas, and Acc promoters (Supplementary table S3). Promoter sequences were identified using UCSC genome browser. Results are represented as agarose gel scans (end-point PCR) as well as fold enrichment (qPCR).

2.3.7 Methylation analysis:

A. Methylated DNA immunoprecipitation (MeDIP): MeDIP assays were performed as described previously by (31). Briefly, 6µg of genomic DNA was sheared by series of 3×20 pulses of sonication using Branson Sonifier 250 at power level 2 on the machine. Sonication efficiency was checked by agarose gel electrophoresis and fragment size of DNA was verified approximately 500 kb. 350 µl of TE buffer was added to sonicated DNA and denatured at 95°C for 10 min and then immediately placed on ice for 5 min. Sonicated and denatured DNA was diluted with 100 µl of 5X IP buffer (50 mM Na-phosphate

pH7, 700 mM NaCl, 0.25% Triton X-100) and incubated with 5µg of 5-methylcytosine monoclonal antibody (5-mc) (Epigentek Group Inc, Farmingdale, NY) and with anti-rabbit IgG antibody (Cell Signaling, location) overnight at 4°C with rotation. Protein A/G beads were prewashed with 0.1% PBS-BSA and resuspended in 40 µl of 1X IP buffer. Beads were added to DNA-Antibody complex and incubate for 2 hrs at 4°C on rotating platform. Beads-DNA- antibody complex were washed three times with 1X IP buffer and after washing complex were re-suspended in 250 µl of digestion buffer (50 mM Tris HCl pH 8, 10 mM EDTA, 0.5%SDS) containing 3.5 µl of proteinase-k (Sigma Aldrich, St. Louis, MO, USA) and then incubated at 55°C on a rotating platform. DNA purification was performed by phenol: chloroform: isoamyl alcohol extraction, and resuspended in 30 µl of TE buffer. Methylated enriched DNA was amplified by real time PCR by using different primers that covers CpG sites of promoter of Srebp-1c, Fas, and Nrf2 (Supplementary table S4). Methylation status of these promoters was plotted in the form of fold enrichment.

B. Pyrosequencing: DNA methylation quantitation of CpG sites was performed by Pyrosequencing technology using PyroMark MD (Qiagen, Santa Clarita CA). Firstly, Pyrosequencing assays for interest region of Nrf2 promoter were designed with PyroMark Assay Design Software version 2.0. DNeasy Blood & Tissue Kit (Qiagen, Santa Clarita CA, catalog number: 69504) was used to isolate total genomic from frozen liver tissues and DNA concentrations were determined by using spectrophotometer (Nanodrop

ND1000, ThermoFischer Scientific, Waltham, MA, USA). Genomic DNA was bisulfide converted by using EZ DNA Methylation™ Kit (Zymo Research, Irvine, CA, catalog number: D5001). Briefly, sodium bisulfite was added to approximately 1 µg of genomic DNA, converting unmethylated cytosines to uracil, which are replaced with thymine during PCR; methylated cytosines remain unchanged. After bisulfite conversion, amplification of Nrf2 gene regions of interest was performed using PyroMark PCR Kit (Qiagen, Santa Clarita CA), forward primer (50 pmol), and biotinylated reverse primer (50 pmol) in a 25 µl PCR reaction system. The PCR conditions, forward, reverse and sequencing primers and biotin labeling for all assays are shown in table 2. The PyroMark MD Pyrosequencer platform (Qiagen) was utilized according to manufacturer suggested protocol to quantify DNA methylation at the selected CpG sites (computed by Pyro Q-CpG Software). Percent DNA methylation calculated by standard curve by quantifying methylation of commercially available 0% and 100% methylated control DNA (80-8060M-PreMix Mouse Methylation Controls- Premix Set, EpigenDx Inc, Hopkinton MA) on each 96-well plate.

2.3.8 Cell culture and transient transfection reporter gene assay:

Human Srebp1c promoter of 1565 bp corresponding to the 5′ upstream region cloned in pGL3-basic luciferase vector was graciously donated by Dr. Marta Casado (Instituto de Biomedicina de Valencia, Valencia, Spain). Expression plasmid p3XFLAG-myc-CMV-26 (EV26) was obtained from Sigma-Aldrich (St Louis, MO). NRF2 ORF cloned into EV26 was graciously donated by Dr. Jose

Manautou (University of Connecticut, Storrs, CT). HepG2 cells were cultured in DMEM containing 25mM glucose, 10% fetal bovine serum, 1% penicillin-streptomycin (10,000 U/mL) and 1% non- essential amino acid (NEAA) under the humidified atmosphere of 95% air to 5 %CO2 at 37°C. Co-transfections (Srebp1c luciferase reporter constructs and transcription factor expression plasmids) were performed using Lipofectamine 3000 (Life Technologies, Tarrytown NY) according to the manufacturer's manual. For all transfections, plasmid DNA used per well were 75ng for Srebp promoter construct, 15ng of Nrf2 expression plasmid and 10ng null renilla luciferase (pRL-CMV) as internal control. After 24 hrs of transfection, cells were lysed by 1× passive lysis buffer and preceded for luciferase activity. For Nrf2 activator treatment experiments, after 24 hrs of Sreb1c luc promoter plasmid transfection, cell were treated with oleanolic acid (50uM) and sulforaphane (10uM) in 0.05% DMSO 12hrs. After treatment, cells were lysed with 1× passive lysis buffer and luciferase activity was measured relative firefly/renilla luciferase Dual-Luciferase® Reporter Assay System (Promega, Madison, CA) with GloMax™ Luminometer (Promega, Madison, CA) according to manufacturer's protocol.

2.3.9 Statistical Analysis. Control and treated groups were analyzed by Student's t-test. Asterisk * indicates statistically significant difference between the control and BPA treated group ($p<0.05$).

2.4 RESULTS

2.4.1 Effects of perinatal peripubertal bisphenol A (PNPP BPA) exposure on body weight, liver weight and hepatic lipid accumulation. Prior to present study, pilot study on PNPP BPA exposure was performed in both male and female offspring. Initial data obtained from male mice did not indicate any increase in liver triglycerides or lipogenic gene expression at week 39 (Supplementary figure S1), but treatment related differences were present in tissues from female mice. Based on these results, female mice were chosen for further study. Pilot dose finding studies indicated that free BPA in serum in the dams and pups at PND 32 was below detectable limits. Detectable levels of total BPA in serum of mothers and pups was 0.6-0.7 ng/ml for BPA 25.

Fig. 1A shows changes in body and liver weight between control and BPA treated animals. BPA increased body weight by ~15% compared to control at both ages. Liver weights were similar between treatment groups at both ages. As compared to control, BPA significantly increase hepatic TG content at week 5 by about 33%, but not significant increase in week 39 (Fig.1B). ORO staining of frozen sections revealed more lipid accumulation with BPA in both week 5 and week 39 livers as compared to respective controls. Representative images are presented in fig.1C, and three images from each sample in all the groups were used to quantify lipid deposits and plotted (Fig. 1D)

2.4.2 Effect of PNPP BPA exposure on expression hepatic lipogenic gene expression in female mice at puberty (week 5) and adult (week 39) age. The effect of PNPP BPA exposure on gene expression related to hepatic lipid

metabolism was evaluated by real time PCR. Fig. 2 illustrates the effect of PNPP BPA exposure on expression of transcription factors (Srebp1, Ppar-γ) involved in regulation of hepatic lipid homeostasis as well as key enzymes Acc, Fas and Gpat at both puberty as well as adult age of female offspring. At week 5, except Scd, BPA induced increase in other targets measured was not significant. However, at week 39, Ppar-γ, Fas, Acc, and Gpat mRNA expression was approximately doubled compared to controls (Fig. 2A, 2B).

Figures 3 and 4 depict expression of proteins in liver related to hepatic lipid accumulation in both weeks with BPA exposure. In week 5 females, BPA increased Ppar-γ levels in nuclear fractions by 300% compared to controls. BPA increased pSrebp1 protein levels to two-fold compared to controls. At week 39, significant induction in protein expression of Ppar-γ and Srebp1c was noted (Fig 3A, 3B). At week 5, BPA increased Fas, Acc, and pAcc protein expression by more than 135%, 200% and 135% respectively. At week 39, BPA25 increased Fas and pAcc protein expression by 50 and 75%, but did not significantly increase Acc levels (Fig. 4A, 4B).

2.4.3 PNPP BPA exposure enhanced Nrf2 and Nrf2-dependent protein expression. Messenger RNA and protein expression for Nrf2, and its target enzymes Gclc were determined (Fig. 5). Protein expression of nuclear Nrf2 and total Gclc were increased by 30% or more with BPA treatment in both week 5 and week 39 livers.

To examine whether BPA exposure was associated with increased oxidative stress, reduced GSH was measured in liver. At week 39, hepatic GSH concentration was similar between controls and BPA exposed group

(Supplementary figure S2), indicating a lack of significant oxidative stress in liver.

2.4.4 PNPP BPA exposure was associated with hypomethylation in regions of the mouse Srepb-1c and Nrf2 promoters. The effect of BPA on gene-specific promoter methylation was determined using methylated DNA immunoprecipitation (MeDIP) using 5- methyl cytosine antibody (5-MC) and according to published protocol (31). Promoter sequences for lipogenic targets were analyzed for presence of CpG site on Methprimer (University of California, San Francisco), and these sites were checked for methylation status. In week 5 mice, BPA decreased methylation in regions upstream of the translational start site. BPA treated groups showed less enrichment of 5-MC for Srebp1-c promoter (-231 to -346 and -1325 to -1456), Fas promoter (-306 to -472 and -654 to -832) and at one promoter region checked for Nrf2 (-1059 to -1168) (Fig. 6). In week 39 livers, BPA was associated with markedly less enrichment of methylated DNA at multiple regions. With exception of Srebp-1c promoter region from -231 to -346, other promoter regions checked displayed a uniform decrease in the DNA methylation.

Further, a sequence of Nrf2 promoter (-1405 to -1088) containing 4 CpG sites (CpG#1, 2, 3 and 4 respectively at -1132, -1144, -1147, -1157) was analyzed to determine change in site-specific methylation upon BPA exposure by pyrosequencing using bisulfide converted DNA (Table 1). In week 5, CpG#1 site is significantly less methylated in BPA treated mice as compared to control. No change in three other CpG sites was observed. Interestingly, in week 39, BPA significantly lower percent methylation of other CpG site

(CpG#4). Multiple other regions of the Srebp-1 and Nrf2 promoter were also checked, and displayed no prominent changes in DNA methylation with BPA in week 5 and week 39 mice (Data not shown).

2.4.5 PNPP BPA exposure enhances recruitment of Nrf2 to the promoter of lipogenic genes. In week 5 mice, BPA increased recruitment of Nrf2 to a putative ARE binding site at -120 to -130 upstream of translational start site in mouse Srebp-1c gene as compared to negative control (IgG) depicted transcriptional regulation of Srebp-1c by Nrf2 upon BPA treatment. Interestingly, this transcriptional regulation of lipogenic proteins by Nrf2 was persistent with BPA in week 39 mice as well (Fig 7B). BPA exhibited higher binding of Nrf2 on Srebp-1c, at same region of upstream of translation start site in week 39 females. Real time PCR results also showed higher enrichment of Nrf2 on Srebp-1c promoter upon BPA treatment in both week 5 and week 39 mice (Fig 7C).

2.4.6 Effect of NRF2 Over-expression on transactivation of human Srebp-1c promoter. Co-transfection of reporter genes with NRF2 increased luciferase activity and thus significantly transactivated Srebp1c reporter (Figure 8A) indicating the potential ARE is located in this Srebp1 promoter region. Furthermore, treatment of HepG2 cells with known Nrf2 activators, sulforaphane and oleanolic acid, enhanced transactivation of the Srebp-1c promoter, supporting the presence of functional ARE in Srebp-1c promoter.

2.5 DISCUSSION

Using BPA as a model compound, here we provide a first evidence for Nrf2-mediated environmental chemical induced lipid homeostasis alterations. Presence of functional ARE in the Srebp-1c promoter demonstrates involvement of Nrf2 in hepatic lipid accumulation under the influence of chemical exposure. Moreover, persistent effects of BPA induced steatosis pertinent of DNA hypomethylation are in agreement with published literature that demonstrates epigenetic imprinting capabilities of BPA –reviewed by (32). We report induction of hepatic steatosis with PNPP BPA exposure in young and adult female mice. Our findings are consistent with a recent pediatric study, which demonstrated higher levels of urinary BPA in females as compared to males, with an association with NAFLD (13). Moreover, in human cross-sectional studies, urinary BPA levels correlated positively with BMI more significantly in girls between 9 to 12 years of age than other age groups, implying the sensitivity of pubertal female population to BPA (12). The observed increased lipid level was associated with induction of mRNA and protein expression of enzymes and transcription factors that induce hepatic lipid accumulation. Furthermore, the findings herein have uncovered new mechanisms for PNPP BPA-induced hepatic steatosis through promoter hypomethylation, describing new areas of differential methylation at the Srebp-1c, Fas, and Nrf2 mouse promoters, as well as describe Nrf2 enrichment at new putative AREs in the mouse Srebp-1c promoter.

The Environmental Protection Agency and US Food and Drug Administration published tolerable daily intake (TDI) value for BPA around 50μg/kg, and the

exposure level chosen in current study is lower than TDI. More importantly, published studies suggest that dose of 400µg/kg BW/day in mice resulted in serum levels (0.5ng/ml) of unconjugated BPA much lower than amount noted in human serum after environmental exposure (2 ng/ml) (33). In addition to dose, timing of exposure to potential endocrine disruptors like BPA is also a critical determinant for disease susceptibility (6, 34). Effects of fetal or neonatal exposure of BPA are hypothesized to be as critical as adult exposure (6, 35). As based on 'fetal plasticity' theory any effects that affect embryo can remain persistent for life. In our model, female mice were exposed to BPA during gestation and lactation. Overall, it was observed in the study herein that BPA induced hypomethylation at some sites in the liver genome that persisted (e.g. Srebp1c -1325 to -1456; Fas -654 to -832, -306 to -472; Nrf2 -1059 to -1168), whereas methylation in other sites in the genome differed at weeks 5 and 39. This data suggests the potential that some sites might be persistently "marked", whereas others are more "plastic" with the ability to be more dynamically regulated by methylation-regulating enzymes or changes in methyl donor content. This observation is highly relevant to the field of epigenetics and supports other observations of plasticity in methylation (36). Effects at low dose, as well as exposure time dependent effects support the notion of BPA being a *"critical window of exposure"* compound.

In the current study, as well as published findings (7), liver weights remained unchanged with BPA exposure irrespective of route and time of administration in both mice and rats. Interestingly, BPA exposed rodents exhibited evident hepatic lipid accumulation among several studies (6, 7). A major source of

liver lipids besides dietary consumption is *de novo* synthesis (37). Our observations herein, as well as ones from the latter studies using rodents are supported to some degree by recent finding published associated NAFLD with BPA exposure in children (13). The majority of BPA exposure studies related to NAFLD have focused primarily on disturbances lipid synthesis at the transcriptional level. Induction of Srebp-1c and Ppar-γ in livers was observed across all these studies, and the resulting Fas and Acc induction could be a result of enhanced transcriptional regulation or direct action of BPA on these enzymes. Impairment of β-oxidation can also result in lipid accumulation in liver (38). In our study, down regulation of oxidation regulators in week 5 animals on mRNA level was observed (Supplementary figure S3); however, effect did not remain consistent in adult animals. Further exploration of BPA effect on lipid oxidation is needed.

Early life exposure to BPA caused persistent changes in lipogenesis that were observed in adult even after stopping the exposure in current study. In previous study, *in utero* and lactational exposure of BPA showed accumulation of lipid in adult rat liver by induction of Srebp-1c and related genes; however the study did not reveal the mechanism of lifelong effect of early exposure but they postulated the epigenetic regulation of lipogenic pathway (7). In present study, PNPP exposure of BPA did changes at lipogenic as well as Nrf2 gene specific promoter methylation when analyzed by MedIP. Potential of BPA to cause gene specific promoter methylation changes have also been studied in other genes involved in insulin signaling pathway which resulted in disturbances of adulthood glucose homeostasis (39). BPA induced

hypomethylation was evident in week 5 as well as week 39 animals; however, extent of hypomethylation differed between ages. These differences in age-dependent methylation patterns need further investigation. Gene and protein expression changes in adult age also appeared more prominent in adult mice as opposed to younger mice. Less uniform epigenetic results, associated with less prominent changes in gene expression in week 5 animals suggest that biological effects exerted by early life BPA exposure of a major concern in adult population. Moreover, lack of perfect correlation between DNA methylation changes and gene/ protein expression changes also imply possibility of involvement of other epigenetic mechanisms besides promoter methylation.

BPA-mediated induction of lipid synthesis enzyme expression has been demonstrated (6), however the upstream mechanism by which BPA imparts this upregulation remains unknown. One potential mechanism could be via upregulation of Nrf2 expression and regulation of lipogenic genes as previously described (28, 40). Although most commonly studied for countering oxidative stress, Nrf2 can be upstream regulator of adipogenesis through Ppar-γ and Cebp-β transcriptional regulation in rodent pre-adipocytes (29, 30). Along with adipose tissue, the role of Nrf2 in regulation of hepatic lipid synthesis is an area under investigation. Direct in vitro exposure of BPA in human embryonic kidney (HEK) cells induced nuclear level of Nrf2 (41). Similarly, present study depicted induction of Nrf2 expression at mRNA as well nuclear protein level upon PNPP exposure to BPA. With the help of ChIP assay in our study we showed novel binding of Nrf2 on consensus ARE

sequence on Srebp-1c promoter. Moreover, BPA exposure enhanced this binding and hence we can infer that BPA induced expression of Srebp-1c expression in our model is possibly mediated through Nrf2 regulation. Transfection of Nrf2 in HepG2 cells, as well as its activation by known chemicals oleanolic acid and sulforaphane demonstrated luciferase activity at the Srebp-1c promoter reporter. These findings establish novel function for Nrf2 from transcriptional regulation of hepatic denovo lipogenesis.

Overall, the present study provides the mechanistic exploration of exposure to environment toxicants like BPA for adulthood metabolic disorders like hepatic steatosis. Because of persistent mechanisms such as epigenetic imprinting, exposure to environmental chemicals exerts biological effects not only based on amount, but on the time of exposure. We addressed promoter methylation changes caused by PNPP BPA exposure, but certainly other epigenetic mechanisms need to be explored in detail as well, to obtain more comprehensive picture regarding these persistent effects. Histone modifications or microRNA changes (42, 43) that are known to be affected in or known to cause NAFLD also need elucidation in regard to environmental toxicity. Also, considering ubiquitous expression and function of Nrf2, its role in environmental toxicity is vital to study. Here we provide evidence for binding of Nrf2 on promoters of lipogenic genes, and the binding increases with BPA exposure. In conclusion, PNPP BPA induced lipogenic effects were demonstrated in this study, and detailed epigenetic and Nrf2-mediated mechanisms were elucidated.

2.6 FIGURE LEGENDS

Figure 1: Perinatal peripubertal (PNPP) exposure to bisphenol A affects body weight and hepatic lipid accumulation in female CD1 mice. A) Body weight and liver weight. Statistical differences between the groups were determined by Student's t-test. Asterisk (*) represents significant difference in weights between BPA treated and vehicle treated animals of same age group ($p \leq 0.05$). **B)** Hepatic triglyceride (TG) quantification. **C)** Oil red o (ORO) staining of lipids in the liver tissue. Representative images are displayed in 200X magnification. **D)** Quantification of oil red staining density from all the samples.

Figure 2: Perinatal peripubertal (PNPP) exposure to bisphenol A increases mRNA expression of lipogenic targets in livers of female CD1 mice (A. Week 5; B. Week 39). mRNA was quantified using real time polymerase chain reaction (RT-PCR) using primers specific for sterol regulatory element binding protein 1c (Srebp-1c), peroxisome proliferator activated receptor gamma (Ppar-γ), fatty acid synthase (Fas), acetyl coA carboxylase (Acc), and glycerol-3-phosphate acetyl transferase (Gpat). Raw data was normalized to respective control expression, and statistical differences between the groups were analyzed by Student's t-test. Asterisk (*) represents significant difference in expression between BPA treated and control animals ($p \leq 0.05$).

Figure 3: Perinatal peripubertal (PNPP) exposure to bisphenol A increases protein expression of lipogenic transcription factors in livers

of female CD1 mice (A. Week 5; B. Week 39). Nuclear proteins were detected for expression using specific antibodies for peroxisome proliferator activated receptor gamma (Ppar-γ), sterol regulatory element binding protein 1c (Srebp-1c), and phosphorylated Srebp-1c. The blots were developed using autoradiography and the mean blot intensity is presented in percent protein expression format. Statistical differences between the groups were analyzed by Student's t-test. Asterisk (*) represents significant difference in expression between BPA treated and control animals ($p \leq 0.05$).

Figure 4: Perinatal peripubertal (PNPP) exposure to bisphenol A increases protein expression of lipid synthesis enzymes in livers of female CD1 mice (A. Week 5; B. Week 39). Protein expression was quantified by western blot using specific antibodies for fatty acid synthase (Fas), acetyl CoA carboxylase (Acc) and phosphorylated Acc. The blots were developed using autoradiography and the mean blot intensity is presented in percent protein expression format. Statistical differences between the groups were analyzed by Student's t-test. Asterisk (*) represents significant difference in expression between BPA treated and control animals ($p \leq 0.05$).

Figure 5: Perinatal peripubertal (PNPP) exposure to bisphenol A and nuclear factor E2 related factor 2 (Nrf2) signaling in livers of female CD1 mice. A) Nrf2 and its target gene glutamate cysteine ligase (Gclc) expression in livers of week 5 animals. mRNA expression was quantified using real time polymerase chain reaction (RT-PCR) using primers specific for Nrf2 and Gclc. **B)** Protein expression of nuclear Nrf2 and Gclc. Protein expression was quantified by western blot using specific antibodies for Nrf2 and glutamate

cysteine ligase (Gclc). The blots were developed using autoradiography and the mean blot intensity is presented in percent protein expression format. **C)** Nrf2 and Gclc mRNA expression in week 39 animals. **D)** Protein expression of nuclear Nrf2 and Gclc in week 39 animals. Statistical differences between the groups were analyzed by Student's t-test. Asterisk (*) represents significant difference in expression between BPA treated and control animals ($p \leq 0.05$).

Figure 6: Effect of Perinatal peripubertal exposure of BPA on promoter methylation of Srebp-1c, Fas and Nrf2 analyzed by methylated DNA immunoprecipitation (MeDIP). Genomic DNA (6µg) was sonicated, denatured and subjected to immunoprecipitation by using 5-methyl cytosine or IgG antibody. Agarose beads were used to recover enriched methylated DNA. After purification real time PCR were performed to amplify methylated DNA fragments using different primers covering promoter sequences containing CpG sites. CpG sites in Promoter sequences of Srebp-1c, Fas and Nrf2 (**A**, **B** and **C** respectively) up to 2 kb upstream of translational start site were analyzed to check methylation effects of PNPP BPA. Results are plotted in the form of fold enrichment.

Figure 7: Chromatin immunoprecipitation of nuclear factor E2 related factor 2 (Nrf2) on Srebp-1c gene promoter. A. Nrf2 recruitment on promoter of Srebp-1c (Schematic representation). Liver tissues of BPA treated both young as well as adult female offsprings mice were homogenized with PBS. Homogenate was cross-linked by adding 1% formaldehyde for 10 min and crosslinking was stopped by 125 mM glycine solution. Crosslinked chromatin was sheared and immunoprecipitated with anti-Nrf2 or anti-rabbit IgG antibody

overnight at 4°C with rotation. Antibody-chromatin complex was recovered by adding preblocked Dynabeads Protein A. After reverse crosslinking and purification Nrf2 and IgG precipitated DNA were subjected to **B.** End point PCR, **C.** Real time PCR amplification by using primers as enlisted in supplementary table S3, which covers putative ARE consensus sequence on promoter of Srebp-1c. Results are plotted in the form of fold enrichment compared to negative control.

Figure 8: Nrf2 mediated transactivation of human Srebp-1 *in vitro*. A. Transcription factor NRF2 expression plasmid were transiently co-transfected with the Srebp-1 promoter luciferase reporter constructs (-1.5kb) or pGL3 basic, in HepG2 cells for 24hrs in serum free DMEM media. Luciferase activity was measured as relative firefly/renilla luciferase and was recorded as relative light units data are presented as mean fold change ± SEM. Statistical differences between the groups were analyzed by one-way ANOVA followed by Duncan's posthoc test. Asterisk (*) represents significant difference in expression between BPA treated and control animals ($p \leq 0.05$). **B**. Effect of Nrf2 activators on Srebp-1c directed reporter gene activity: Srebp-1c promoter luciferase reporter constructs or pGL3 basic were transiently transfected into HepG2 cell. After 24 hrs of transfection HepG2 cell were treated with the oleanolic acid (50uM) and sulforaphane (10uM) along with DMSO (0.05%) for 12hrs. Luciferase activity was measured using a commercial kit.

2.7 FUNDING INFORMATION:

This work was supported by National Institute of Health [5R01ES016042 and 5K22ES013782] to AS, and by Rhode Island IDeA Network of Biomedical Research Excellence Award [P20RR016457-10] from the National Center for Research Resources.

2.8 ACKNOWLEDEGEMENTS: We thank Maureen Driscoll, Supriya Kulkarni, Jialin Xu for technical help with experimental methods. Genomic Sequencing Center (GSC) at University of Rhode Island and Rhode Island IDeA Network for Excellence in Biomedical Research (RI-INBRE) provided instrumentation necessary for the experiments.

2.9 TABLES:

Table 1: Site specific methylation (%) of 4 CpG sites for Nrf2 promoter upon PNPP BPA exposure in week 5 and 39 age of mice. Values were adjusted to a standard curve of control DNA (ranging between 0 and 100%) run for each CpG site on the corresponding experimental plate for each sample. Asterisk * represents statistically significant difference between control and BPA treated groups ($p<0.05$).

Week 5	CpG #1	CpG #2	CpG #3	CpG #4
Control	20.47 ± 2.44	7.46 ± 1.62	2.39 ± 0.90	8.16 ± 1.88
BPA	11.61 ± 1.74*	6.52 ± 1.47	5.16 ± 2.24	10.84 ± 2.67

Week 39	CpG #1	CpG #2	CpG #3	CpG #4
Control	13.26 ± 0.61	6.44 ± 1.23	4.38 ± 1.74	19.03 ± 0.9
BPA	15.70 ± 3.30	6.49 ± 0.95	2.44 ± 1.26	7.64 ± 2.42*

Table 2: PCR conditions for Pyro-Sequencing

Primer/sequence to analyze	Nrf2 Assay
Forward PCR primer	GTAGTTAAAGAAGTATGTTTGGGAATGA
Reverse PCR primer	Biotin-TATAATCTCATAAAACCCCACCTCTC
Sequencing primer (5' to 3')	ATAATAAGAATTATATTAAAGGG
Amplicon length	318
Temperature	58
Number of cycles	45

2.10 REFERENCES:

1. Liangpunsakul S, Chalasani N. Treatment of Nonalcoholic Fatty Liver Disease. Curr Treat Options Gastroenterol 2003;6:455-463.

2. Bedogni G, Nobili V, Tiribelli C. Epidemiology of fatty liver: an update. World J Gastroenterol 2014;20:9050-9054.

3. Li Z, Clark J, Diehl AM. The liver in obesity and type 2 diabetes mellitus. Clin Liver Dis 2002;6:867-877.

4. Al-Eryani L, Wahlang B, Falkner KC, Guardiola JJ, Clair HB, Prough RA, Cave M. Identification of Environmental Chemicals Associated with the Development of Toxicant-associated Fatty Liver Disease in Rodents. Toxicol Pathol 2014.

5. Wahlang B, Beier JI, Clair HB, Bellis-Jones HJ, Falkner KC, McClain CJ, Cave MC. Toxicant-associated steatohepatitis. Toxicol Pathol 2013;41:343-360.

6. Marmugi A, Ducheix S, Lasserre F, Polizzi A, Paris A, Priymenko N, Bertrand-Michel J, et al. Low doses of bisphenol A induce gene expression related to lipid synthesis and trigger triglyceride accumulation in adult mouse liver. Hepatology 2012;55:395-407.

7. Wei J, Sun X, Chen Y, Li Y, Song L, Zhou Z, Xu B, et al. Perinatal exposure to bisphenol A exacerbates nonalcoholic steatohepatitis-like phenotype in male rat offspring fed on a high-fat diet. J Endocrinol 2014;222:313-325.

8. Beydoun HA, Khanal S, Zonderman AB, Beydoun MA. Sex differences in the association of urinary bisphenol-A concentration with selected indices of glucose homeostasis among U.S. adults. Ann Epidemiol 2014;24:90-97.

9. Edlow AG, Chen M, Smith NA, Lu C, McElrath TF. Fetal bisphenol A exposure: concentration of conjugated and unconjugated bisphenol A in amniotic fluid in the second and third trimesters. Reprod Toxicol 2012;34:1-7.

10. Hines M, Swinburn K, McIntyre S, Novak I, Badawi N. Infants at risk of cerebral palsy: a systematic review of outcomes used in Cochrane studies of pregnancy, childbirth and neonatology. J Matern Fetal Neonatal Med 2014:1-13.

11. Ashley-Martin J, Dodds L, Arbuckle TE, Ettinger AS, Shapiro GD, Fisher M, Morisset AS, et al. A birth cohort study to investigate the association between prenatal phthalate and bisphenol A exposures and fetal markers of metabolic dysfunction. Environ Health 2014;13:84.

12. Li DK, Miao M, Zhou Z, Wu C, Shi H, Liu X, Wang S, et al. Urine bisphenol-A level in relation to obesity and overweight in school-age children. PLoS One 2013;8:e65399.

13. Khalil N, Ebert JR, Wang L, Belcher S, Lee M, Czerwinski SA, Kannan K. Bisphenol A and cardiometabolic risk factors in obese children. Sci Total Environ 2014;470-471:726-732.

14. Newbold RR, Padilla-Banks E, Jefferson WN, Heindel JJ. Effects of endocrine disruptors on obesity. Int J Androl 2008;31:201-208.

15. Ben-Jonathan N, Hugo ER, Brandebourg TD. Effects of bisphenol A on adipokine release from human adipose tissue: Implications for the metabolic syndrome. Mol Cell Endocrinol 2009;304:49-54.

16. Alonso-Magdalena P, Vieira E, Soriano S, Menes L, Burks D, Quesada I, Nadal A. Bisphenol A exposure during pregnancy disrupts glucose homeostasis in mothers and adult male offspring. Environ Health Perspect 2010;118:1243-1250.

17. Angle BM, Do RP, Ponzi D, Stahlhut RW, Drury BE, Nagel SC, Welshons WV, et al. Metabolic disruption in male mice due to fetal exposure to low but not high doses of bisphenol A (BPA): evidence for effects on body weight, food intake, adipocytes, leptin, adiponectin, insulin and glucose regulation. Reprod Toxicol 2013;42:256-268.

18. Bastos Sales L, Kamstra JH, Cenijn PH, van Rijt LS, Hamers T, Legler J. Effects of endocrine disrupting chemicals on in vitro global DNA methylation and adipocyte differentiation. Toxicol In Vitro 2013;27:1634-1643.

19. Murphy SK, Yang H, Moylan CA, Pang H, Dellinger A, Abdelmalek MF, Garrett ME, et al. Relationship between methylome and transcriptome in patients with nonalcoholic fatty liver disease. Gastroenterology 2013;145:1076-1087.

20. Pogribny IP, Tryndyak VP, Bagnyukova TV, Melnyk S, Montgomery B, Ross SA, Latendresse JR, et al. Hepatic epigenetic phenotype predetermines individual susceptibility to hepatic steatosis in mice fed a lipogenic methyl-deficient diet. J Hepatol 2009;51:176-186.

21. Lee JH, Friso S, Choi SW. Epigenetic mechanisms underlying the link between non-alcoholic fatty liver diseases and nutrition. Nutrients 2014;6:3303-3325.

22. Sookoian S, Rosselli MS, Gemma C, Burgueno AL, Fernandez Gianotti T, Castano GO, Pirola CJ. Epigenetic regulation of insulin resistance in nonalcoholic fatty liver disease: impact of liver methylation of the peroxisome

proliferator-activated receptor gamma coactivator 1alpha promoter. Hepatology 2010;52:1992-2000.

23. Cordero P, Campion J, Milagro FI, Martinez JA. Transcriptomic and epigenetic changes in early liver steatosis associated to obesity: effect of dietary methyl donor supplementation. Mol Genet Metab 2013;110:388-395.

24. Gracia A, Elcoroaristizabal X, Fernandez-Quintela A, Miranda J, Bediaga NG, M MdP, Rimando AM, et al. Fatty acid synthase methylation levels in adipose tissue: effects of an obesogenic diet and phenol compounds. Genes Nutr 2014;9:411.

25. Uriarte G, Paternain L, Milagro FI, Martinez JA, Campion J. Shifting to a control diet after a high-fat, high-sucrose diet intake induces epigenetic changes in retroperitoneal adipocytes of Wistar rats. J Physiol Biochem 2013;69:601-611.

26. Schneider KS, Chan JY. Emerging role of Nrf2 in adipocytes and adipose biology. Adv Nutr;4:62-66.

27. Xu J, Kulkarni SR, Donepudi AC, More VR, Slitt AL. Enhanced Nrf2 activity worsens insulin resistance, impairs lipid accumulation in adipose tissue, and increases hepatic steatosis in leptin-deficient mice. Diabetes;61:3208-3218.

28. More VR, Xu J, Shimpi PC, Belgrave C, Luyendyk JP, Yamamoto M, Slitt AL. Keap1 knockdown increases markers of metabolic syndrome after long-term high fat diet feeding. Free Radic Biol Med 2013;61:85-94.

29. Hou Y, Xue P, Bai Y, Liu D, Woods CG, Yarborough K, Fu J, et al. Nuclear factor erythroid-derived factor 2-related factor 2 regulates transcription of CCAAT/enhancer-binding protein beta during adipogenesis. Free Radic Biol Med 2012;52:462-472.

30. Pi J, Leung L, Xue P, Wang W, Hou Y, Liu D, Yehuda-Shnaidman E, et al. Deficiency in the nuclear factor E2-related factor-2 transcription factor results in impaired adipogenesis and protects against diet-induced obesity. J Biol Chem 2010;285:9292-9300.

31. Guerrero-Bosagna C, Settles M, Lucker B, Skinner MK. Epigenetic transgenerational actions of vinclozolin on promoter regions of the sperm epigenome. PLoS One 2010;5.

32. Ferreira LL, Couto R, Oliveira PJ. Bisphenol A as epigenetic modulator: setting the stage for carcinogenesis? Eur J Clin Invest 2015;45 Suppl 1:32-36.

33. Taylor JA, Vom Saal FS, Welshons WV, Drury B, Rottinghaus G, Hunt PA, Toutain PL, et al. Similarity of bisphenol A pharmacokinetics in rhesus

monkeys and mice: relevance for human exposure. Environ Health Perspect 2011;119:422-430.

34. Chapin RE, Adams J, Boekelheide K, Gray LE, Jr., Hayward SW, Lees PS, McIntyre BS, et al. NTP-CERHR expert panel report on the reproductive and developmental toxicity of bisphenol A. Birth Defects Res B Dev Reprod Toxicol 2008;83:157-395.

35. Liu J, Yu P, Qian W, Li Y, Zhao J, Huan F, Wang J, et al. Perinatal bisphenol A exposure and adult glucose homeostasis: identifying critical windows of exposure. PLoS One 2013;8:e64143.

36. Tang WY, Morey LM, Cheung YY, Birch L, Prins GS, Ho SM. Neonatal exposure to estradiol/bisphenol A alters promoter methylation and expression of Nsbp1 and Hpcal1 genes and transcriptional programs of Dnmt3a/b and Mbd2/4 in the rat prostate gland throughout life. Endocrinology 2012;153:42-55.

37. Postic C, Girard J. Contribution of de novo fatty acid synthesis to hepatic steatosis and insulin resistance: lessons from genetically engineered mice. J Clin Invest 2008;118:829-838.

38. Matsuzaka T, Shimano H. Molecular mechanisms involved in hepatic steatosis and insulin resistance. J Diabetes Investig 2011;2:170-175.

39. Ma Y, Xia W, Wang DQ, Wan YJ, Xu B, Chen X, Li YY, et al. Hepatic DNA methylation modifications in early development of rats resulting from perinatal BPA exposure contribute to insulin resistance in adulthood. Diabetologia 2013;56:2059-2067.

40. Xu J, Kulkarni SR, Donepudi AC, More VR, Slitt AL. Enhanced Nrf2 activity worsens insulin resistance, impairs lipid accumulation in adipose tissue, and increases hepatic steatosis in leptin-deficient mice. Diabetes 2012;61:3208-3218.

41. Chepelev NL, Enikanolaiye MI, Chepelev LL, Almohaisen A, Chen Q, Scoggan KA, Coughlan MC, et al. Bisphenol A activates the Nrf1/2-antioxidant response element pathway in HEK 293 cells. Chem Res Toxicol 2013;26:498-506.

42. Panera N, Gnani D, Crudele A, Ceccarelli S, Nobili V, Alisi A. MicroRNAs as controlled systems and controllers in non-alcoholic fatty liver disease. World J Gastroenterol 2014;20:15079-15086.

43. Aagaard-Tillery KM, Grove K, Bishop J, Ke X, Fu Q, McKnight R, Lane RH. Developmental origins of disease and determinants of chromatin structure: maternal diet modifies the primate fetal epigenome. J Mol Endocrinol 2008;41:91-102.

2.11 FIGURES:

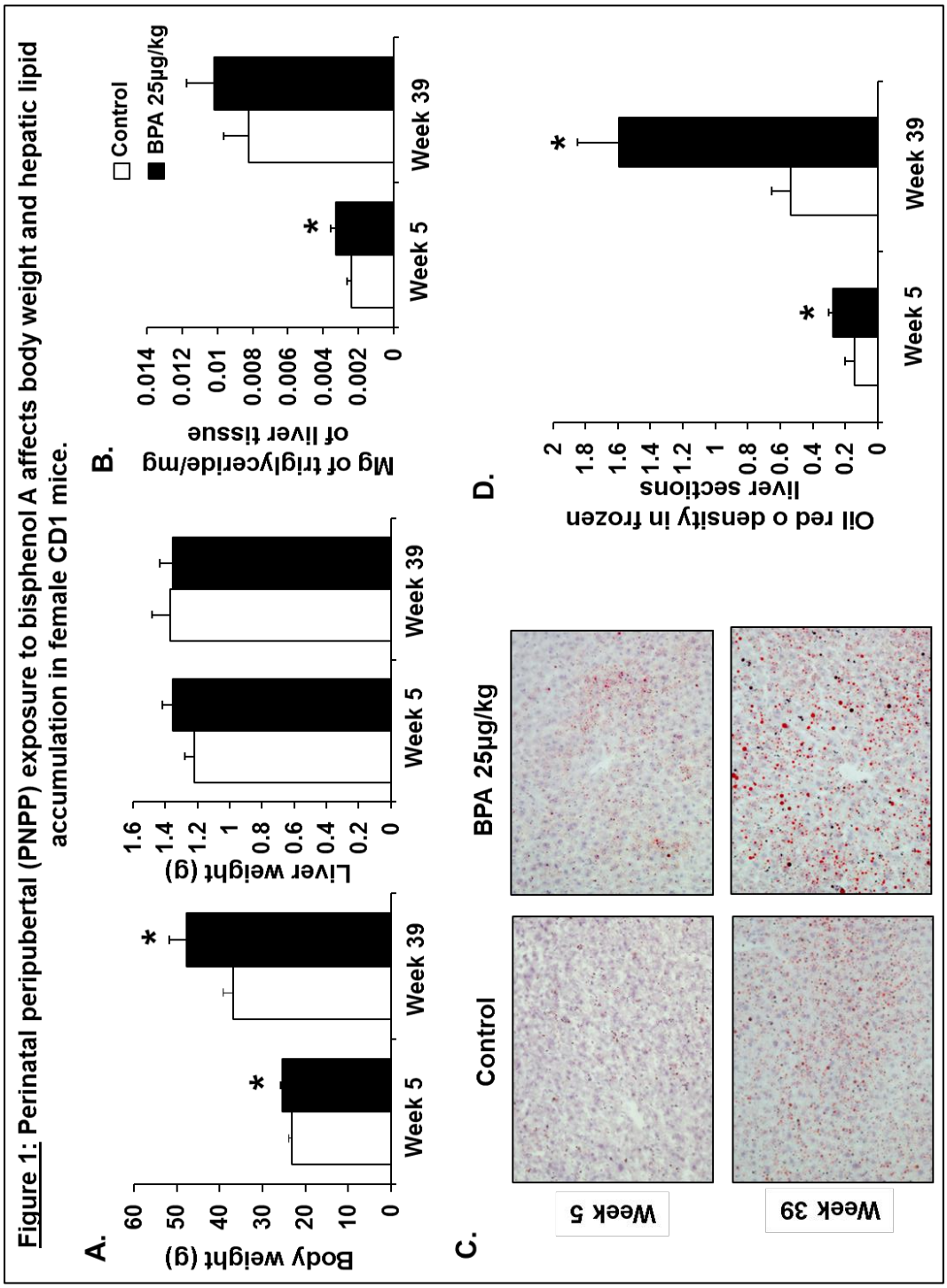
Figure 1: Perinatal peripubertal (PNPP) exposure to bisphenol A affects body weight and hepatic lipid accumulation in female CD1 mice.
A.
Body weight (g)
Liver weight (g)
Week 5
Week 39
B.
Mg of triglyceride/mg of liver tissue
Control
BPA 25µg/kg
C.
Control
BPA 25µg/kg
Week 5
Week 39
D.
Oil red o density in frozen liver sections
*

Figure 2: Perinatal peripubertal (PNPP) exposure to bisphenol A increases mRNA expression of lipogenic targets in livers of female CD1 mice

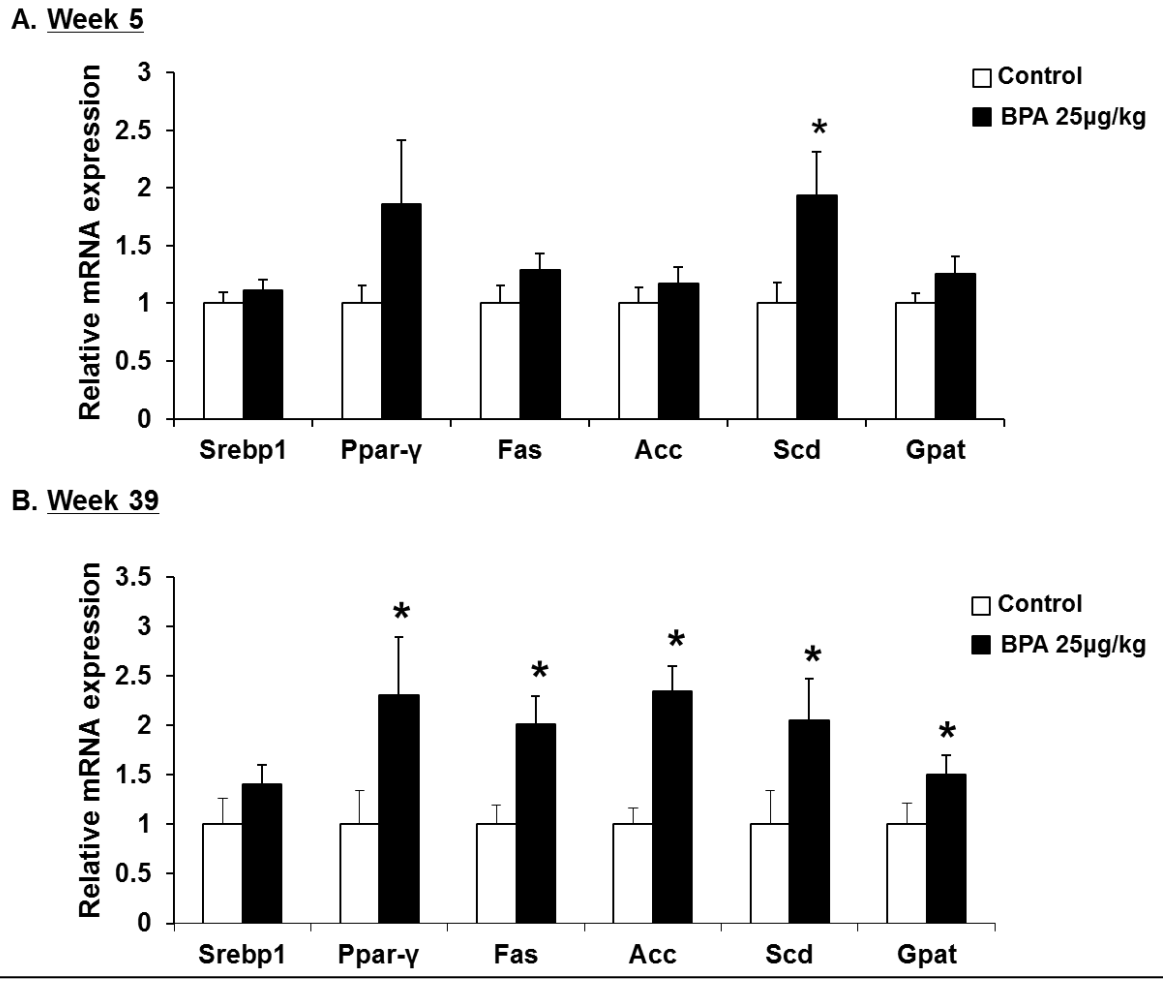

Figure 3: Perinatal peripubertal (PNPP) exposure to bisphenol A increases protein expression of lipogenic transcription factors in livers of female CD1 mice

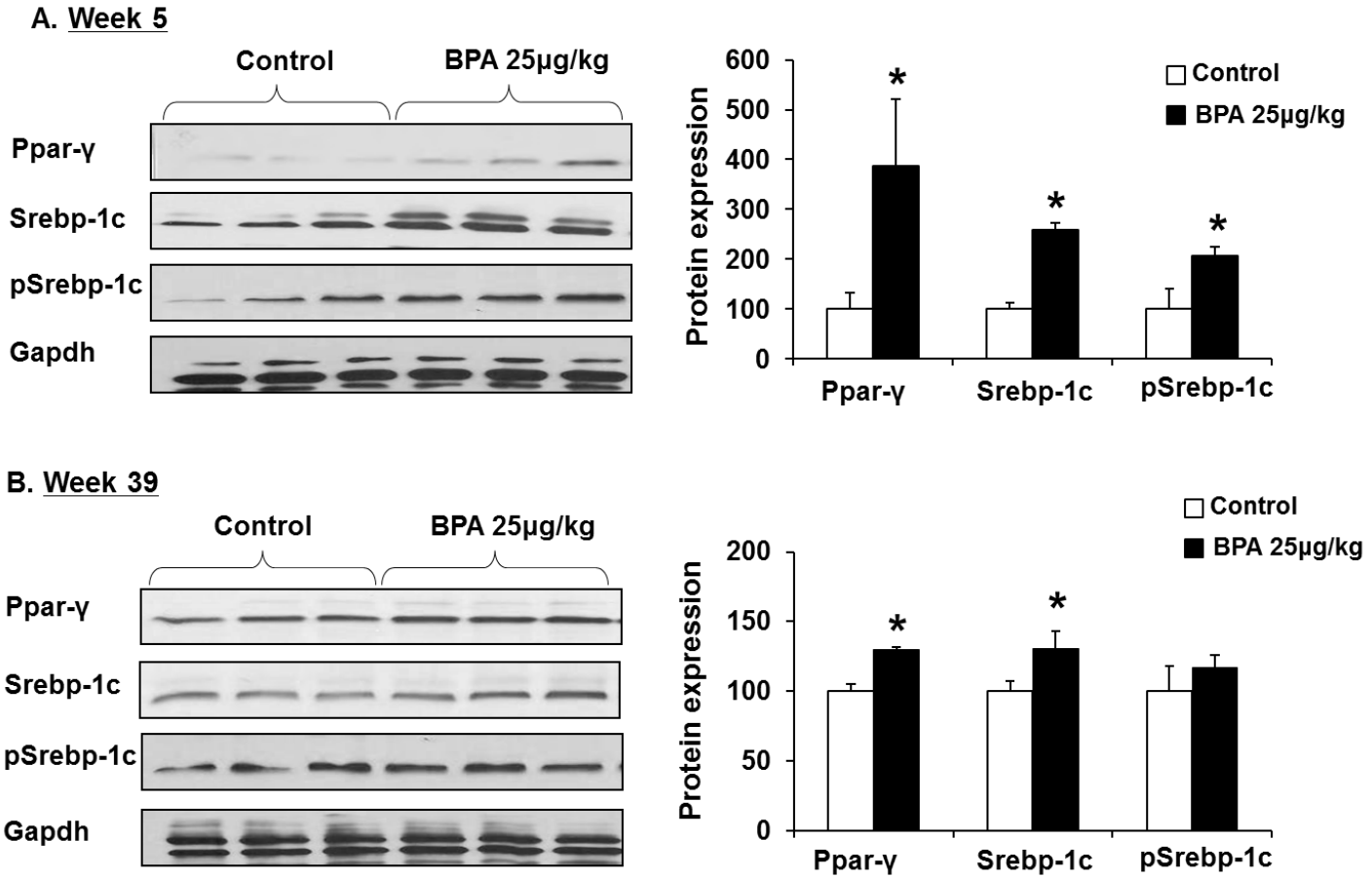

Figure 4: Perinatal peripubertal (PNPP) exposure to bisphenol A increases protein expression of lipid synthesis enzymes in livers of female CD1 mice

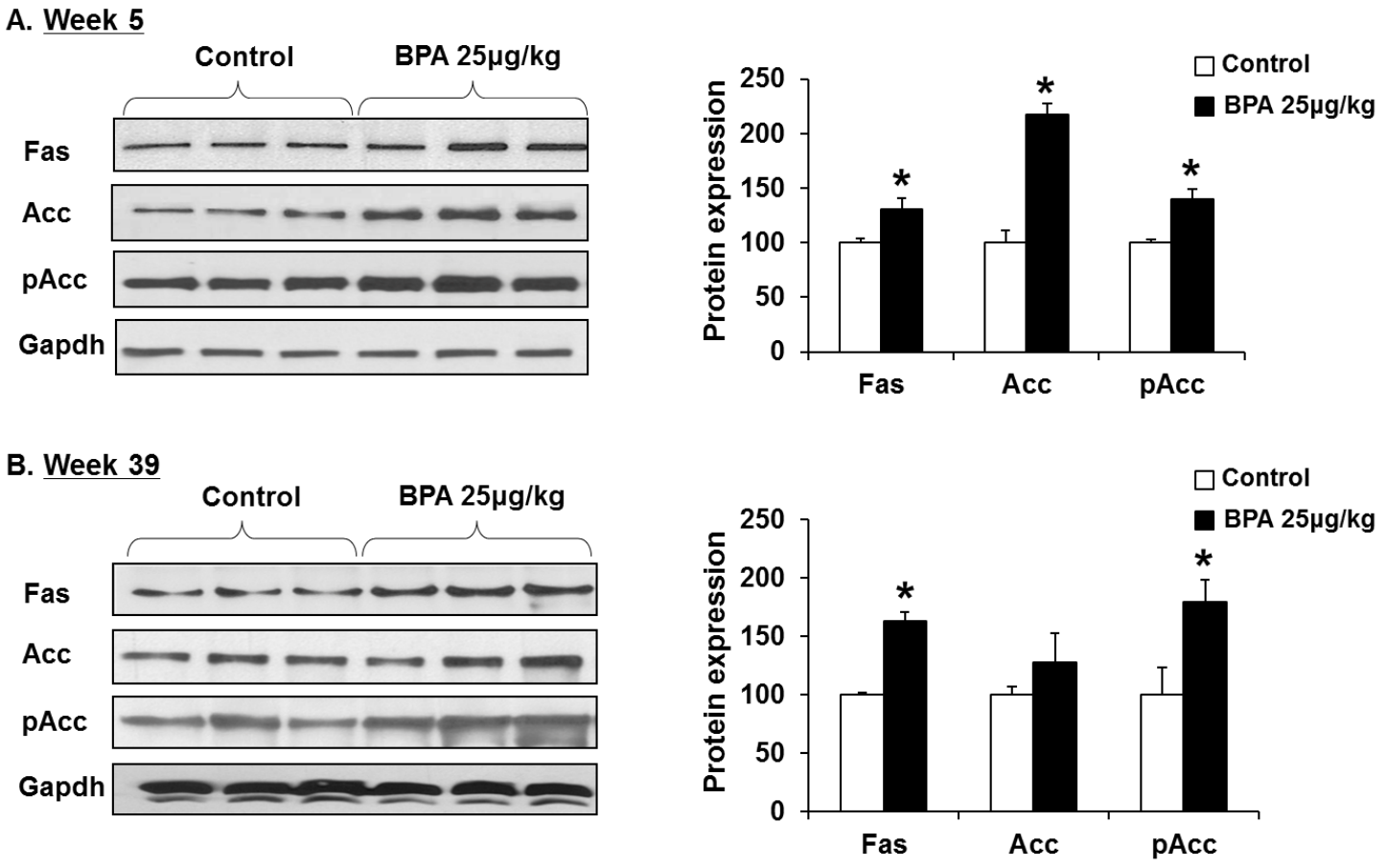

Figure 5: Perinatal peripubertal (PNPP) exposure to bisphenol A and nuclear factor E2 related factor 2 (Nrf2) signaling in livers of female CD1 mice.

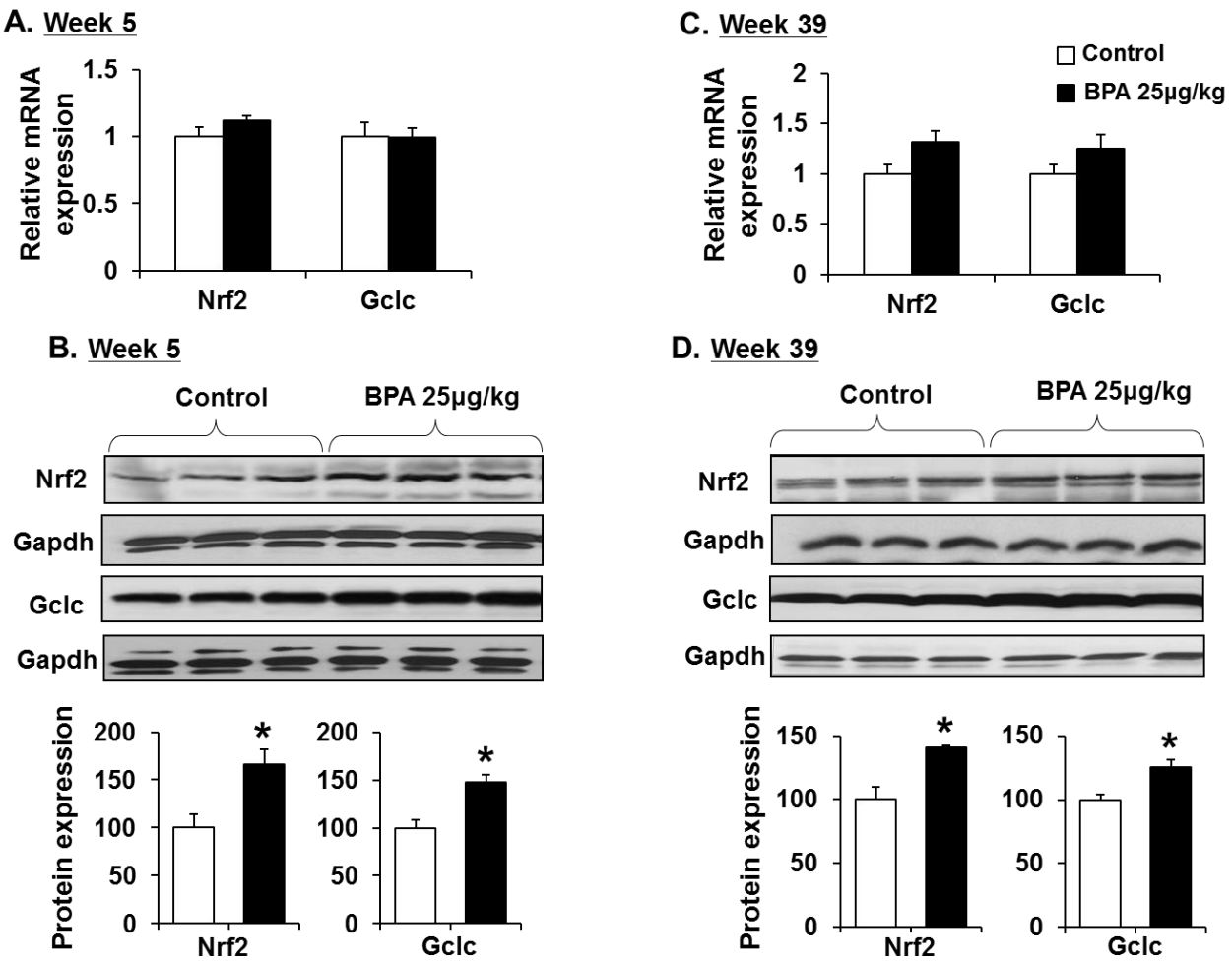

Figure 6: Effect of Perinatal peripubertal exposure of BPA on promoter methylation of Srebp-1c, Fas and Nrf2 analyzed by methylated DNA immunoprecipitation (MeDIP)

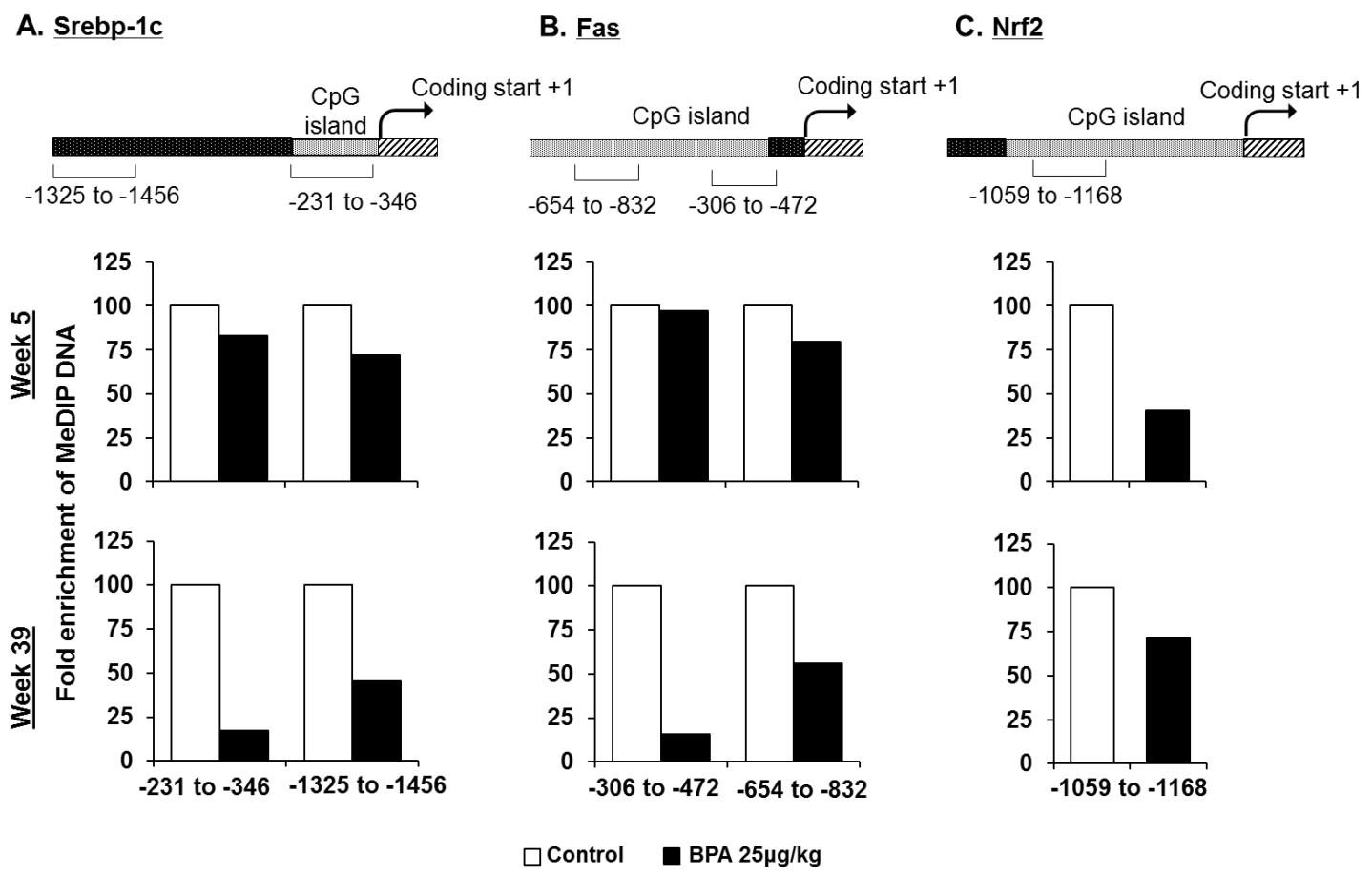

Figure 7: Chromatin immunoprecipitation of nuclear factor E2 related factor 2 (Nrf2) on Srebp-1c promoter

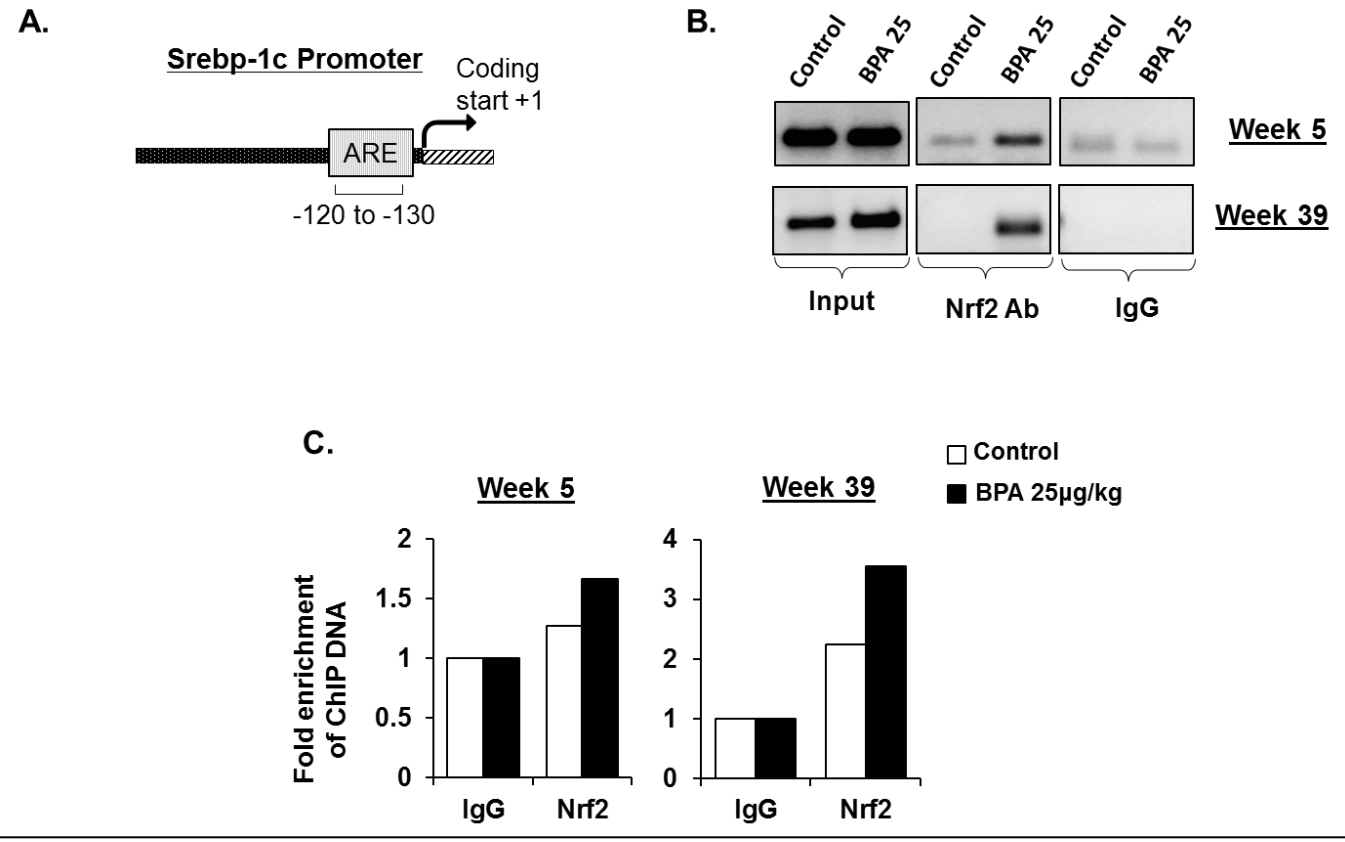

Figure 8: **Nrf2 mediated transactivation of human Srebp-1 *in vitro***

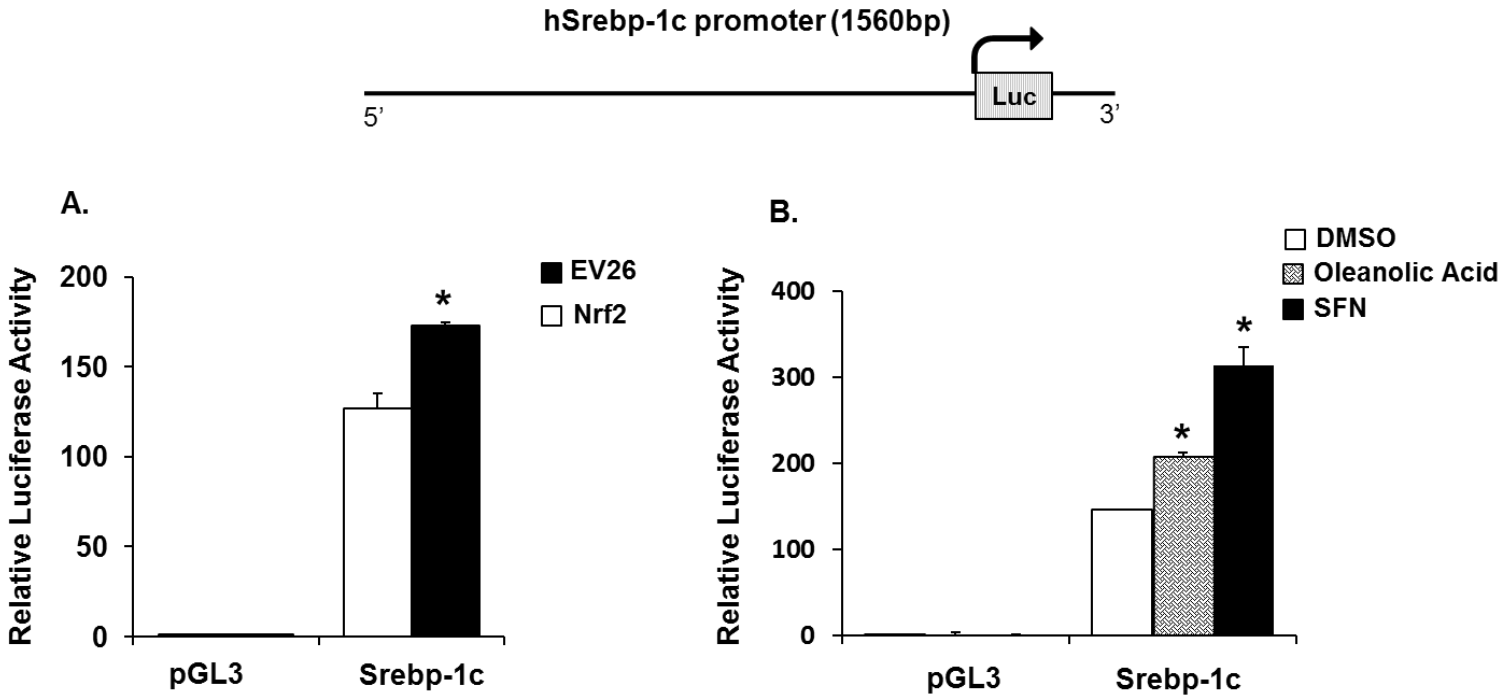

2.12 SUPPLEMENTARY DATA:

Supplementary figure S1: Effect of perinatal peripubertal (PNPP) BPA exposure on hepatic triglyceride (TG) and mRNA expression in male offsprings at week 39 of age. A. TG quantification. **B.** Gene expression of lipogenic targets. Raw data was normalized to respective control expression, and statistical differences between the groups were analyzed by Student's t-test. Asterisk (*) represents significant difference in expression between BPA treated and control animals ($p \leq 0.05$).

Supplementary figure S2: Glutathione (GSH) levels in the livers of week 39 mice exposed to PNPP BPA. Liver tissue was homogenized and the GSH was quantified by commercial kit from Promega (Madison, WI). Raw data was normalized to respective control expression, and statistical differences between the groups were analyzed by Student's t-test.

Supplementary figure S3: Perinatal peripubertal (PNPP) exposure to bisphenol A increases mRNA expression of β-oxidation targets in livers of female CD1 mice (A. Week 5; B. Week 39). Total RNA was extracted from liver tissue by phenol-chloroform extraction using TRIzol® reagent. Messenger RNA was converted to cDNA and subsequently quantified using real time polymerase chain reaction (RT-PCR) using primers specific for peroxisome proliferator activated receptor alpha (Ppar-α), cytochrome P450 4a10 (Cyp4a10), carnitine palmitoyltransferase 1a (Cpt1a). Raw data was normalized to respective control expression, and statistical differences

between the groups were analyzed by Student's t-test. Asterisk (*) represents significant difference in expression between BPA treated and control animals ($p \leq 0.05$).

Supplementary table S1: Primer sequence for quantitative RT-PCR

Supplementary table S2: List of primary and secondary antibodies for western blot and chromatin immunoprecipitation

Supplementary table S3: Primer sequence for amplification of DNA from chromatin immunoprecipitation

Supplementary table S4: Primer sequence for Methylated DNA immunoprecipitation output amplification

Supplementary figure S1: Effect of perinatal peripubertal (PNPP) BPA exposure on hepatic triglyceride (TG) and mRNA expression in male offsprings at week 39 of age

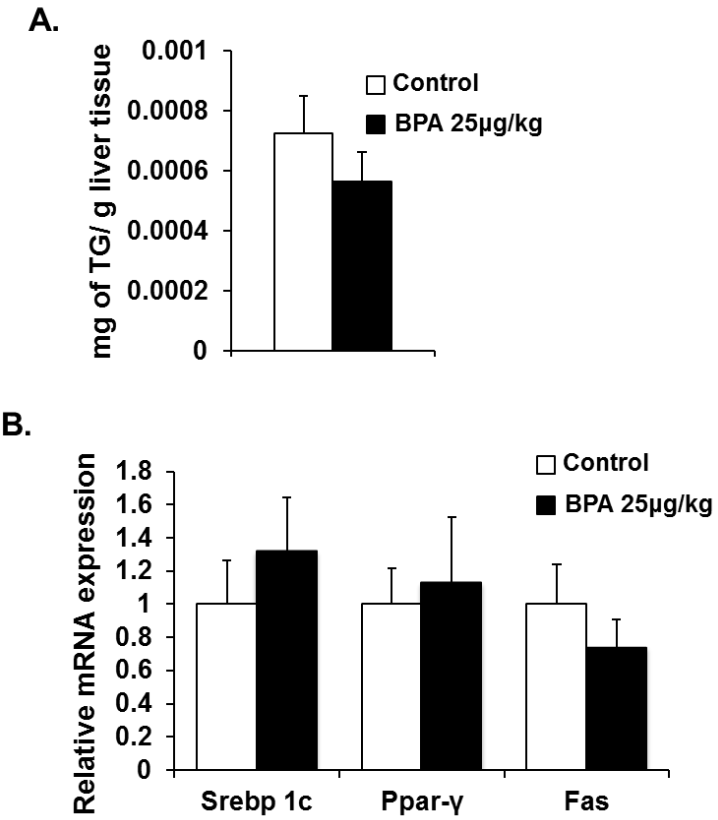

Supplementary figure S2: Glutathione (GSH) levels in the livers of week 39 mice exposed to PNPP BPA

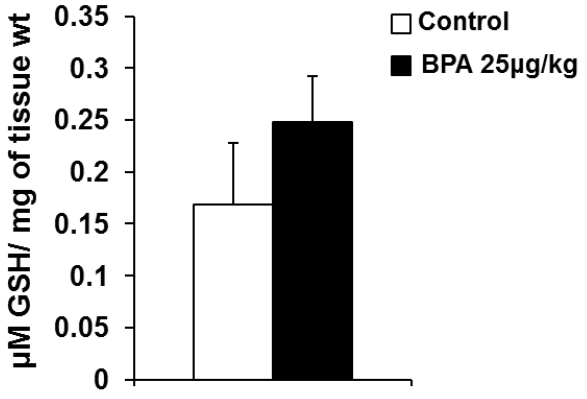

Supplementary figure S3: Perinatal peripubertal (PNPP) exposure to bisphenol A increases mRNA expression of β-oxidation targets in livers of female CD1 mice

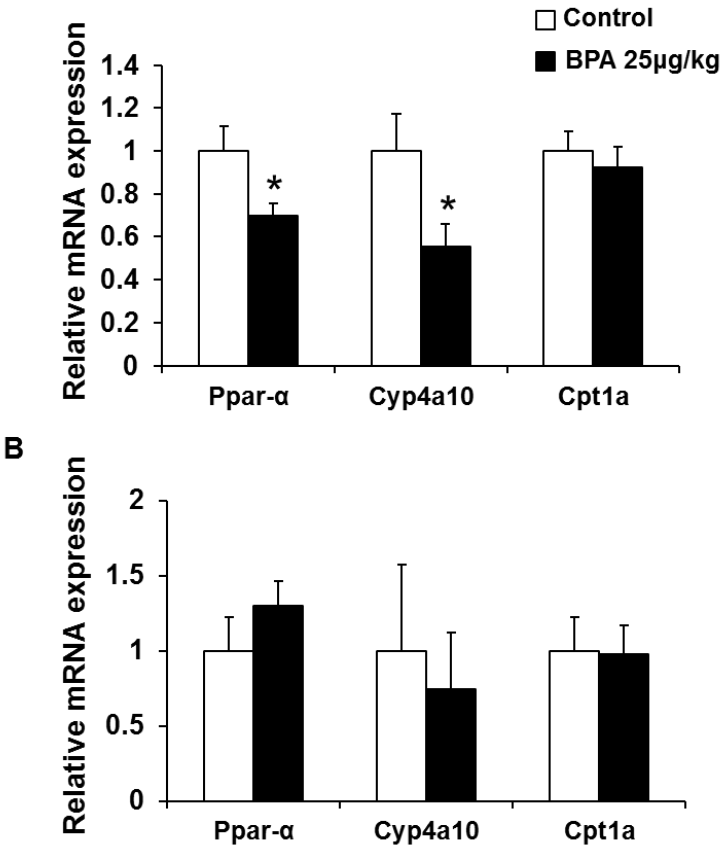

Supplementary table S1: Primer sequence for quantitative RT-PCR

Gene	Forward	Reverse
Srebp1c	GCAGCCACCATCTAGCCTG	CAGCAGTGAGTCTGCCTTGAT
Ppar-γ	CTCTGTTTTATGCTGTTATGGGTGA	GGTCAACAGGAGAATCTCCCAG
Fas	GGAGGTGGTGATAGCCGGTAT	TGGGTAATCCATAGAGCCCAG
Acc	GATGAACCATCTCCGTTGGC	GACCCAATTATGAATCGGGAGTG
Gpat	ACAGTTGGCACAATAGACGTTT	CCTTCCATTTCAGTGTTGCAGA
Nrf2	TCTTGGAGTAAGTCGAGAAGTGT	GTTGAAACTGAGCGAAAAAGGC
Keap1	CTGCCCAATTCATGGCTCACA	CTTAGGGTGGATGCCTTCGAT
Nqo1	AGGATGGGAGGTACTCGAATC	TGCTAGAGATGACTCGGAAGG
Gclc	GGGGTGACGAGGTGGAGTA	GTTGGGGTTTGTCCTCTCCC
B2M	TTCTGGTGCTTGTCTCACTGA	CAGTATGTTCGGCTTCCCATTC

Supplementary table S2: List of primary and secondary antibodies for western blot and chromatin immunoprecipitation assay

Antibody name	Primary/ Secondary	Protein fraction	Application	Source
Gapdh/ B-actin	Primary	Total, Membrane	WB	Cell Signaling Tech
Acc-1	Primary	Total	WB	Cell Signaling Tech
pAcc-1	Primary	Total	WB	Cell Signaling Tech
Ppar-γ	Primary	Total	WB	Cell Signaling Tech
Srebp1c	Primary	Total	WB	Active Motif
			ChIP	Active Motif
p-Srebp1c		Total	WB	Cell Signaling Tech
Nrf2	Primary	Nuclear	WB	Gift from Dr. Schmidt's lab
			ChIP	Cell Signaling Tech
Gclc	Primary	Total	WB	Abcam
Anti-mouse	Secondary	-	WB	Sigma Aldrich
Anti-rat	Secondary	-	WB	Sigma Aldrich, St Louis, MO
Anti-rabbit	Secondary	-	WB	Sigma Aldrich, St Louis, MO

Supplementary table S3: Primer sequence for ChIP

Promoter	Predicted ARE (Considering Coding start site as +1)	Forward	Reverse
Srebp 1c	-120 to -130	TAGGCGAGCTGTCAGGAT	TCTCGGCCAGTGTCTGT

Supplementary table S4: Primer sequence for methylated DNA immunoprecipitation (MeDIP)

Promoter	Location (coding start site +1)	Number of CpG sites	Forward	Reverse
Srebp1c	-231 to -347	2	CAGCAAGACTAGGAAGTGAGTT	GGCCTTGGCTTCTTCTGTAT
Srebp1c	-1325 to -1456	2	CTGGGACAGGCTATTTGAGTT	GGCTTCACCAGGACACATT
Fas	-306 to -472	5	TGTTCCCTCTGGGTCCTAA	CAGTTGCCTACTGGATGCT
Fas	- 654 to -832	9	CAGCTTGGAGAAGGCAGATG	CTGGTCGAACACTTTGTAACCT
Nrf2	-1059 to-1169	4	GGTCACCACAACACGAACTA	GACTCTCAGGGTTCCTTTACAC

MANUSCRIPT 3:

PFOS INDUCES ADIPOGENESIS AND GLUCOSE UPTAKE IN ASSOCIATION WITH ACTIVATION OF NRF2 SIGNALING PATHWAY

Jialin Xu[1,2#], Prajakta Shimpi[2#], Laura Armstrong[2], Deanna Salter[2], and Angela L. Slitt[2]

[1]Institute of Biochemistry and Molecular Biology, College of Life and Health Sciences, Northeastern University, Shenyang, P. R. China, 110819

[2]Department of Biomedical and Pharmaceutical Sciences, University of Rhode Island, Kingston, RI 02881

# Both authors contributed equally to the manuscript

Manuscript under revision in *"Toxicology and Applied Pharmacology (TAAP)"* journal

3.1 ABSTRACT:

PFOS is a chemical of nearly ubiquitous exposure in humans. Recent studies have associated PFOS exposure to adipose tissue-related effects. The present study was to determine whether PFOS alters the process of adipogenesis in mouse and human preadipocytes and regulates insulin-stimulated glucose uptake. In murine-derived 3T3-L1 preadipocytes, PFOS enhanced hormone-induced differentiation to adipocytes and adipogenic gene expression, increased insulin-stimulated glucose uptake at concentrations ranging from 10 to 100 μM, and enhanced Glut4 and Insulin receptor substrate-1 expression. Nrf2, Nqo1 and Gclc were significantly induced in 3T3-L1 cells treated with PFOS, along with a robust induction of antioxidant response element (ARE) reporter in mouse embryonic fibroblasts isolated from ARE-hPAP transgenic mice by PFOS treatment. Chromatin immunoprecipitation assays further illustrated that PFOS increased Nrf2 binding to ARE sites in mouse Nqo1 promoter, suggesting that PFOS activated Nrf2 signaling in murine-derived preadipocytes. Additionally, PFOS administration in mice (0.1mg/kg BW/day) induced adipogenic gene expression and activated Nrf2 signaling in epididymal white adipose tissue. Moreover, human visceral preadipocytes illustrated that PFOS (5 and 50 μM) promoted adipogenesis and increased cellular lipid accumulation. It was observed that PFOS increased Nrf2 binding to ARE sites in association with Nrf2 signaling activation, induction of Ppar-γ

and Cebpα expression, and increased adipogenesis. This study points to a potential role PFOS in dysregulation of adipose tissue expandability, and warrants further investigations on the adverse effects of persistent pollutants on human health.

Key words: PFOS, Nrf2, Ppar-γ, adipogenesis, glucose uptake, ARE

3.2 INTRODUCTION

Perfluorooctanesulfonate (PFOS) and Perfluorooctanoic acid (PFOA) are organic fluoroalkyl chemicals widely used in industrial and consumer applications as powerful surfactants and building material components, as they are stable at high temperature and nonflammable (Olsen *et al.*, 2005). These two chemicals have been detected worldwide in the environment, including drinking water (Skutlarek *et al.*, 2006), atmosphere air (Shoeib *et al.*, 2005), soil, sediments (Boulanger *et al.*, 2005), and even the wildlife in the Antarctic Pole (Giesy and Kannan, 2001). Average human serum PFOS and PFOA content has decreased between 2000 and 2005 due to the phase out of perfluorooctanesulfonyl-fluoride (POSF, C8F17SO2F)-based materials by the primary global manufacturer, 3M Company, in May 2000 (Olsen *et al.*, 2007b), but the related health effects still remain a concern. Although have been banned in United States and Europe, PFOS and PFOS-related chemicals are still currently produced in China.

Importantly, PFOS and PFOA are readily absorbed and poorly eliminated from humans. Increased renal absorption via transport mechanisms is suspected to be the mechanism that contributes to the relatively long serum half-lives observed in humans (Olsen *et al.*, 2007a), which has been estimated to 5.4 (PFOS) and 3.8 (PFOA) years. Because of its persistence in the body and presence in populations across the world, it is important to assess potential health effects. Liver is the major organ affected by

exposure of PFOS in animal model, as it is known to deposit in liver and is associated with increased liver weight in rats, mice, and monkeys (Chang *et al.*, 2012; Wan *et al.*, 2012). Exposure of PFOS has been shown to induce further undesirable effects, such as increased hepatic lipid accumulation along with significant induction of CD36 and lipoprotein lipase (Lpl) expression, which resulted in disturbance of lipid metabolism and excessive fatty liver (Wan *et al.*, 2012). In addition, dietary administration of PFOS in mice (0.005%, w/w) for 10 days reduced serum cholesterol and triglycerides levels, and induced a moderate hepatomegaly (Qazi *et al.*, 2010). More recent publications reported that exposure of PFOS altered expression of genes mainly involved in lipid modulation, energy metabolism, reproduction, hormone regulation, suggesting a role for PFOS in regulating lipid metabolism and development (Hu *et al.*, 2005; Hagenaars *et al.*, 2008). The observed hepatomegaly that results from PFOS administration is due to peroxisome proliferator-activated receptor (Ppar) activation (Takacs and Abbott, 2007; Bjork and Wallace, 2009). Rosen *et al.* also reported that PFOS may modulate various gene expression related to lipid metabolism, inflammation, and xenobiotic metabolism via Ppar-α independent mechanisms, such as the modest activation of constitutive and rostane receptor (CAR) and Ppar-γ signaling pathway (Rosen *et al.*, 2010). And PFOA was reported to induce various xenobiotic metabolism genes, which were under the control of CAR and transcription factor of nuclear factor

erythoid 2-related factor 2 (Nrf2) (Rosen *et al.*, 2008). However, PFOS effects on adipogenesis and white adipose tissue expansion is still unknown.

Adipogenesis is a process involving sequential coordinated gene induction (Rosen and Spiegelman, 2000). CCAAT/enhancer-binding protein (Cebp) δ and Cebp-β induce the expression of Ppar-γ, which activates Cebp-α, and these two transcriptional factors can work in concert to maintain the differentiated status. Gain-of-function experiments that forced Ppar-γ and/or in combination with potential agonists demonstrated that non-adipogenic, fibroblast cells can be transdifferentiated to adipocytes (Wu *et al.*, 1995). Emerging data points to new regulators of Ppar-γ expression, such as transcription factor of Nrf2, regulated lipid metabolism and the process of adipogenesis (Shin *et al.*, 2007; Pi *et al.*, 2010). Classically, Nrf2 binds to antioxidant-responsive elements (ARE), induces expression of a battery of detoxification and antioxidant genes to counter cellular electrophilic and oxidative stress (Kensler *et al.*, 2007; Klaassen and Reisman, 2010). Pi *et al.* reported that an ARE element exists in mouse Ppar-γ promoter, and loss of Nrf2 reduced Ppar-γ expression and prevented the process of adipogenesis in 3T3-L1 preadipocytes (Pi *et al.*, 2010). This work provided a link between Nrf2 and adipogenesis. Other studies have demonstrated that too much Nrf2 activation can also perturb adipogeneis. An early study by Kensler described Nrf2 prevented

adipogenesis via modulating Aryl hydrocarbon receptor Signaling (Shin *et al.*, 2007). Our previous results demonstrated that enhanced Nrf2 activity via Keap1-knockdown inhibited white adipose tissue expansion and the adipocyte differentiation, suggesting the Nrf2-independent mechanism involved in Keap1-knockdown (Xu *et al.*, 2012). Additionally, PFOS increased cellular reactive oxygen species (ROS) content, induced the antioxidant signaling of Nrf2 and Heme oxygenase-1 (Ho-1) expression levels, suggesting the relationship between PFOS administration and Nrf2 signaling activation (Shi and Zhou, 2010) from *in vitro* study.

To evaluate the effect of PFOS on adipogenesis, and further explore its effect on regulating white adipose tissue expansion and the development of obesity, 3T3-L1 preadipocytes were induced to differentiation to adipocytes with the presence of PFOS. The cellular lipid content and adipogenic gene expression was evaluated. Additionally, glucose uptake was determined in the mature adipocytes with PFOS administration. Lastly, PFOS-induced adipogenic effects were also evaluated in a whole animal model with daily PFOS administration and in human visceral preadipocytes. The current study demonstrates that PFOS induces Nrf2 activation in association with promoting Ppar-γ and Cebp-α signaling, and induction of adipogenesis that increases lipid accumulation in 3T3-L1 preadipocytes. Moreover, pro-adipogenic effects were observed in human visceral preadipocytes exposed to PFOS.

3.3 MATERIALS AND METHODS

3.3.1 Chemicals. Heptadecaperfluorooctanesulfonic acid potassium salt (#77282, PFOS), insulin (#I6634), dexamethasone (#D4902, DEX) isobutylmethylxanthine (#I5879, IBMX), and Oil Red O (#O0625) were got from Sigma-Aldrich (St. Louis, MO). Ethanol, methanol, and isopropanol, MTT solution and other chemicals without specific illustration were got from Thermo Fisher Scientific Inc. (Waltham, MA)

3.3.2 Animals and PFOS administration. 10-week-old male C57BL/6 mice weighing approximately 30 grams were purchased from Charles River Laboratories (Wilmington, MA). The mice were housed under a controlled temperature (22-25 °C) with relative humidity (30-70%), lighting (12 hrs, light-dark cycles) environment and acclimated for 5 weeks on the standard rodent chow to allow for additional weight gain. At 15 weeks of age, the mice were then fed a purified rodent chow (AIN-93G Growth Purified Diet, TestDiet, St. Louis, MO). At 21 weeks of age, mice (n=8) were administered water as vehicle (Veh) via oral gavage (5mL/kg) or PFOS (0.1mg/kg, 5mL/kg) for 6 weeks. Body weight and food intake were monitored daily and recorded. Epididymal white adipose tissue (WAT) was collected, snap frozen with liquid nitrogen, and stored at -70°C until analysis. All procedures were conducted in accordance with the NIH Guidelines for the Care and Use of Laboratory Animals and were approved by the University of Rhode Island Animal Care and Use Committee.

3.3.3 Acute cytotoxicity assay. A minimum of 5 replicates of 7,500 3T3-L1 preadipocytes per well were plated in 96-well plates and allowed to adhere to the plate for approximately 12 hrs, at which time the media was removed and replaced with fresh media containing varying concentrations of PFOS in DMSO (1nM, 5nM, 10nM, 100nM, 500nM, 1μM, 5 μM, 10μM, 50μM, 100μM). Cells were subsequently incubated for an additional 48 hrs. Then 20 μL MTT solution (5 mg/mL in PBS) was added and the plate was incubated for another 3 hrs. The supernatant was removed carefully and 150 μL MTT solvent (4 mM HCl, 0.1% NP-40 in isopropanol) was added to each well. The plate was covered with foil and agitated on an orbital shaker for 15 mins. The cell viability was determined by measuring the absorbance at 590 nm with 620 nm as reference filter. Relative cell viability (%) was displayed using vehicle (0.1% DMSO)-treated samples as a standard.

3.3.4 Cell culture and 3T3-L1 pre-adipocyte differentiation. Mouse 3T3-L1 (ATCC® CL-173™) preadipocytes were obtained from ATCC (American Type Culture Collection, Manassas, VA, USA) and maintained in high-glucose DMEM medium supplemented with 10% fetal bovine serum (FBS). 3T3-L1 pre-adipocyte differentiation was induced according to the protocol described previously (Shin *et al.*, 2007; Xu *et al.*, 2012). Briefly, 2 days post 100% confluence, 3T3-L1 preadipocytes were stimulated to differentiation to adipocytes in a standard adipogenic differentiation

medium (DMEM containing 10%FBS, 10μg/mL insulin, 1μM DEX, 0.5mM IBMX), which was considered Day 0. Cells were cultured in the latter media for Days 0-3 and then cultured in DMEM containing 10%FBS and 10 μg/mL insulin for the remaining days. Media was refreshed every 2 days. Cell treatment and corresponding assay were described as **Figure 1A**.

3.3.5 Human visceral preadipocytes culture and induction to adipocytes. Poietics™ Human visceral preadipocytes (Donor #: 24711; Lot #:0000313366; Cat #: PT-5005) were obtained from Lonza (Lonza Walkersville, Inc., Walkersville, MD) and maintained in PBM-2 media according to the manufacturer's instructions. The preadipocytes were plated at 8,700 cells per well. Cells were induced to differentiation to adipocytes by switching with the differentiated media of PBM-2 supplementing with dexamethasone, isobutylmethylxanthine and insulinSingleQuots™ 24 hrs post 100% confluence and keep in the same media for the next 11 days. Cells were treated with DMSO (0.1%) or PFOS (5 or 50μM) in quadruplicates. Oil red O was used to image the lipid droplets. The cellular lipid was purified via isopropanol extraction and the lipid content was quantified spectrophotometrically at what 520 nm. Cell treatment and corresponding assay were described as **Figure 1B**.

3.3.6 RNA isolation and quantitative real-time PCR. Total RNA was isolated using TRIzol reagent (Invitrogen, CA) according to the manufacturer's instructions. One microgram of total RNA was converted to

cDNA and mRNA levels were quantified by quantitative real-time PCR using a Roche LightCycler 480 System (Roche Applied Science, Mannheim, Germany). SYBR green chemistry was used and relative target gene expression was normalized to 18S rRNA. The primers used are listed in Supplementary Table 1.

3.3.7 Oil Red O staining. 3T3-L1 preadipocytes or human visceral preadipocytes were induced to differentiation to adipocytes. The supernatant was removed and cell layer was washed twice with 2 mL ice-cold PBS. Cells were fixed with 10% formalin at 4°C for 30 mins, then stained with Oil Red O solution (six parts Oil Red O stock solution [0.5% Oil Red O in 100% isopropanol] and four parts H_2O) for 60 mins. Cells were counterstained with hematoxylin and mounted in glycerin jelly (Carolina Biological Supply Company, Burlington, NC).

3.3.8 Measurement of triglycerides in 3T3-L1 preadipocytes. 3T3-L1 preadipocytes plated on 60-mm dishes were induced to adipocytes for 8 days. Lipids were extracted according to a previous protocol (Xu *et al.*, 2012). Triglycerides content were determined with reagent kits (Pointe Scientific, Inc, MI), and the absorbance was measured spectrophotometrically at 520 nm. Relative triglycerides content (%) was displayed using differentiation medium containing 0.1% DMSO - treated cells as a standard.

3.3.9 Glucose uptake assay. Glucose uptake in 3T3-L1 mature

adipocytes was measured by using 2-[*N*-(7-nitrobenz-2-oxa-1,3-diazol-4-yl) amino]-2-deoxy-d-glucose (2-NBDG) according to the manufacturer's instructions (Cayman Chemical Company, MI). In brief, 3T3-L1 preadipocytes plated on 96-well fluorescent plates were induced to adipocytes as described above. At Day 11, cells were washed with PBS and then treated with serum-free DMEM containing PFOS (0 - 100μM) or DMSO (0.1%) for 5 hrs. Then cells were washed with sterilized PBS for 3 times, and stimulated with 100 nM insulin for 20 mins in KRPH buffer (20 mM HEPES, 5 mM KH_2PO_4, 1 mM $MgSO_4$, 1 mM $CaCl_2$, 136 mM NaCl, and 4.7 mM KCl, pH 7.4) with the presence of PFOS or DMSO, respectively. Glucose uptake was initiated by the addition of 100 μg/mL 2-NBDG to each well. The fluorescence activity was monitored at an excitation wavelength of 485 nm and an emission wavelength of 535 nm. At least eight replicates for each dosage was performed. Relative glucose uptake was displayed using vehicle-treated group as a standard.

3.3.10 hPAP induction assay. Mouse embryonic fibroblast (MEF) differentiation to adipocytes was performed as described elsewhere (Shin *et al.*, 2007; Xu *et al.*, 2012). MEFs were isolated from 13.5- to 15.5-d post coital mouse embryos from ARE-hPAP transgenic mice, then cells were cultured in DMEM supplemented with 10% FBS in 10 cm culture dishes (Johnson *et al.*, 2002). MEFs were collected and cultured in 6-well plate, 2 days post of 100% confluence, cells were switched to differentiated media

with DMEM containing 10% FBS, 10 μg/mL insulin, 1 μM DEX, 0.5 mM IBMX (Day 0). Three days later, cells were switched to media only containing 10% FBS and 10 μg/mL insulin for the remaining days. And four days post differentiation, total RNA was extracted and the relative mRNA levels of hPAP were measured using quantitative real-time PCR. The detailed design was described as **Figure 1C**.

3.3.11 Chromatin Immunoprecipitation (ChIP) assay. 3T3-L1 cells were induced to adipocytes as described above. Two days post differentiation to adipocytes, cells were harvested and the Chip assay was performed according to the manufacturer's instructions (Active Motif, Carlsbad, CA). Equal amount of sheared chromatin DNA (15 μg) was incubated with anti-Nrf2 antibody (Cell Signaling, Danvers, MA) or IgG as negative control overnight at 4°C. A portion of sheared chromatin DNA was preserved as input (10 μL). Purified DNA was PCR-amplified for 35 cycles (30 s at 94 °C, 30 s at 59 °C, and 30 s at 72 °C) with the primers that cover putative AREs sequences in mouse Nqo-1 promoter.

(Forward: 5'-GCAGTTTCTAAGAGCAGAACG-3')

(Reverse: 5'-GTAGATTAGTCCTCACTCAGCCG-3')

3.3.12 Statistical Analysis. Quantitative data were presented as average ± SE. Statistic differences were determined by a one-way ANOVA followed by a Duncan's Multiple Range *post hoc* test. All statistical tests with $P<0.05$ were considered significant.

3.4 RESULTS:

3.4.1 PFOS induces adipogenesis in 3T3-L1 preadipocytes. In order to explore the association of PFOS exposure and adipocyte differentiation, we determined the effect of PFOS concentrations on 3T3-L1 pre-adipocyte viability. No overt toxicity was observed at <50μM in the current study (**Figure 1D**). 3T3-L1 preadipocytes were differentiated to adipocytes in the presence of differentiated cocktail with or without PFOS. Oil Red O staining of mature lipid-containing adipocytes at Day 8 was performed to evaluate PFOS effects on adipogenesis. Figure 2A illustrates that high concentrations of PFOS (1-100μM) increased lipid accumulation in 3T3-L1 adipocytes compared to vehicle-treated group (**Figure 2A**). However, staining was similar between vehicle- and PFOS-treated groups treated with concentrations less than 1μM (1-500nM), except there was lower lipid content at the dosage of 5nM (**Figure, 2B,** data not shown). Similar to the observed staining, higher PFOS concentrations (1-50μM) increased triglyceride content in 3T3-L1 adipocytes by more than 20% above control, but this effect was not observed with the relatively lower PFOS concentrations (1-100 nM) (**Figure 2B**). The data suggest that PFOS has the potential to potentiate induction of mouse preadipocyte differentiation to mature adipocytes and promote lipid accumulation.

3.4.2 PFOS increases adipogenic gene expression in 3T3-L1 preadipocytes. The underlying molecular mechanisms for PFOS function

on adipogenesis were evaluated. 3T3-L1 preadipocytes were induced to adipocytes with PFOS administration for continuous 3 days, total RNA was extracted and the relative mRNA levels of genes related with adipogenesis of Cebp-α, Ppar-γ, Fabp4 and Lpl were determined. There is no significant difference for these four genes expression between vehicle- and PFOS-treated groups at Day1. After induction to adipocytes for 3 days (Day3), Cebp-α, Ppar-γ, Fabp4 and Lpl were significantly induced in both groups; with induction being significantly higher in PFOS-treated adipocytes than vehicle-treated group (increased by 32.2-, 14.2-, 8.6-, and 19.7-fold, respectively), suggesting PFOS increased adipogenic gene expression, which may contribute to the increased adipogenesis (**Figure 3A**). Additionally, the mRNA levels of Nrf2 and two target genes, Nqo1 and Gclc were determined. After 3 days of induction to adipocytes (Day 3), PFOS significantly increased Nrf2, Nqo1 and Gclc mRNA levels in 3T3-L1 adipocytes than vehicle-treated group by more than 15-fold, suggesting that PFOS has the potential to activate Nrf2 signaling in preadipocytes (**Figure 3B**).

3.4.3 PFOS promotes insulin-stimulated glucose uptake in 3T3-L1 adipocytes. In order to assess the metabolic consequence of PFOS treatment in 3T3-L1 preadipocytes, insulin-stimulated glucose uptake were monitored in vehicle- and PFOS-treated adipocytes. After 3T3-L1 preadipocytes were differentiated to adipocytes for 10 days, cells were

exposed to PFOS for 5 hrs, then 2-NBDG was added, and the fluorescence activity was monitored. There was no significant difference between the low dose PFOS treatments (1 and 5 μM) and vehicle-treated group. However, insulin-stimulated glucose uptake was significantly higher in PFOS-treated at the concentration of 10 μM than vehicle-treated group (by 26%). And a dose-dependent increase of glucose uptake by PFOS-treatment was observed, with the highest induction being at the dosage of 100 μM (61.0% higher than vehicle) (**Figure 4A**). The gene expression related to insulin signaling and glucose metabolism was monitored. Low dose PFOS treatment (1 μM) did not affect Ppar-γ, Srebp-1c, Glut4, Irs-1, and Insr gene expression. However, treatment with 10 or 50 μM PFOS increased Ppar-γ, Srebp-1c, Glut4 and Irs-1 expression compared to vehicle-treated group, but with similar Insr expression between vehicle- and PFOS-treated groups (**Figure 4B**). It was hypothesized that in the early induction process, PFOS might induce the antioxidant response, then leading to Nrf2 activation that augmented Ppar-γ induction (Shi and Zhou, 2010). PFOS (1 μM) did not induce Nrf2 or Nqo1 expression, but expression was induced by about 30% in cells treated with 10 and 50 μM PFOS, suggesting the potential role of PFOS activating Nrf2 signaling in mature adipocytes (**Figure 4C**).

3.4.4 Adipogenic gene expression and Nrf2 signaling is increased in white adipose tissue from mice administered PFOS. C57BL/6 male

mice were administered PFOS for 6 weeks (0.1mg/kg BW/day) and the transcript levels corresponding to adipogenesis and Nrf2 signaling were measured in epididymal WAT. PFOS significantly increased the expression of adipogenic genes, including Cebp- α, Ppar-γ, Fabp4 and Lpl in WAT (by 66.4%, 93.2%, 73.3%, and 67.6%). Srebp1c and Insr, related with insulin signaling, were significantly induced after PFOS administration (by 67.2% and 59.7%), along with the increasing tread of Glut4 and Irs-1 expression (by 44.1% and 25.9%) (**Figure 5A**). Additionally, PFOS significantly induced Nrf2, Nqo1 and Gclc mRNA levels (by 97.2%, 173.0% and 87.3%), suggesting enhanced Nrf2 signaling in WAT of mice administrated with PFOS. Expression of Ho-1, Multidrug resistance-associated protein (Mrp) 2, Mrp4, UDP-glucuronosyltransferase (Ugt) 1a6, and Superoxide dismutase-1 (Sod-1), which are highly associated with Nrf2 signaling (Thimmulappa *et al.*, 2002; Dreger *et al.*, 2009), were increased in the current study. PFOS decreased Cytochrome P450, family 7, subfamily A, polypeptide 1 (Cyp7a1) by 78.5% after PFOS treatment, which is consistent with the previous study (Chang *et al.*, 2009).

3.4.5 PFOS increased lipid accumulation in differentiated human visceral preadipocytes. Human visceral preadipocytes were obtained and differentiated to adipocytes, and cellular lipid content was evaluated by Oil red O staining. Eleven days post-differentiation, PFOS (5 and 50 μM) significantly increased staining in mature adipocytes (**Figure 6A**).

Furthermore, the stain was extracted and quantified spectrophotometrically. Figure 6B illustrates that PFOS increased staining in adipocytes by 48% at 5 μM and 40% at 50 μM, suggesting PFOS may increase adipogenesis in human visceral preadipocytes, contribute to enhance lipid accumulation in PFOS-treated group (**Figure 6B**).

3.4.6 PFOS increases Antioxidant Response Element activity and enhances Nrf2 enrichment at the ARE element in mouse Nqo1 promoter. Some recent work indicates that the Nrf2 pathway is inducible in MEFs and adipose tissue (Shin *et al.*, 2007; Xu *et al.*, 2012). In order to determine whether PFOS induces Nrf2 signaling and might increase adipogenesis via the Nrf2 signaling pathway, MEFs from ARE-hPAP transgenic mice (Johnson *et al.*, 2002) were isolated and differentiated to adipocytes with or without PFOS for 4 days. Next, hPAP mRNA levels were measured by quantitative real-time PCR. PFOS treatment (50 μM) doubled hPAP mRNA levels compared to vehicle controls (Figure 7), highly suggesting PFOS increased ARE binding activity (**Figure 7A**). Furthermore, to determine whether the increased ARE binding was via the increased Nrf2 binding in PFOS treatment, Chip assay was carried out. Figure 7B and 7C illustrate that two days into differentiation, PFOS increased Nrf2 binding to ARE sites in mouse Nqo1 promoter (by 31%), suggesting that Nrf2 binding was increased after PFOS treatment during the differentiation process (**Figure 7B, 7C**).

3.5 DISCUSSION:

PFOS has been manufactured for over 60 years. Epidemiological studies and recent research with PFOS primarily focuses on widespread exposure (Giesy and Kannan, 2001; Olsen *et al.*, 2005), hepatic effects in humans (Nelson *et al.*, 2010), primates (Chang *et al.*, 2012) and rodents (Wan *et al.*, 2012), and metabolic perturbations (Wan *et al.*, 2012). However, PFOS effects on adipogenesis or adipocyte health is largely undescribed, yet is of growing concern because of the growing population of obese people worldwide. In the current study, we demonstrated that PFOS augmented adipocyte differentiation, increased the expression of key transcription factors of Ppar-γ and Cebp-α involved in adipogenesis, and increased ARE binding activity and activation of Nrf2 signaling, which increase the binding to promoters for oxidative stress-related and adipogenic genes, suggesting the potential roles of PFOS regulating white adipose tissue expansion and the related obesity.

The activation of Ppar-γ by PFOS suggested that PFOS has Ppar-α independent mechanism, which is in agreement with the previous study (Rosen *et al.*, 2010). PFOS increased liver weight and caused hypertrophy, which related with the activation of peroxisome proliferator, consistent with the effects of Ppar-α activator WY14,643. Also, PFOS induced both mouse and human Ppar-α activation, but exerted a greater level of induction of mouse Ppar-α than human Ppar-α at similar

concentrations (Takacs and Abbott, 2007). It has been reported that PFOS increased Ppar-γ luciferance reporter plasmid activity at the concentration from 1 μM to 100 μM, with little toxicity at 250 μM (Takacs and Abbott, 2007), illustrated that the dose 50 μM used in the current study is the optimal concentration for PFOS treatment.

Ppar-γ activation is the key process for adipocyte differentiation in 3T3-L1 preadipocytes. Ppar-γ is needed for adipose tissue formation in mice, and in a loss-of-function experiment, adipocyte differentiation and white adipose tissue expansion was impaired, and did not develop glucose intolerance and insulin resistance, suggesting the central role for adipogenesis (Jones *et al.*, 2005). We failed to observe adipose tissue expansion in mice administered with PFOS (0.1 mg/kg BW/day) for 6 weeks (Data not shown). This lack of effect could be explained by the relatively low dose of PFOS has been used in the current study, but is consistent with other reports. Qazi *et al.* have used 0.005% (W/W) dietary treatment of PFOS for 10 days with male mice, resulted in significant reductions for serum cholesterol and triglycerides content (Qazi *et al.*, 2010). And male BALB/c mice fed with HFD with the exposure of PFOS at the dose of 5 or 20 mg/kg BW/day for 14 days, exhibited reduced serum lipid and lipoprotein content, but significantly increased hepatic lipid accumulation, probably via Pparα-independent pathway (Wang *et al.*, 2014). Also, compared to liver, PFOS deposits to a much lower concentration in white adipose tissue (Maestri *et*

al., 2006). So perhaps the low dose of PFOS administered might not have a positive induction in adipose tissue expansion *in vivo*, despite this treatment inducing adipogenic gene expression at transcriptional levels. The second possible reason is that PFOS has a potential function to induce Ppar-α activation (Shipley *et al.*, 2004). Increased Ppar-α in adipose tissue could induce lipolysis and promote β-oxidation (Reddy and Hashimoto, 2001; Goto *et al.*, 2011), which is beneficial to prevent the lipid accumulation to adipose tissue and decrease white adipose tissue mass. It was noted that contradict results have been reported that PFOS administration reduced white adipose tissue mass, the ventral fat was significantly reduced when mice treated with PFOS (20 mg/kg BW/day) for 14 days, even in normal diet and HFD-group, which related with the reduced secretion and impaired function of low density lipoproteins (Wang *et al.*, 2014).

It is interesting to note that PFOS increased insulin-stimulated glucose uptake in differentiated adipocytes. A previous study reported that higher serum PFOS concentration was positively associated with increased serum insulin levels and insulin resistance (Lin *et al.*, 2009), which contrasts with the current study. And Nelson *et al*. reported that higher serum PFOA and PFOS concentration was positively associated with serum cholesterol levels, but displayed a weak association with body weight and insulin resistance (Nelson *et al.*, 2010). Another *in vivo* study performed on rats,

which the pregnant rats were given with PFOS (0.5 or 1.5 mg/kg BW/day) from gestation day 0 to postnatal day 21. The pups displayed impaired glucose tolerance and enhanced insulin resistance index, suggesting PFOS disrupted insulin signaling in integrate animal study (Lv *et al.*, 2013). In the current *in vitro* study, we demonstrated that PFOS increased insulin-induced glucose uptake and increased gene expression related to insulin signaling. One possible reason is that PFOS increased adipogenesis in 3T3-L1 preadipocytes and enhanced adipogenesis increases capacity for glucose uptake (Nugent *et al.*, 2001). Also, enhanced Ppar-γ and Glut4 expression will help to promote glucose uptake, as well as improve insulin signaling and insulin-response activity. Our previous study reported that enhanced Nrf2 activity by Keap1-KD increased glucose tolerance, and increased insulin-stimulated Akt phosphorylation without Glut4 expression change (Xu *et al.*, 2013), suggesting activation Nrf2 can promote insulin signaling, contribute to positively regulate glucose uptake in differentiated 3T3-L1 preadipocytes.

The study herein reported that PFOS could induce Nrf2 activation in preadipocytes. PFOS administration has been shown to increase ROS production, which induces oxidative stress and activate Nrf2 signaling (Qian *et al.*, 2010). ARE consensus elements are the typical transcriptional factor binding sites, which are described to induce the antioxidant gene expression for Nrf2 target genes, such as Ho1, Gclc, Nqo1, and Multiple

resistance-associated proteins to provide a protective role against oxidative and cytochemical stress (Nguyen *et al.*, 2009). Also, ARE sites have been reported in the promoter of Pparγ and Cebpα, which are responsible for 3T3-L1 preadipocytes adipogenesis (Pi *et al.*, 2010). ARE binding was enhanced after PFOS treatment in MEFs isolated from transgenic mice that harbor a ARE sequence coupled to a hPAP reporter, suggesting activation of genes via ARE sites is a process that occurs via PFOS-induced adipogenesis. Chip assay revealed that PFOS treatment increased Nrf2 binding to ARE sites in the mouse Nqo1 promoter in 3T3-L1 cells cultured in induction media for 4 days, further confirming that PFOS administration can induce Nrf2 signaling via ARE binding during adipogenesis.

Overall, this study reported that novel effects of PFOS in inducing Ppar-γ and Cebp-α expression and adipogenesis, via enhancing ARE binding activity and Nrf2 signaling in preadipocytes (**Figure 7D**). Additionally, PFOS increased insulin-stimulated glucose uptake and increased gene expression related with insulin signaling. This study points out the potential roles of PFOS promoting adipose tissue differentiation and the related metabolic conditions of obesity consequentially.

3.6 ACKNOWLEDGEMENTS:

This work was supported by National Institute of Health [5R01ES016042] to AS, and in part, by Rhode Island IDeA Network of Biomedical Research Excellence [P20RR016457-10] from the National Center for Research Resources, National Institute of Health [5K22ES013782]. JX was also supported by the National Science Foundation of China [81570788 and 81341102], and Fundamental Research Funds for Northeastern University [N130220001].

3.7 REFERENCES:

Bjork, J. A., and Wallace, K. B. (2009). Structure-activity relationships and human relevance for perfluoroalkyl acid-induced transcriptional activation of peroxisome proliferation in liver cell cultures. *Toxicol Sci* 111, 89-99.

Boulanger, B., Vargo, J. D., Schnoor, J. L., and Hornbuckle, K. C. (2005). Evaluation of perfluorooctane surfactants in a wastewater treatment system and in a commercial surface protection product. *Environ Sci Technol* 39, 5524-5530.

Chang, S. C., Ehresman, D. J., Bjork, J. A., Wallace, K. B., Parker, G. A., Stump, D. G., and Butenhoff, J. L. (2009). Gestational and lactational exposure to potassium perfluorooctanesulfonate (K+PFOS) in rats: toxicokinetics, thyroid hormone status, and related gene expression. *Reprod Toxicol* 27, 387-399.

Chang, S. C., Noker, P. E., Gorman, G. S., Gibson, S. J., Hart, J. A., Ehresman, D. J., and Butenhoff, J. L. (2012). Comparative pharmacokinetics of perfluorooctanesulfonate (PFOS) in rats, mice, and monkeys. *Reprod Toxicol* 33, 428-440.

Dreger, H., Westphal, K., Weller, A., Baumann, G., Stangl, V., Meiners, S., and Stangl, K. (2009). Nrf2-dependent upregulation of antioxidative enzymes: a novel pathway for proteasome inhibitor-mediated cardioprotection. *Cardiovasc Res* 83, 354-361.

Giesy, J. P., and Kannan, K. (2001). Global distribution of perfluorooctane sulfonate in wildlife. *Environ Sci Technol* 35, 1339-1342.

Goto, T., Lee, J. Y., Teraminami, A., Kim, Y. I., Hirai, S., Uemura, T., Inoue, H., Takahashi, N., and Kawada, T. (2011). Activation of peroxisome proliferator-activated receptor-alpha stimulates both differentiation and fatty acid oxidation in adipocytes. *J Lipid Res* 52, 873-884.

Hagenaars, A., Knapen, D., Meyer, I. J., van der Ven, K., Hoff, P., and De Coen, W. (2008). Toxicity evaluation of perfluorooctane sulfonate (PFOS) in the liver of common carp (Cyprinus carpio). *Aquat Toxicol* 88, 155-163.

Hu, W., Jones, P. D., Celius, T., and Giesy, J. P. (2005). Identification of genes responsive to PFOS using gene expression profiling. *Environ Toxicol Pharmacol* 19, 57-70.

Johnson, D. A., Andrews, G. K., Xu, W., and Johnson, J. A. (2002). Activation of the antioxidant response element in primary cortical neuronal cultures derived from transgenic reporter mice. *J Neurochem* 81, 1233-1241.

Jones, J. R., Barrick, C., Kim, K. A., Lindner, J., Blondeau, B., Fujimoto, Y., Shiota, M., Kesterson, R. A., Kahn, B. B., and Magnuson, M. A. (2005). Deletion of PPARgamma in adipose tissues of mice protects against high fat diet-induced obesity and insulin resistance. *Proc Natl Acad Sci U S A* 102, 6207-6212.

Kensler, T. W., Wakabayashi, N., and Biswal, S. (2007). Cell survival responses to environmental stresses via the Keap1-Nrf2-ARE pathway. *Annu Rev Pharmacol Toxicol* 47, 89-116.

Klaassen, C. D., and Reisman, S. A. (2010). Nrf2 the rescue: effects of the antioxidative/electrophilic response on the liver. *Toxicol Appl Pharmacol* 244, 57-65.

Lin, C. Y., Chen, P. C., Lin, Y. C., and Lin, L. Y. (2009). Association among serum perfluoroalkyl chemicals, glucose homeostasis, and metabolic syndrome in adolescents and adults. *Diabetes Care* 32, 702-707.

Lv, Z., Li, G., Li, Y., Ying, C., Chen, J., Chen, T., Wei, J., Lin, Y., Jiang, Y., Wang, Y., Shu, B., Xu,

B., and Xu, S. (2013). Glucose and lipid homeostasis in adult rat is impaired by early-life exposure to perfluorooctane sulfonate. *Environ Toxicol* 28, 532-542.

Maestri, L., Negri, S., Ferrari, M., Ghittori, S., Fabris, F., Danesino, P., and Imbriani, M. (2006). Determination of perfluorooctanoic acid and perfluorooctanesulfonate in human tissues by liquid chromatography/single quadrupole mass spectrometry. *Rapid Commun Mass Spectrom* 20, 2728-2734.

Nelson, J. W., Hatch, E. E., and Webster, T. F. (2010). Exposure to polyfluoroalkyl chemicals and cholesterol, body weight, and insulin resistance in the general U.S. population. *Environ Health Perspect* 118, 197-202.

Nguyen, T., Nioi, P., and Pickett, C. B. (2009). The Nrf2-antioxidant response element signaling pathway and its activation by oxidative stress. *J Biol Chem* 284, 13291-13295.

Nugent, C., Prins, J. B., Whitehead, J. P., Savage, D., Wentworth, J. M., Chatterjee, V. K., and O'Rahilly, S. (2001). Potentiation of glucose uptake in 3T3-L1 adipocytes by PPAR gamma agonists is maintained in cells expressing a PPAR gamma dominant-negative mutant: evidence for selectivity in the downstream responses to PPAR gamma activation. *Mol Endocrinol* 15, 1729-1738.

Olsen, G. W., Burris, J. M., Ehresman, D. J., Froehlich, J. W., Seacat, A. M., Butenhoff, J. L., and Zobel, L. R. (2007a). Half-life of serum elimination of perfluorooctanesulfonate,perfluorohexanesulfonate, and perfluorooctanoate in retired fluorochemical production workers. *Environ Health Perspect* 115, 1298-1305.

Olsen, G. W., Huang, H. Y., Helzlsouer, K. J., Hansen, K. J., Butenhoff, J. L., and Mandel, J. H. (2005). Historical comparison of perfluorooctanesulfonate, perfluorooctanoate, and other fluorochemicals in human blood. *Environ Health Perspect* 113, 539-545.

Olsen, G. W., Mair, D. C., Reagen, W. K., Ellefson, M. E., Ehresman, D. J., Butenhoff, J. L., and Zobel, L. R. (2007b). Preliminary evidence of a decline in perfluorooctanesulfonate (PFOS) and perfluorooctanoate (PFOA) concentrations in American Red Cross blood donors. *Chemosphere* 68, 105-111.

Pi, J., Leung, L., Xue, P., Wang, W., Hou, Y., Liu, D., Yehuda-Shnaidman, E., Lee, C., Lau, J., Kurtz, T. W., and Chan, J. Y. (2010). Deficiency in the nuclear factor E2-related factor-2 transcription factor results in impaired adipogenesis and protects against diet-induced obesity. *J Biol Chem* 285, 9292-9300.

Qazi, M. R., Abedi, M. R., Nelson, B. D., DePierre, J. W., and Abedi-Valugerdi, M. (2010). Dietary exposure to perfluorooctanoate or perfluorooctane sulfonate induces hypertrophy in centrilobular hepatocytes and alters the hepatic immune status in mice. *Int Immunopharmacol* 10, 1420-1427.

Qian, Y., Ducatman, A., Ward, R., Leonard, S., Bukowski, V., Lan Guo, N., Shi, X., Vallyathan, V., and Castranova, V. (2010). Perfluorooctane sulfonate (PFOS) induces reactive oxygen species (ROS) production in human microvascular endothelial cells: role in endothelial permeability. *J Toxicol Environ Health A* 73, 819-836.

Reddy, J. K., and Hashimoto, T. (2001). Peroxisomal beta-oxidation and peroxisome proliferator-activated receptor alpha: an adaptive metabolic system. *Annu Rev Nutr* 21, 193-230.

Rosen, E. D., and Spiegelman, B. M. (2000). Molecular regulation of adipogenesis. *Annu Rev Cell Dev Biol* 16, 145-171.

Rosen, M. B., Lee, J. S., Ren, H., Vallanat, B., Liu, J., Waalkes, M. P., Abbott, B. D., Lau, C., and

Corton, J. C. (2008). Toxicogenomic dissection of the perfluorooctanoic acid transcript profile in mouse liver: evidence for the involvement of nuclear receptors PPAR alpha and CAR. *Toxicol Sci* 103, 46-56.

Rosen, M. B., Schmid, J. R., Corton, J. C., Zehr, R. D., Das, K. P., Abbott, B. D., and Lau, C. (2010). Gene Expression Profiling in Wild-Type and PPARalpha-Null Mice Exposed to Perfluorooctane Sulfonate Reveals PPARalpha-Independent Effects. *PPAR Res* 2010.

Shi, X., and Zhou, B. (2010). The role of Nrf2 and MAPK pathways in PFOS-induced oxidative stress in zebrafish embryos. *Toxicol Sci* 115, 391-400.

Shin, S., Wakabayashi, N., Misra, V., Biswal, S., Lee, G. H., Agoston, E. S., Yamamoto, M., and Kensler, T. W. (2007). NRF2 modulates aryl hydrocarbon receptor signaling: influence on adipogenesis. *Mol Cell Biol* 27, 7188-7197.

Shipley, J. M., Hurst, C. H., Tanaka, S. S., DeRoos, F. L., Butenhoff, J. L., Seacat, A. M., and Waxman, D. J. (2004). trans-activation of PPARalpha and induction of PPARalpha target genes by perfluorooctane-based chemicals. *Toxicol Sci* 80, 151-160.

Shoeib, M., Harner, T., Wilford, B. H., Jones, K. C., and Zhu, J. (2005). Perfluorinated sulfonamides in indoor and outdoor air and indoor dust: occurrence, partitioning, and human exposure. *Environ Sci Technol* 39, 6599-6606.

Skutlarek, D., Exner, M., and Farber, H. (2006). Perfluorinated surfactants in surface and drinking waters. *Environ Sci Pollut Res Int* 13, 299-307.

Takacs, M. L., and Abbott, B. D. (2007). Activation of mouse and human peroxisome proliferator-activated receptors (alpha, beta/delta, gamma) by perfluorooctanoic acid and perfluorooctane sulfonate. *Toxicol Sci* 95, 108-117.

Thimmulappa, R. K., Mai, K. H., Srisuma, S., Kensler, T. W., Yamamoto, M., and Biswal, S. (2002). Identification of Nrf2-regulated genes induced by the chemopreventive agent sulforaphane by oligonucleotide microarray. *Cancer Res* 62, 5196-5203.

Wan, H. T., Zhao, Y. G., Wei, X., Hui, K. Y., Giesy, J. P., and Wong, C. K. (2012). PFOS-induced hepatic steatosis, the mechanistic actions on beta-oxidation and lipid transport. *Biochim Biophys Acta* 1820, 1092-1101.

Wang, L., Wang, Y., Liang, Y., Li, J., Liu, Y., Zhang, J., Zhang, A., Fu, J., and Jiang, G. (2014). PFOS induced lipid metabolism disturbances in BALB/c mice through inhibition of low density lipoproteins excretion. *Sci Rep* 4, 4582.

Wu, Z., Xie, Y., Bucher, N. L., and Farmer, S. R. (1995). Conditional ectopic expression of C/EBP beta in NIH-3T3 cells induces PPAR gamma and stimulates adipogenesis. *Genes & development* 9, 2350-2363.

Xu, J., Donepudi, A. C., Moscovitz, J. E., and Slitt, A. L. (2013). Keap1-knockdown decreases fasting-induced fatty liver via altered lipid metabolism and decreased fatty acid mobilization from adipose tissue. *PLoS One* 8, e79841.

Xu, J., Kulkarni, S. R., Donepudi, A. C., More, V. R., and Slitt, A. L. (2012). Enhanced Nrf2 activity worsens insulin resistance, impairs lipid accumulation in adipose tissue, and increases hepatic steatosis in leptin-deficient mice. *Diabetes* 61, 3208-3218.

3.8 FIGURE LEGENDS:

Figure 1. MTT assay of PFOS on 3T3-L1 preadipocytes. The illustration of study design on **(A)** 3T3-L1 preadipocytes, **(B)** human visceral preadipocytes, and **(C)** mouse embryonic fibroblasts. **(D)** 3T3-L1 preadipocytes were exposed to PFOS at concentration of 1nM, 5nM, 10nM, 100nM, 500nM, 1μM, 5μM, 10μM, 50μM, 100μM or DMSO in DMEM with 10% FBS for 48 hrs. PFOS toxicity at different dosage was determined by MTT assay. N=5. *, P<0.05, PFOS-treated vs. vehicle (**Veh**).

Figure 2. Non-cytotoxic levels of PFOS enhances lipid content in differentiated 3T3-L1 preadipocytes. Cells were differentiated 2 days post 100% confluences (Day 0) by switching with differentiated media containing 10μg/mL insulin, 1μM dexamethasone, 0.5 mM isobutylmethylxanthine in DMEM with 10% FBS for the first 3 days; then switch to media only containing 10 μg/mL insulin in DMEM with 10% FBS for the additional 5 days. Indicated concentration of PFOS or vehicle was included in media from Day 0 to Day 8. **(A)** Representative images of Oil red O staining of 3T3-L1 preadipocytes at indicated concentration of PFOS. **(B)** Lipids were extracted from differentiated 3T3-L1 adipocytes by using chloroform/ methanol mixture, and triglycerides (TG) content was determined spectrophotometrically. Relative triglycerides content (%) was displayed using differentiated media containing DMSO (0.1%) - treated cells as a standard (**Veh**). *, P<0.05, PFOS-treated vs. vehicle (**Veh**).

Figure 3. PFOS increases adipogenic gene expression and induced Nrf2 signaling in 3T3-L1 preadipocytes. 3T3-L1 preadipocytes were induced to differentiation to adipocytes with or without PFOS (50 μM) for 3 days. Total RNA was extracted at the indicated time. Relative mRNA levels were quantified by quantitative real-time PCR. PFOS increased adipogenic gene expression of Cebp-α, Ppar-γ, Fabp4, Lpl **(A),** and increased Nrf2 signaling of Nrf2, Nqo1, Gclc **(B)** mRNA levels in 3T3-L1 preadipocytes All data were normalized to 18S rRNA levels. *, P<0.05, PFOS-treated vs. vehicle (**Veh**)..

Figure 4. PFOS promotes insulin-stimulated glucose uptake in 3T3-L1 adipocytes. (A) 3T3-L1 preadipocytes were induced to differentiation to adipocytes for 10 days, then treated with PFOS (1, 5, 10, 50, 100 μM) for 5 hrs. Glucose uptake of differentiated 3T3-L1 preadipocytes was determined by using 2-NBDG according to the manufactory instruction. The fluorescence activity was monitored at an excitation wavelength of 485 nm and an emission wavelength of 535 nm. Relative glucose uptake was displayed using vehicle-treated group as a standard. Total RNA was extracted from 3T3-L1 adipocytes after treated with PFOS (10 μM or 50 μM) for 5 hrs. Relative mRNA levels of **(B)** Ppar-γ, Srebp-1c, Glut4, Irs-1, Insr and **(C)** Nrf2, Nqo1 were quantified by quantitative real-time PCR. All

data were normalized to 18S rRNA levels. *, P<0.05, PFOS-treated vs. vehicle (**Veh**).

Figure 5. Adipogenic gene expression and Nrf2 signaling of Nrf2 and Nqo1 expression increase in white adipose tissue (WAT) from mice administered PFOS. Mice were administrated with PFOS (0.1mg/kg BW/day) for 6 weeks. Epididymal white adipose tissue was collected and total RNA was extracted. **(A, B)** Relative mRNA levels of the indicated gene were quantified by quantitative real-time PCR. All data were normalized to 18S rRNA levels. *, P<0.05, PFOS-treated vs. vehicle (**Veh**).

Figure 6. PFOS increased lipid accumulation in differentiated human visceral preadipocytes. Human visceral preadipocytes obtained from Lonza were induced to differentiation to adipocytes by switch with the differentiated media contain dexamethasone, isobutylmethylxanthine and insulinSingleQuots^{TM} according to the manufacturer's instructions, with PFOS (5 or 50 μM) or not (0.1% DMSO) for 11 days. **(A)** Representative images of Oil Red O staining of differentiated human visceral preadipocytes treated with PFOS at indicated concentration. **(B)** Staining of lipids was extracted from differentiated human visceral preadipocytes via isopropanol isolation, and the lipid content was determined spectrophotometrically. Relative lipid content (%) was displayed using differentiated media

containing DMSO (0.1%) - treated cells as a standard (**Veh**). *, P<0.05, PFOS-treated vs. vehicle (**Veh**).

Figure 7. PFOS increases hPAP expression and enhances Nrf2 enrichment at ARE sites in mouse Nqo1 promoter. **(A)** Mouse embryonic fibroblasts isolated from ARE-hPAP transgenic mice were induced to differentiation to adipocytes for 4 days, then incubated with PFOS (50 μM) for additional 4 days. Total RNA was extracted and hPAP mRNA levels were quantified by quantitative real-time PCR. All data were normalized to 18S rRNA levels. *, P<0.05, PFOS-treated vs. vehicle (**Veh**). **(B)** 3T3-L1 cells were induced to differentiation for 2 days. Cells were collected for chromatin immunoprecipitation assays using either Nrf2 antibody or IgG as the negative control. A primer targeted for antioxidant response element in mouse Nqo1 promoter was used for PCR amplification. Non-immunoprecipitated chromation (1%) was used as an input control. **(C)** Relative ChIP signal for PFOS function on Nrf2 enrichment to ARE element of mouse Nqo1 promoter. **(D)** The work-flow for PFOS increased adipogenesis via activating Nrf2 signaling and inducing Cebp-α, Ppar-γ expression in preadipocytes.

3.9 FIGURES:

Figure 1: Illustration of study design and MTT assay of PFOS on 3T3-L1 preadipocytes

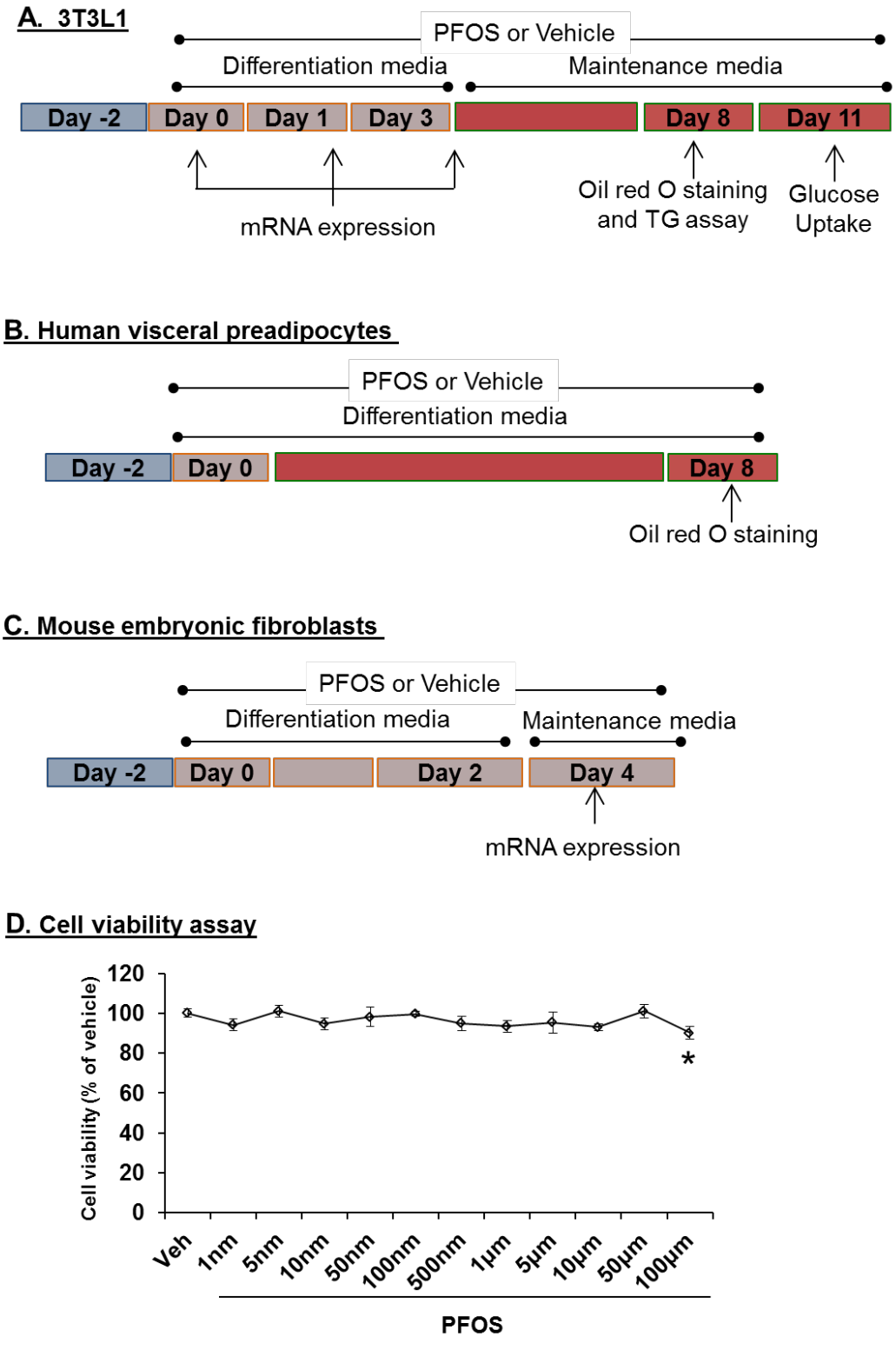

Figure 2: Non-cytotoxic levels of PFOS enhances lipid content in differentiated 3T3-L1 preadipocytes

A. Oil Red O Staining

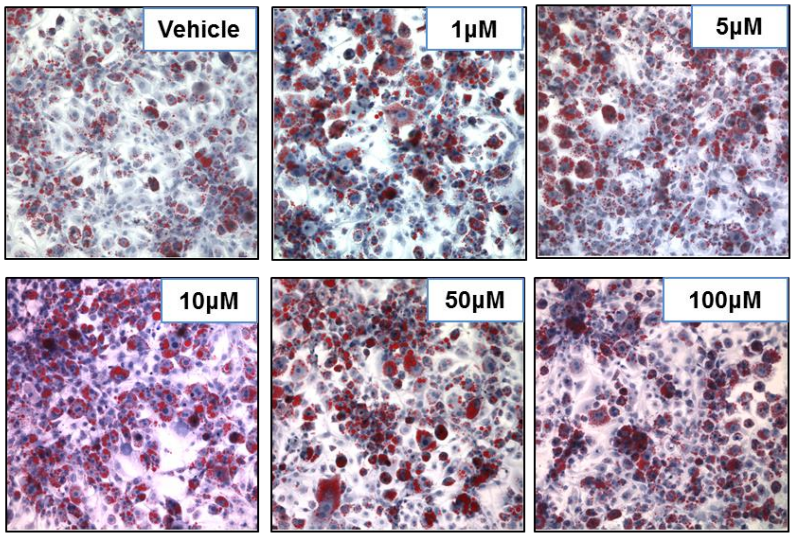

B. Triglyceride

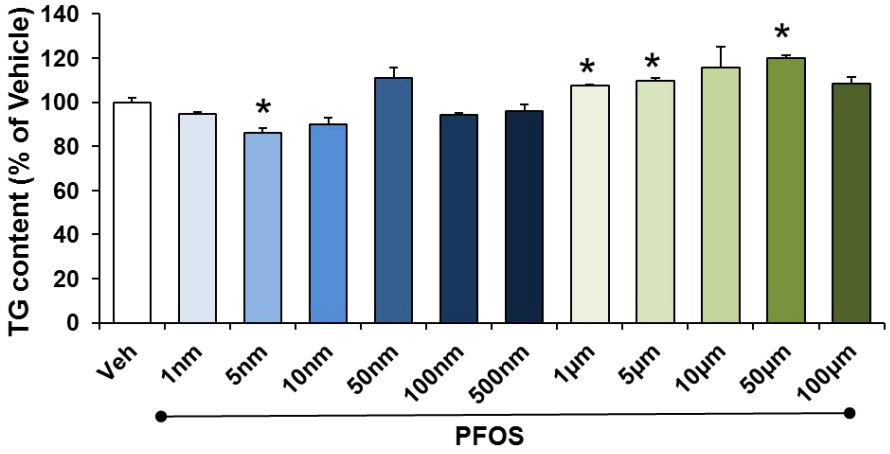

Figure 3: PFOS increases adipogenic gene expression and induced Nrf2 signaling in 3T3-L1 preadipocytes

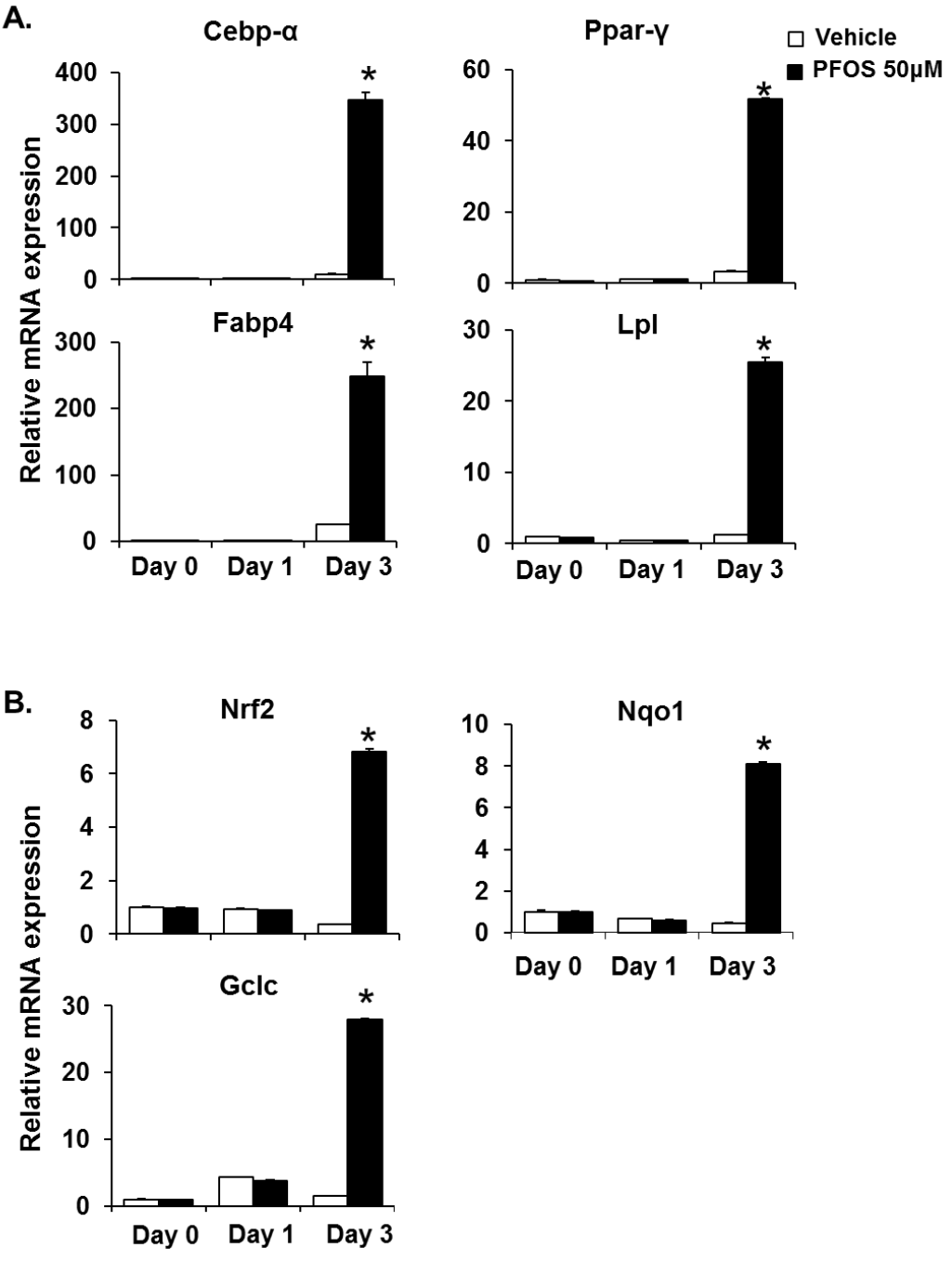

Figure 4: PFOS promotes insulin-stimulated glucose uptake in 3T3-L1 preadipocytes

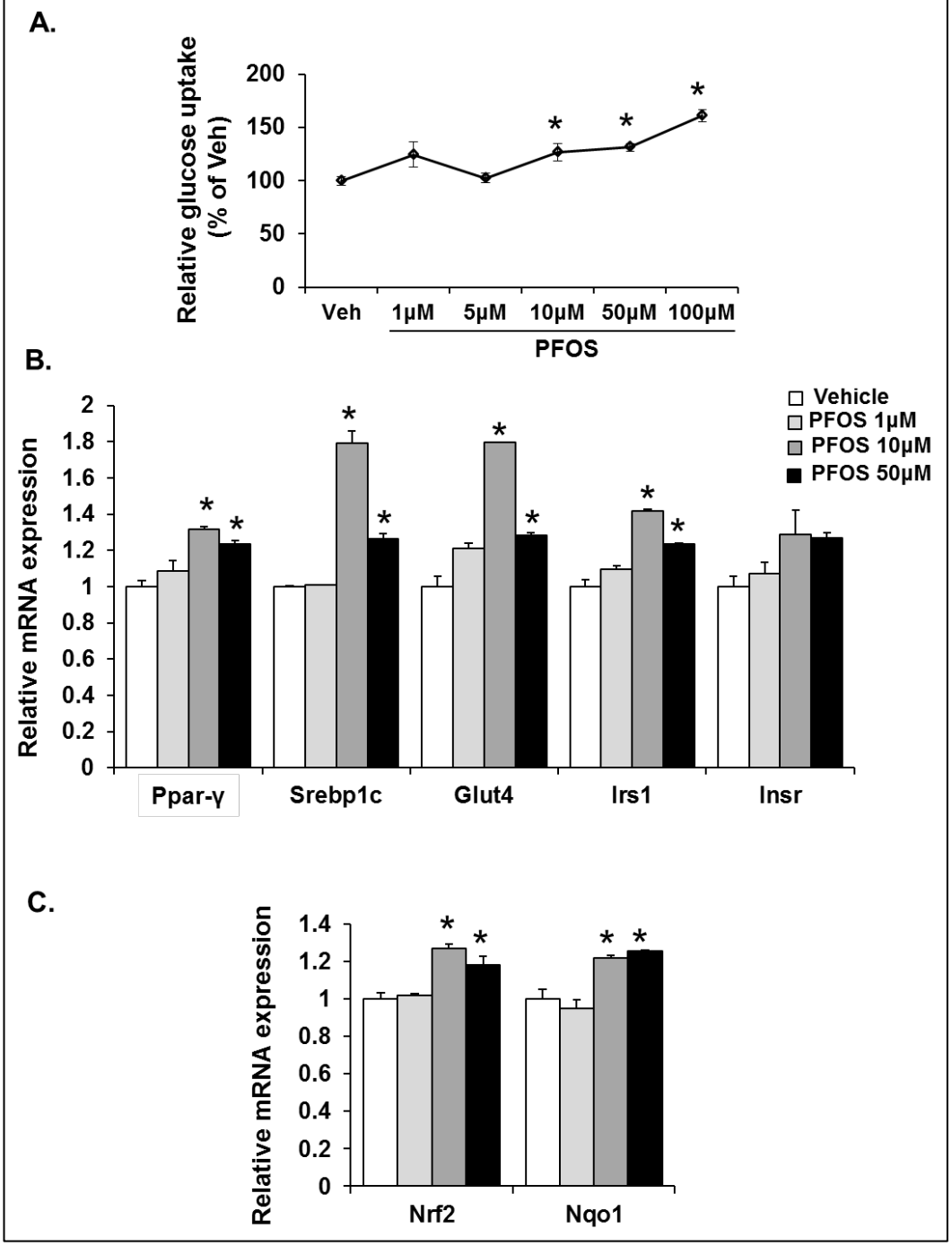

Figure 5: Adipogenic gene expression and Nrf2 signaling of Nrf2 and Nqo1 expression increase in white adipose tissue (WAT) from mice administered PFOS

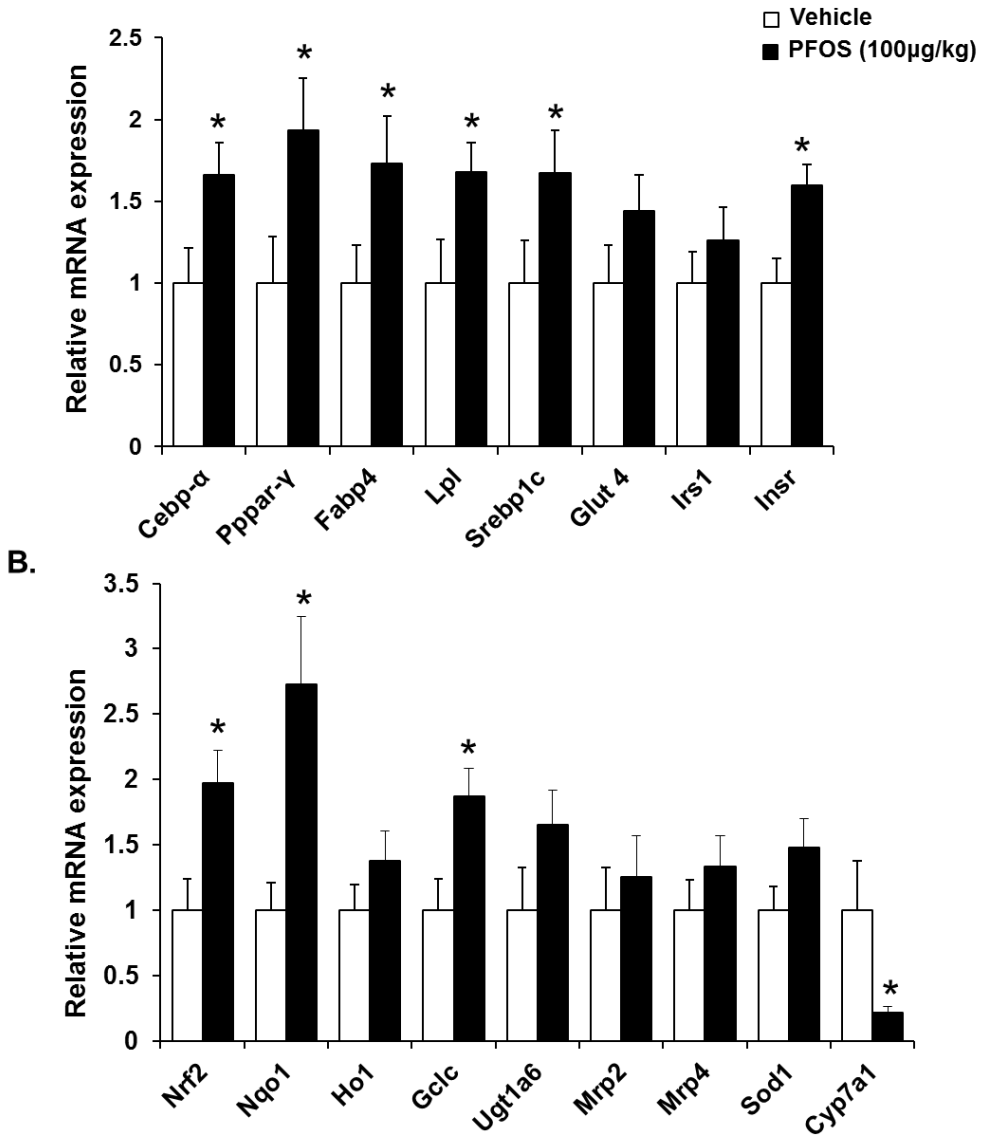

Figure 6: PFOS increased lipid accumulation in differentiated human visceral preadipocytes

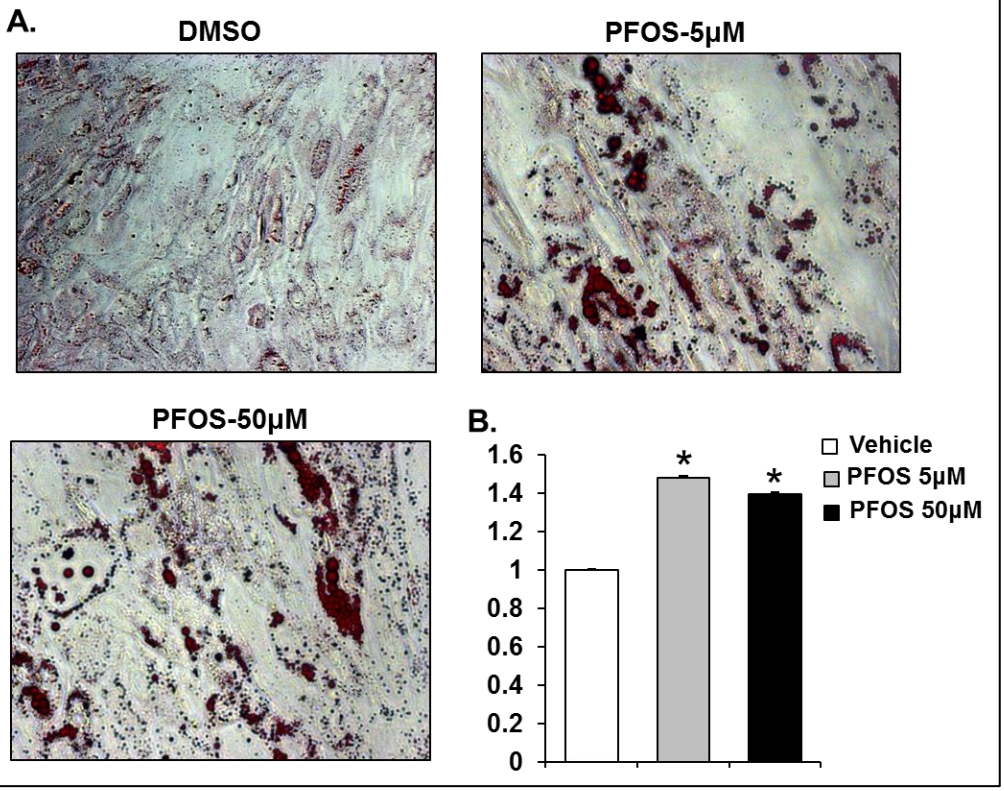

Figure 7: PFOS increases hPAP expression and enhances Nrf2 enrichment at ARE sites in mouse Nqo1 promoter

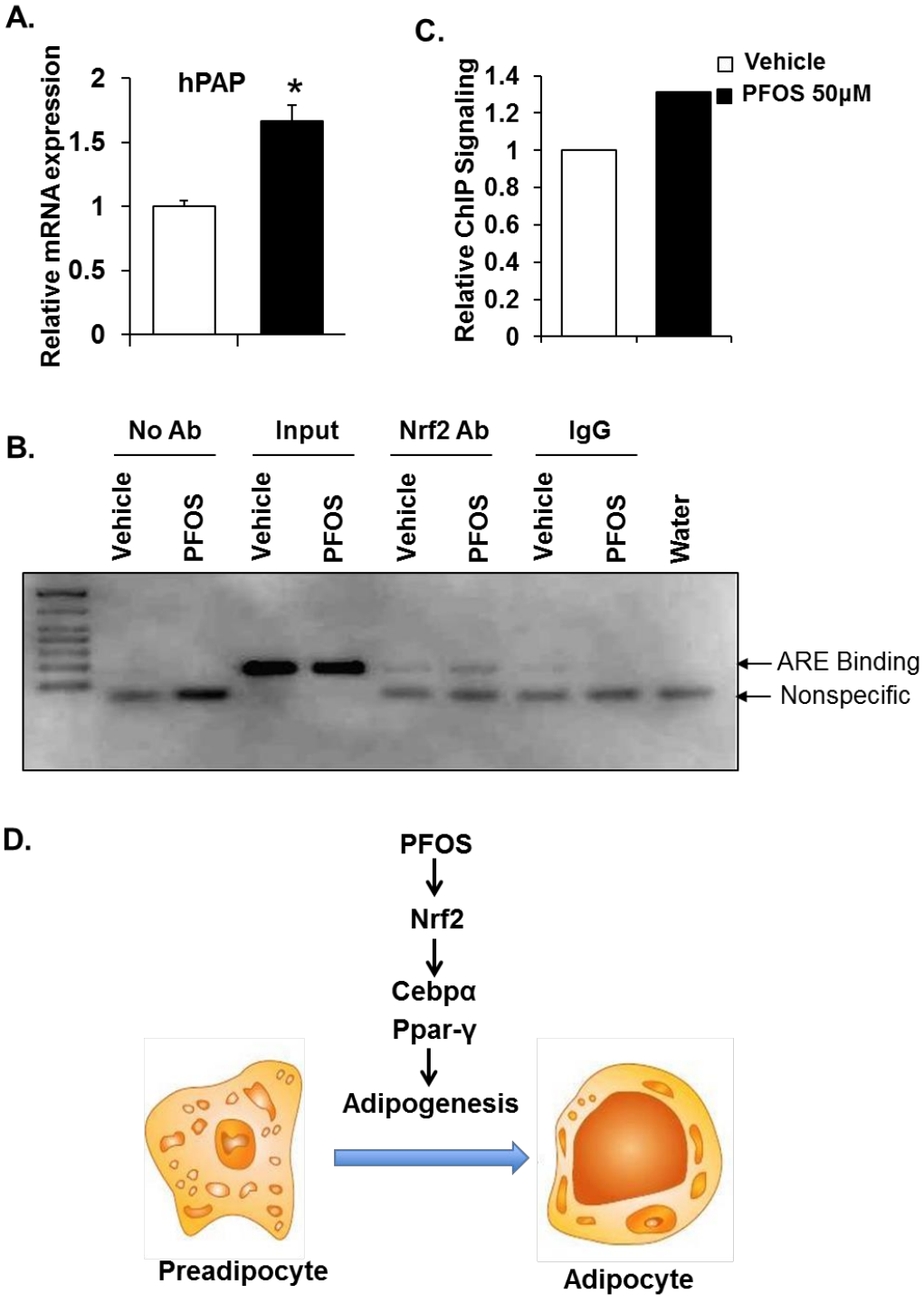

3.10 SUPPLEMENTARY MATERIALS:

Supplementary table 1. Primer sequences for quantitative RT-PCR

Genes	Forward	Reverse
Cebp-α	CAAGAACAGCAACGAGTACCG	GTCACTGGTCAACTCCAGCAC
β2m	TTCTGGTGCTTGTCTCACTGA	CAGTATGTTCGGCTTCCCATTC
Fabp4	AAGGTGAAGAGCATCATAACCCT	TCACGCCTTTCATAACACATTCC
Glut4	GTGACTGGAACACTGGTCCTA	CCAGCCACGTTGCATTGTAG
Gclc	GGGGTGACGAGGTGGAGTA	GTTGGGGTTTGTCCTCTCCC
hPAP	TTGCCCCAAATCTCAACTTC	TGGGTAGCTGGGACTACAGG
Insr	ATGGGCTTCGGGAGAGGAT	GGATGTCCATACCAGGGCAC
Irs-1	TCTACACCCGAGACGAACACT	TGGGCCTTTGCCCGATTATG
Nqo1	AGGATGGGAGGTACTCGAATC	TGCTAGAGATGACTCGGAAGG
LPL	GGGAGTTTGGCTCCAGAGTTT	TGTGTCTTCAGGGGTCCTTAG
Nrf2	TCTTGGAGTAAGTCGAGAAGTGT	GTTGAAACTGAGCGAAAAAGGC
Ppar-γ	CTCTGTTTTATGCTGTTATGGGTGA	GGTCAACAGGAGAATCTCCCAG
Srebp-1c	GCAGCCACCATCTAGCCTG	CAGCAGTGAGTCTGCCTTGAT
18S	AGTCCCTGCCCTTTGTACACA	CGATCCGAGGGCCTCACTA

SUMMARY AND CONCLUSION

1. Perinatal peripubertal exposure of bisphenol A increases predisposition to NAFLD, in younger as well as adult mice. Developmental exposure of environmental chemical like bisphenol A exerts epigenetic modification of lipogenic genes**.** This gives a novel plausible mechanism of involvement of early age epigenetic imprinting for rising prevalence of childhood obesity. Childhood lipid homeostasis disturbances may have its roots in perinatal toxicity of environmental chemicals.
2. PFOS exposure augmented differentiation of preadipocytes to adipocytes, hence increased overall fat cell number. Thus, indirectly study has demonstrated obesogenic property of PFOS. PFOS also increased glucose uptake in adipocytes.
3. In both BPA induced hepatic steatosis and PFSO induced adipogensis, activation of Nrf2 was evident, supporting recent literature stating role of Nrf2 in lipid homeostasis. Using BPA/ PFOS as a model compounds, novel mechanism of environmental lipid disturbances through Nrf2 mediation were elucidated.

APPENDIX 1:

Objective: Studying the hepatic lipid accumulation with short-term high fat diet feeding in Keap1 knockdown (Keap1 KD) mice

Experimental design: Nine week old WT and Keap1 KD mice were fed 10% or 60% kCal fat diet for 5 weeks, and then euthanized to collect organs. Tissue and serum lipid levels (TG, FFA, LDL/HDL) were detected by commercial kits. For all the figures, differences between the groups were calculated by two-way ANOVA followed by Tukey's multiple comparison tests. Asterisk * represents significant difference between WT and Keap1 KD mice, whereas # represents significant difference between SD and HFD groups.

Synopsis: As elaborated in all the manuscripts in this thesis, elucidating role of Nrf2 in lipid accumulation is one of the primary goals of my research. In this project, mice having diminished expression of Keap1 protein, and subsequently constitutive activation of Nrf2 were utilized. After 5 weeks on HFD, these mice appeared to be protected from lipid accumulation in liver. Keap1 KD mice fed SD as well as HFD contained less hepatic lipids as compared to WT controls (App 1 fig 2). TG content of the white adipose tissue, on the contrary, was higher in Keap1 KD mice relative to controls, on both diets. On both diets, Keap1 KD mice demonstrated increasing trend in LDL/HDL ratio (App 1 fig 2). Lipogenic target mRNA and protein expression was decreased in Keap1 KD mice on SD, and the expression was further diminished in HFD fed groups (App 1 fig 4 and 5). Fatty acid oxidation target expression data was inconclusive. Keap1 KD mice demonstrated high pAmpk

α to Ampk α ratio, and this change was higher with HFD (App 1 fig 6). Ratio of pIrs1 to total Irs1 decreased Keap1 KD in SD fed group, but not in HFD fed group, compared to respective controls (App 1 fig 6).

Appendix 1 figure 1: Body, liver and WAT weight of C57BL/6 (WT) and Keap1 KD mice fed a 10% kCal low fat diet (SD) or 60% kCal high fat diet (HFD)

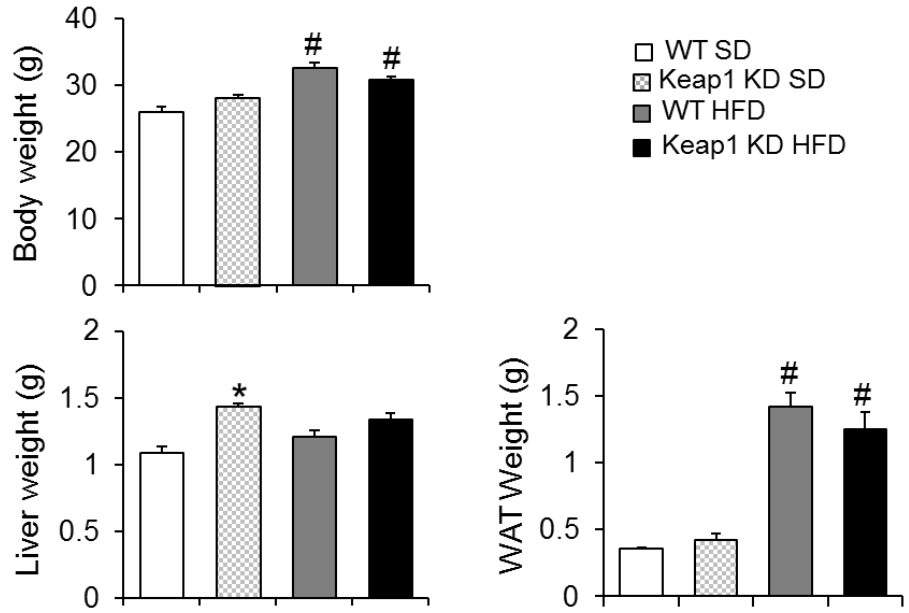

Appendix 1 figure 2: Hepatic, WAT and serum triglyceride (TG), free fatty acid (FFA) content in C57BL/6 (WT) and Keap1 KD mice fed a 10% kCal low fat diet (SD) or 60% kCal high fat diet (HFD).

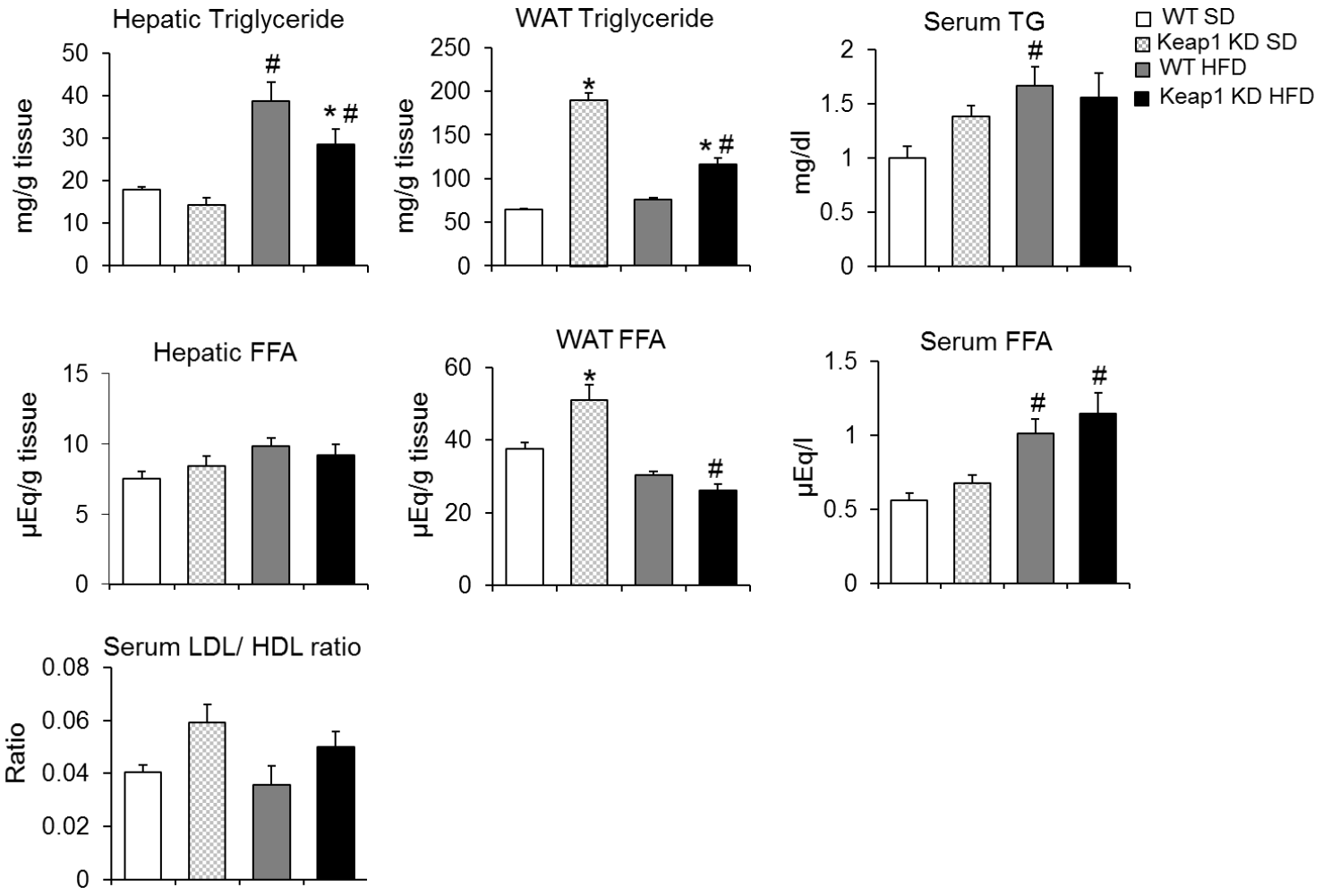

Appendix 1 figure 3: Nrf2 target gene expression in livers and WAT of C57BL/6 (WT) and Keap1 KD mice fed a 10% kCal low fat diet (SD) or 60% kCal high fat diet (HFD)

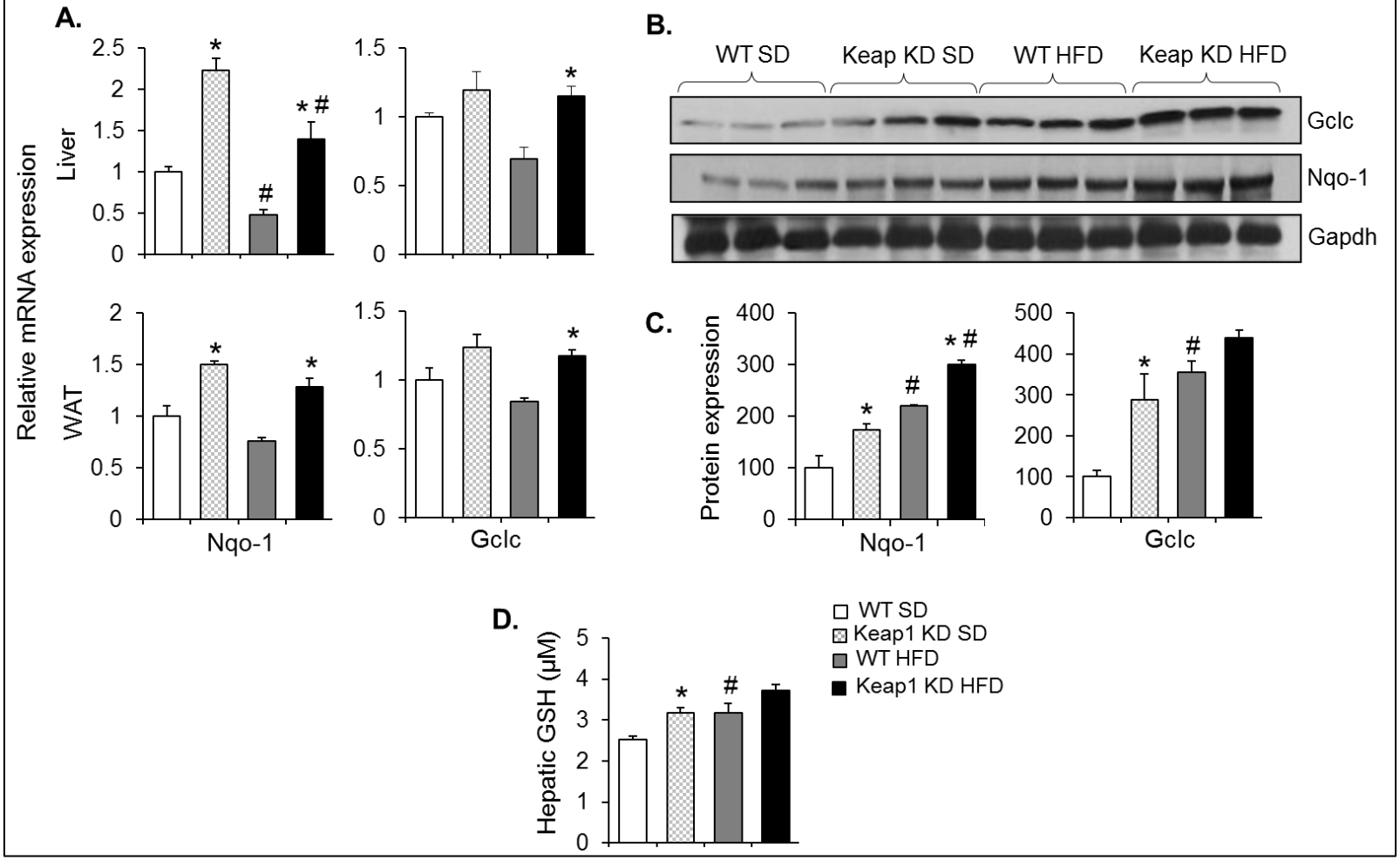

Appendix 1 figure 4: **Lipogenic, lipid oxidation and lipid transport gene expression in livers and of C57BL/6 (WT) and Keap1 KD mice fed a 10% kCal low fat diet (SD) or 60% kCal high fat diet (HFD)**

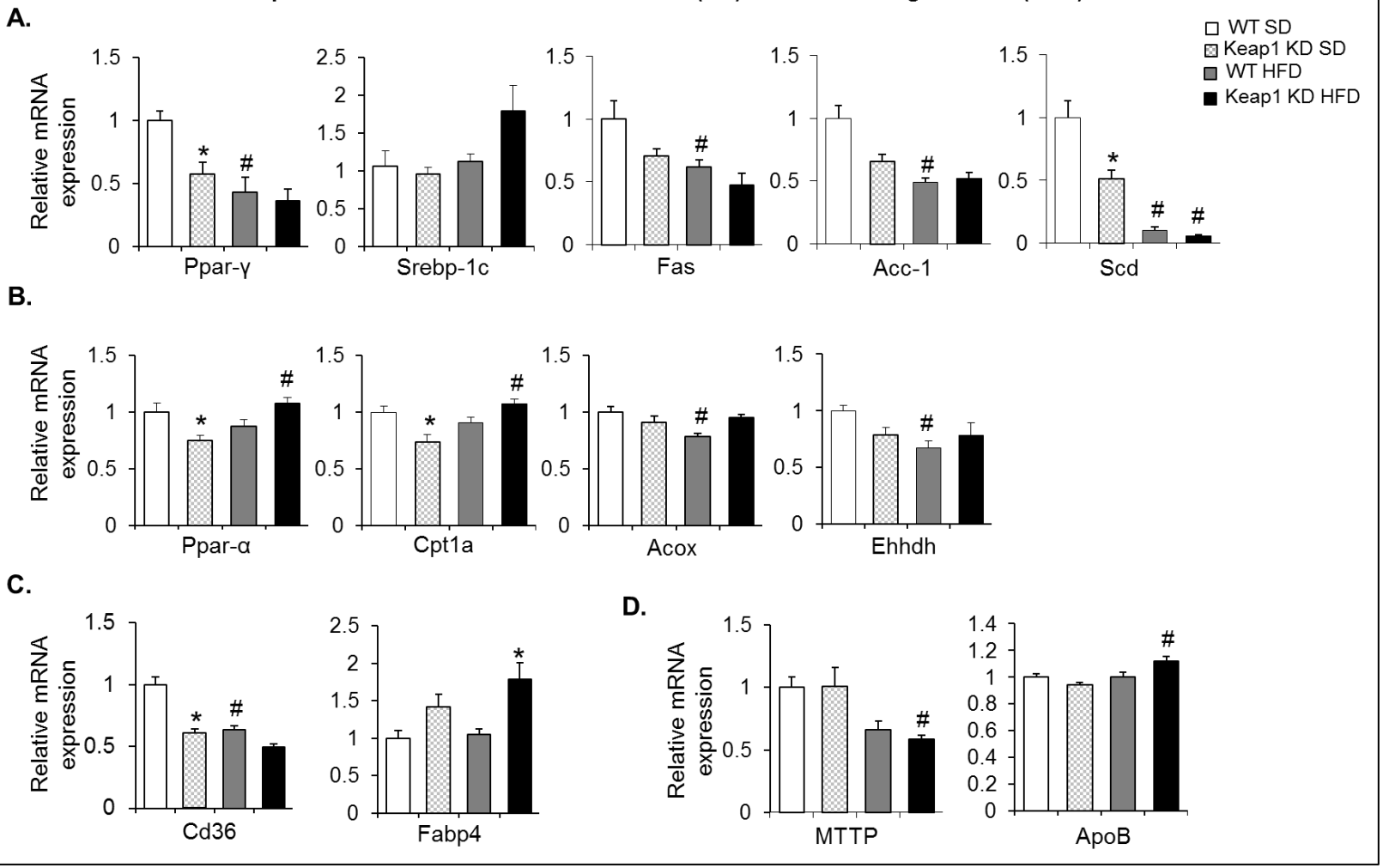

Appendix 1 figure 5:Protein expression of lipogenic enzymes in livers of C57BL/6 (WT) and Keap KD mice fed a 10% kCal low fat diet (SD) or 60% kCal high fat diet (HFD)

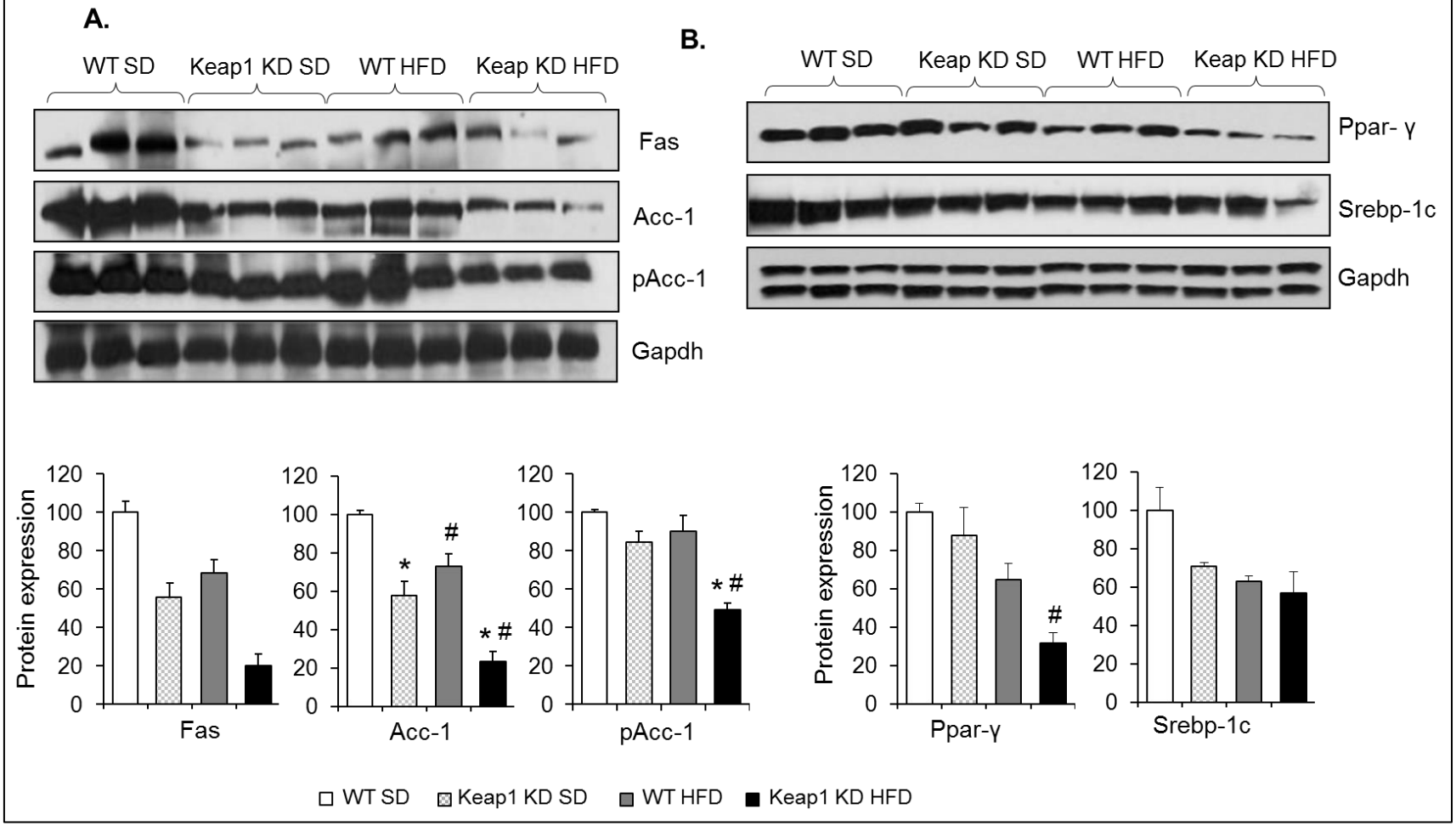

Appendix 1 figure 6: Protein expression of insulin signaling and related targets in livers of C57BL/6 (WT) and Keap KD mice fed a 10% kCal low fat diet (SD) or 60% kCal high fat diet (HFD)

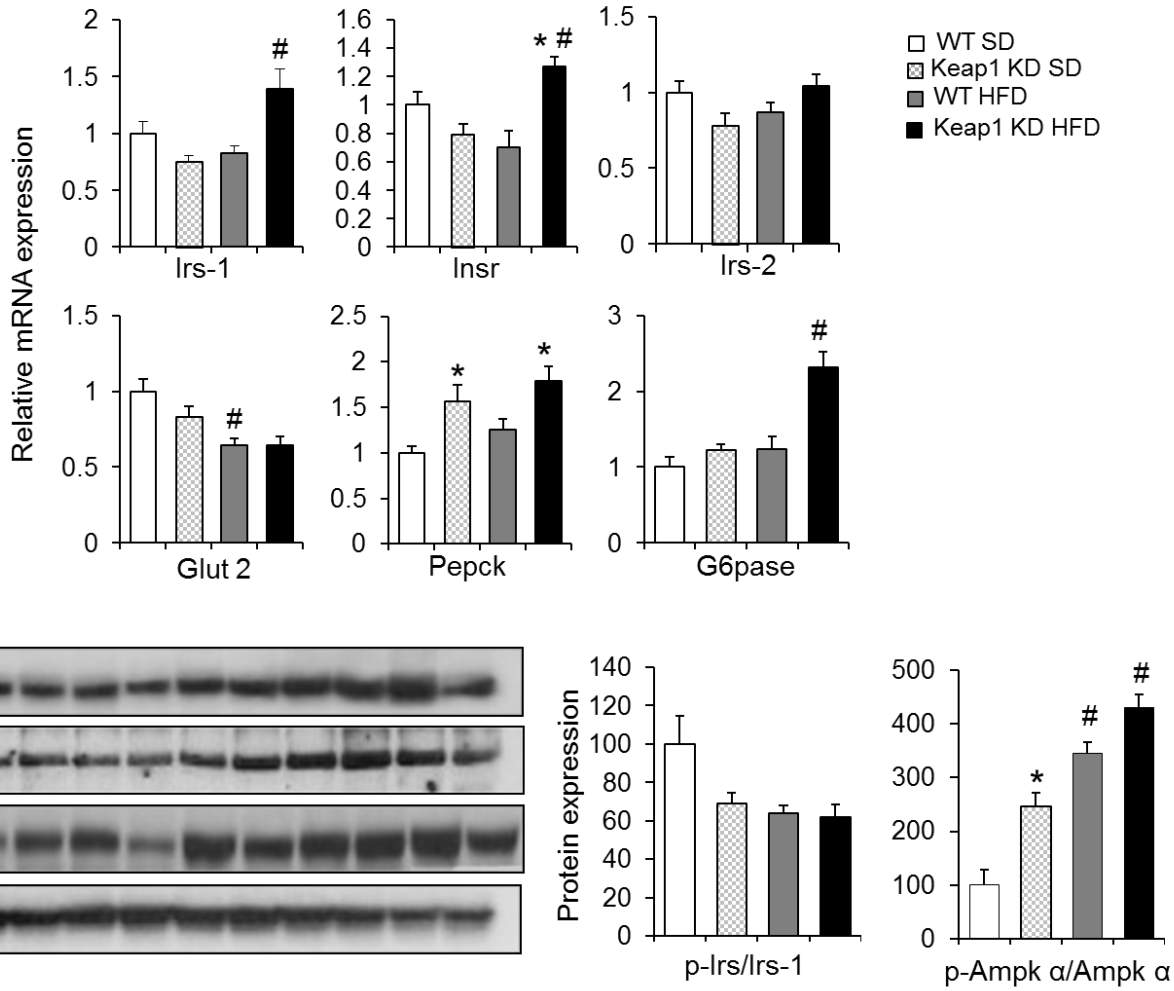

APPENDIX 2:

Objective: Studying the effect of perinatal peripubertal (PNPP) effect of bisphenol A (BPA) on hepatic lipid accumulation and its mechanism in female mice

Experimental design: Pregnant mice were implanted with osmotic pumps containing 250µg/kg BPA or vehicle. The pups were exposed to BPA after birth through milk, and until week 5 of age through drinking water. One set of animals was euthanized at week 5, whereas another set was euthanized at week 39, without any further BPA exposure beyond week 5. The liver tissue was used for lipid accumulation (TG, FFA content), mRNA expression (RT-PCR), protein expression (western blot), promoter methylation (methylated DNA immunoprecipitation), and binding assay (chromatin immunoprecipitation). This data is originally a cohort from studies described in 'manuscript 2', hence all the methods have been described in detail. Differences between the groups were checked with Student's t-test, asterisk * represents significant difference between BPA treated and vehicle group.

Synopsis: The treatment group represented here, BPA 250µg/kg is another treatment cohort from the same study that is presented in 'manuscript 2' of this thesis. Simultaneous study with BPA 25µg/kg and 250µg/kg were performed, and data was compared with vehicle group. Hepatic lipid accumulation (liver TG and oil red o staining) was significantly increased with BPA 25µg/kg but not with BPA 250µg/kg. This is the reason study with this exposure level of BPA was not included in original manuscript. Although phenotypic increase in

hepatic lipids was not evident in BPA 250μg/kg (App 2 fig 1), lipogenic gene expression (App 2 fig 2), protein expression (App 2 fig 3 and 4), Nrf2 signaling (App 2 fig 5), and lipogenic promoter hypomethylation (App 2 fig 6) was altered similar to BPA 25μg/kg exposure. Nrf2 binding on the Srebp-1c promoter was not enhanced by BPA 250μg/kg exposure (App 2 fig 7), indicating transcriptional mechanism of Nrf2 mediated lipid accumulation in liver is evident only in BPA 25μg/kg exposure, but not in BPA 250μg/kg.

Appendix 2 figure 1: **Perinatal peripubertal (PNPP) exposure to bisphenol A affects body weight and hepatic lipid accumulation in female CD1 mice.**

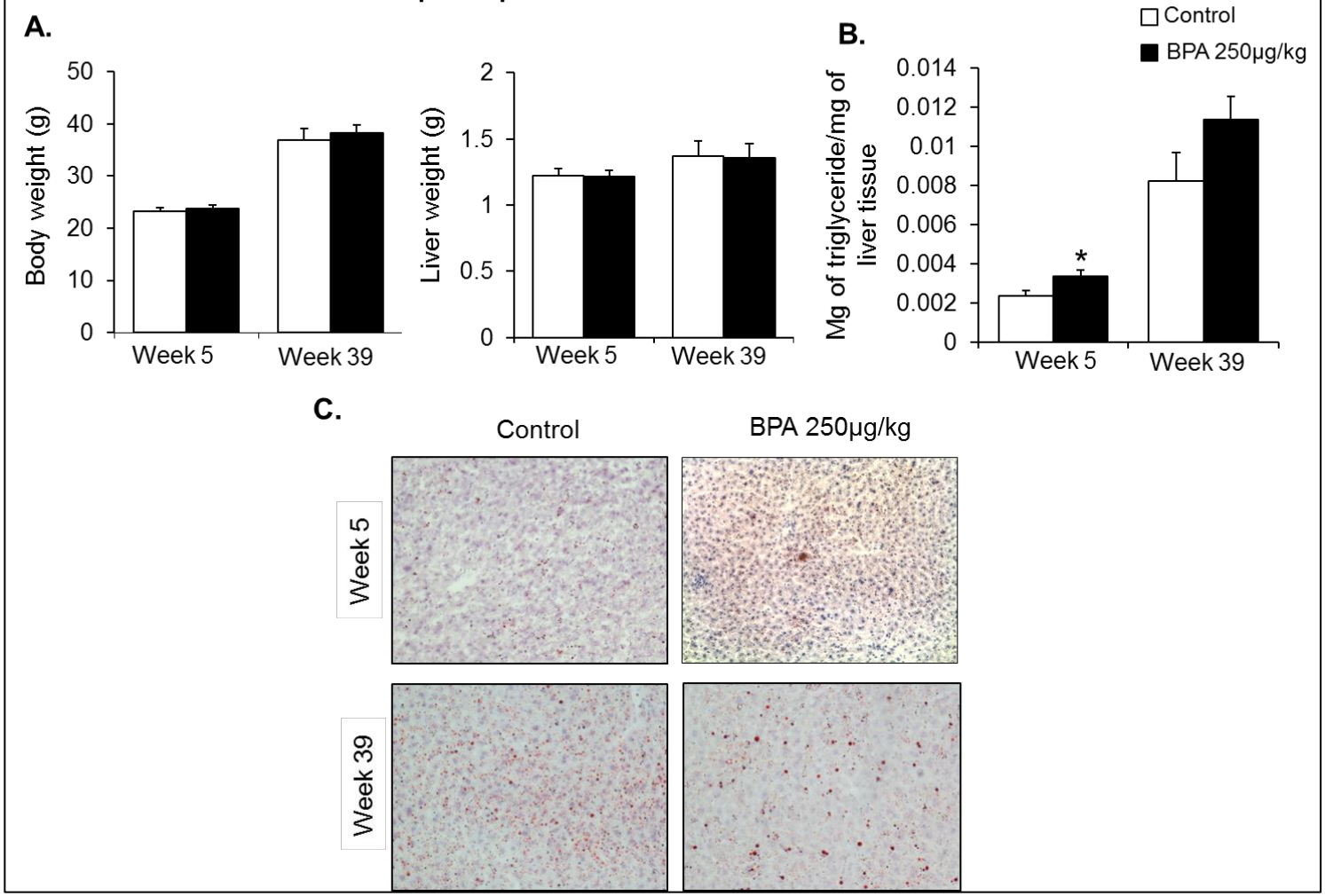

Appendix 2 figure 2: **Perinatal peripubertal (PNPP) exposure to bisphenol A increases mRNA expression of lipogenic targets in livers of female CD1 mice**

A. Week 5

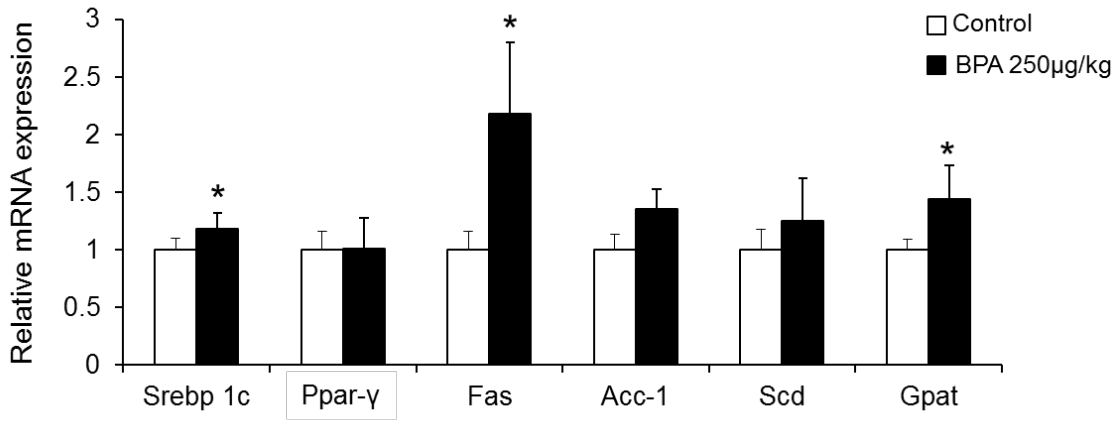

B. Week 39

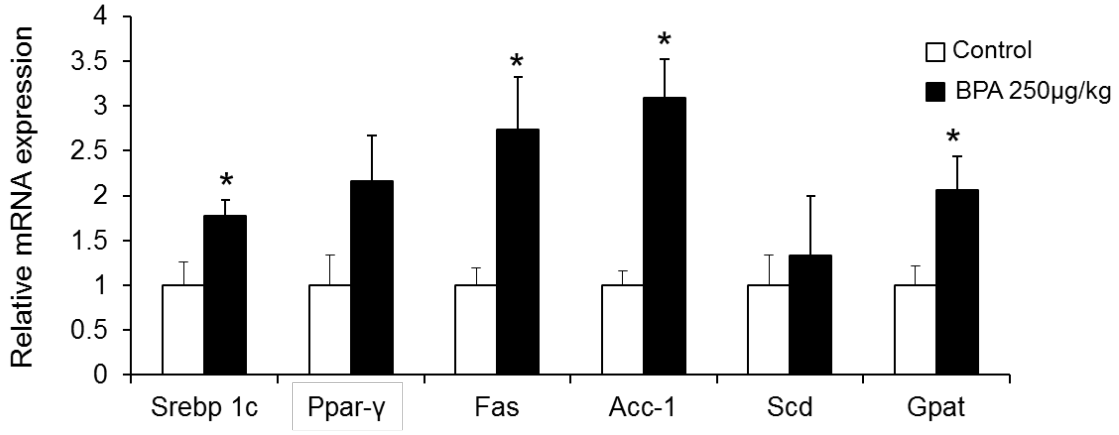

Appendix 2 figure 3: Perinatal peripubertal (PNPP) exposure to bisphenol A increases protein expression of lipogenic transcription factors in livers of female CD1 mice

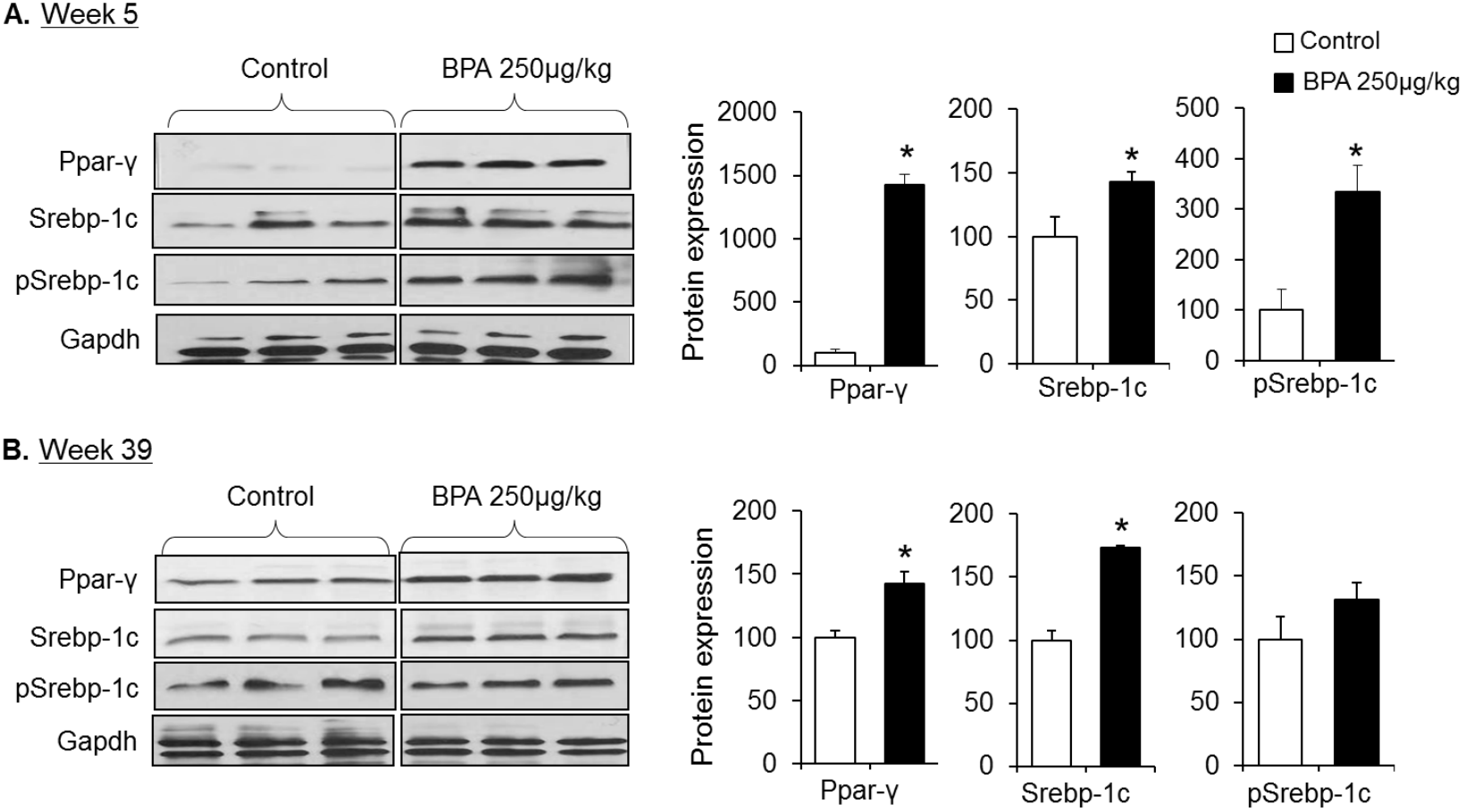

Appendix 2 figure 4: **Perinatal peripubertal (PNPP) exposure to bisphenol A increases protein expression of lipid synthesis enzymes in livers of female CD1 mice**

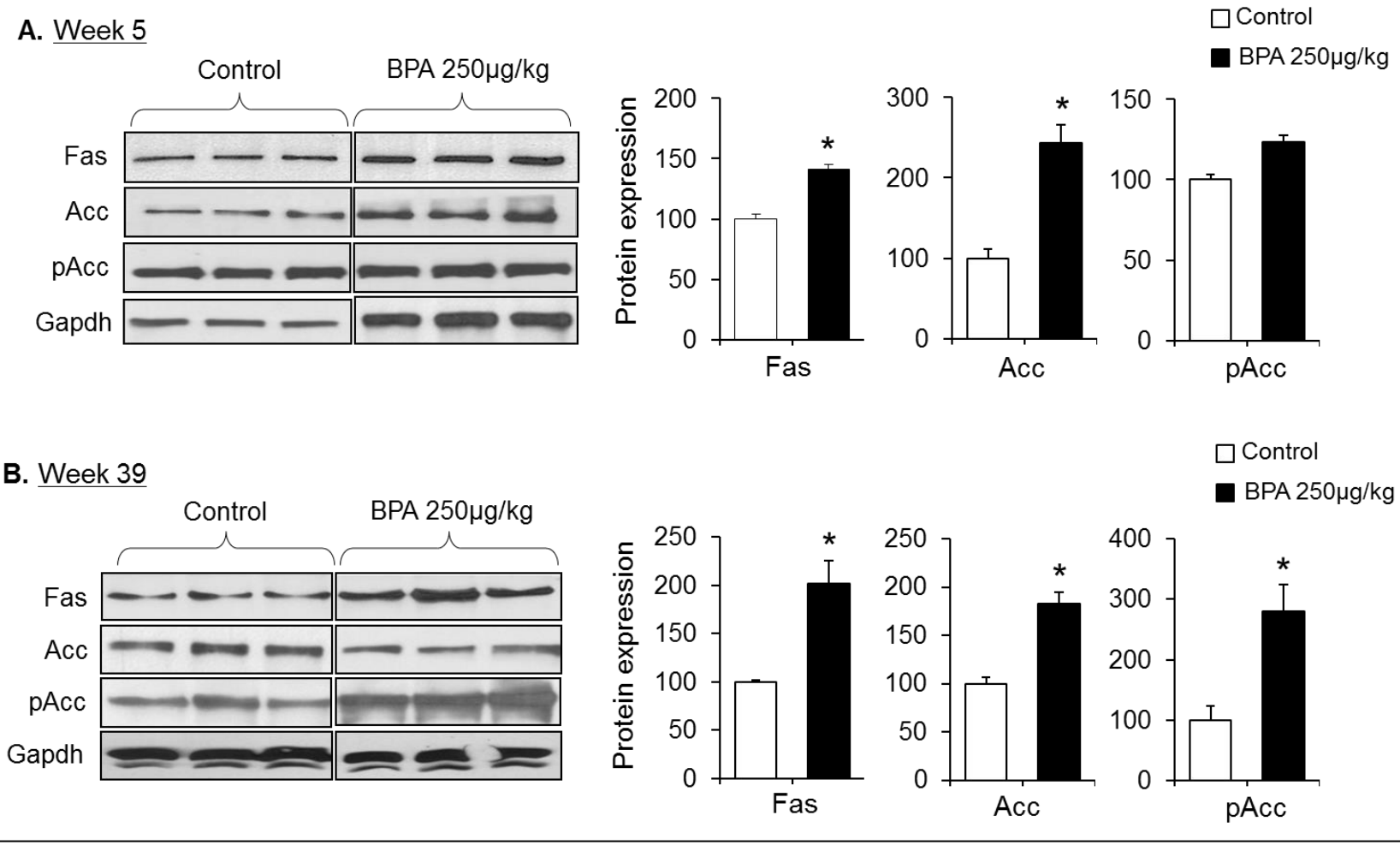

Appendix 2 figure 5: Perinatal peripubertal (PNPP) exposure to bisphenol A and nuclear factor E2 related factor 2 (Nrf2) signaling in livers of female CD1 mice.

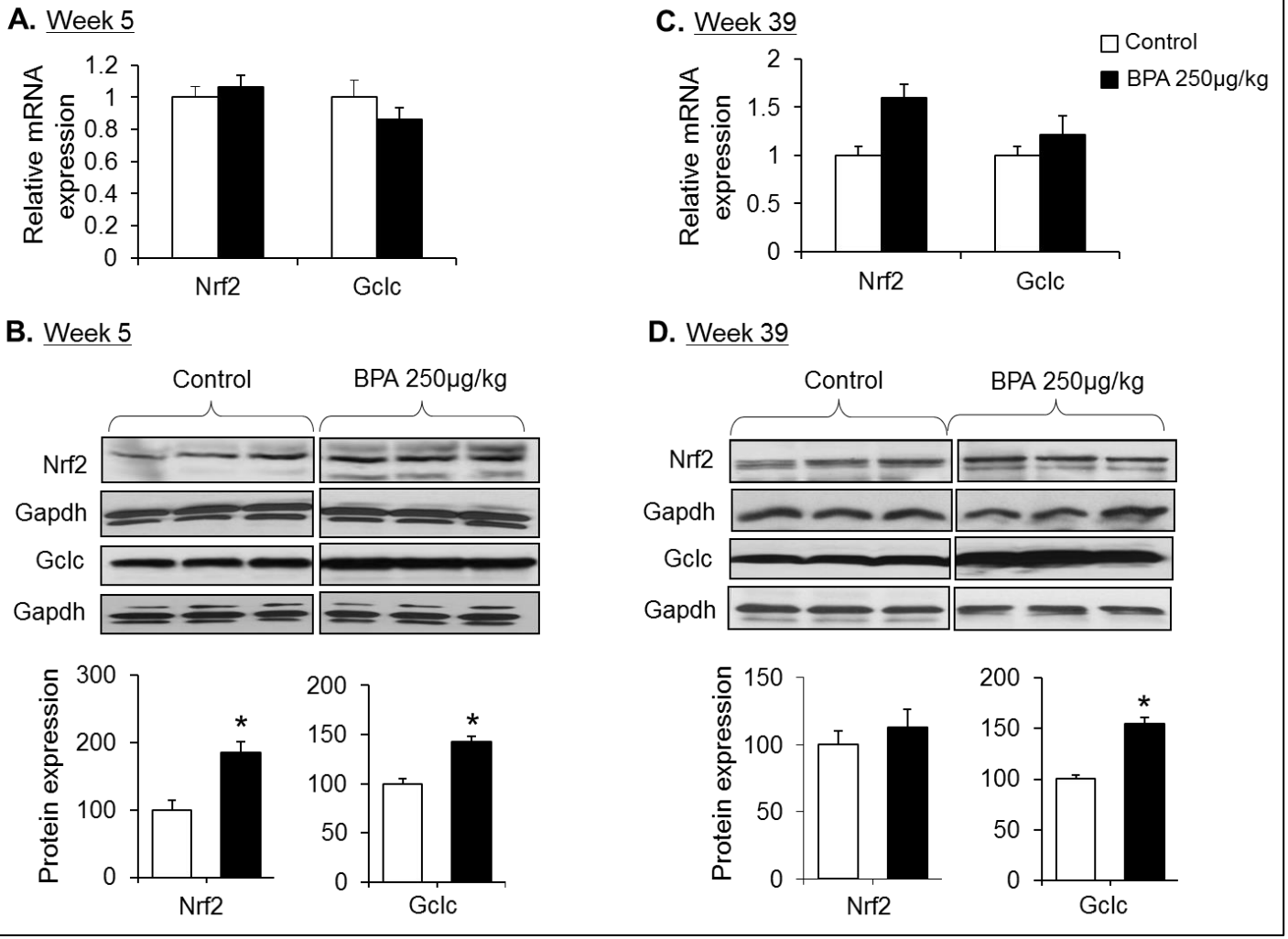

Appendix 2 figure 6: Effect of Perinatal peripubertal exposure of BPA on promoter methylation of Srebp-1c, Fas and Nrf2 analyzed by methylated DNA immunoprecipitation (MeDIP)

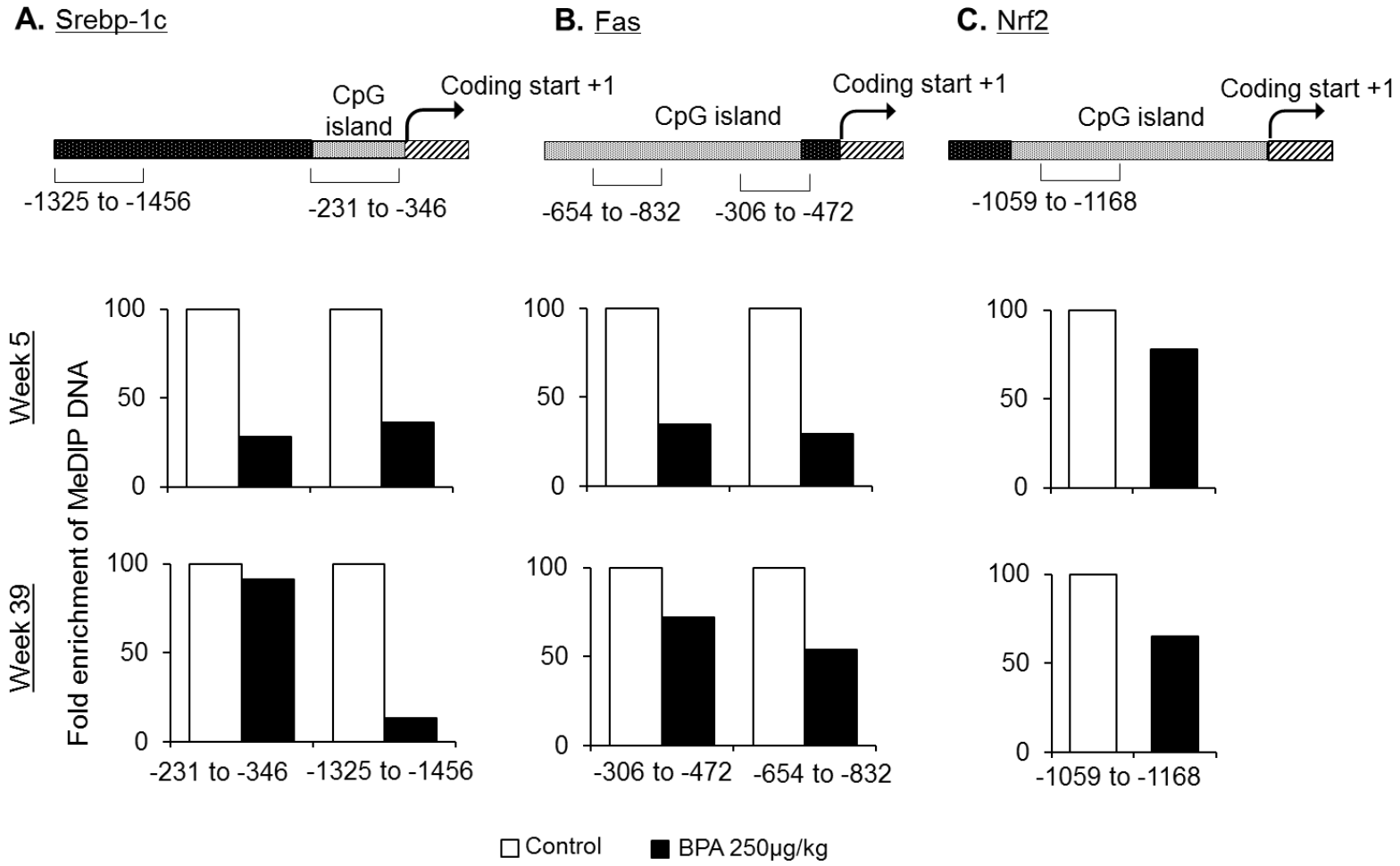

Appendix 2 figure 7: Chromatin immunoprecipitation of nuclear factor E2 related factor 2 (Nrf2) on Srebp-1c gene promoter